VOLUME: 13 NO: 3 YEAR: 2016

ISSN: 1304-530X

TURKISH JOURNAL OF PHARMACEUTICAL SCIENCES

An Official Journal of the Turkish Pharmacists' Association, Academy of Pharmacy

TURKSH
JOURNAL OF PHARMACEUTICAL SCIENCES

Volume: 13, No: 3 Year: 2016

CONTENTS

CONTENTS 13(3) 2016

Original articles

Short communication

Review article

Turk J Pharm Sci 13(3), 285-291, 2016
DOI: 10.4274/tjps.2016.01

ORIGINAL ARTICLE

Wound Healing Potential of Selected Liverworts Growing in Turkey

Türkiye'de Yetişen Bazı Ciğer Otlarının Yara İyileştirici Etkileri

Alev TOSUN[1], İpek SÜNTAR[2], Hikmet KELEŞ[3], Hatice ÖZENOĞLU KİREMİT[4], Yoshinori ASAKAWA[5], Esra KÜPELİ AKKOL[2*]

[1]Ankara University, Faculty of Pharmacy, Department of Pharmacognosy, 06100 Ankara, TURKEY
[2]Gazi University, Faculty of Pharmacy, Department of Pharmacognosy, 06330 Ankara, TURKEY
[3]Afyon Kocatepe University, Faculty of Veterinary, Department of Pathology, 03200 Afyonkarahisar, TURKEY
[4]Adnan Menderes University, Faculty of Education, Department of Biology Education, 09010 Aydın, TURKEY
[5]Tokushima Bunri University, Faculty of Pharmaceutical Sciences, Yamashiro-cho, Tokushima 770-8514, JAPAN

ABSTRACT

The Bryophytes have been traditionally used to cure cuts, burns, external wounds, bacteriosis, pulmonary tuberculosis, neurasthenia, fractures, convulsions, scalds, uropathy, inflammation, fever and pneumonia. Selected eight liverworts growing in Turkey were tested for their wound healing potential. In the present study, *in vivo* wound-healing activities of the ethereal extracts of some liverworts collected from Southern Anatolia were investigated by using linear incision and circular excision experimental patterns subsequently histopathological analysis. For the bioassays, 1% ointment formulations were prepared from the crude extracts. The ethereal extracts from *Reboulia hemisphaerica* (L.) Raddi (Aytoniaceae), *Plagiochasma rupestre* (J.R. Forst et G. Forst) Steph. (Aytoniaceae), and *Targionia hypophylla* L. (Targioniaceae) showed 43.1, 38.3, and 24.1% increase in tensile strength on the linear incision wound test, respectively. The extracts of *Reboulia hemisphaerica*, *Plagiochasma rupestre* and *Targionia hypophylla* also exhibited significant contraction effect with the values of 62.1, 58.0, and 39.8%, respectively, on the circular excision wound model, quite comparable to reference sample. The liverworts have many important biological activities, which are investigated previously. However, the wound healing effects of Turkish liverworts have not been expounded yet. Thus, the results obtained from the present study will be important for the future researches. Moreover, the present study supported the usages of some Bryophytes in some native societies of the world against skin problems, including wound, bruises, burns, etc.

Key words: Wound healing, Liverworts, Bryophytes, Marchantiophyta

ÖZ

Bryofitler geleneksel olarak kesik ve yanık yaralarında, bakteriozis, pulmoner tüberküloz, nevrasteni, kırık, konvülsiyon, üropati, enflamasyon, ateş ve pnömoni tedavisinde kullanılmaktadır. Bu çalışmada, Türkiye'de yetişen ve Anadolu'nun güney kesimlerinden toplanan sekiz ciğer otunun eterli ekstrelerinin *in vivo* yara iyileştirici etkileri çizgisel insizyon ve dairesel eksiyon yara modelleri kullanılarak araştırıldı. Takibinde dokular üzerinde histopatolojik analizler yapıldı. Deneylerde, ham ekstreden hazırlanan %1'lik merhem formülasyonları kullanıldı. İnsizyon yara modelinde, *Reboulia hemisphaerica* (L.) Raddi (Aytoniaceae), *Plagiochasma rupestre* (J.R. Forst et G. Forst) Steph. (Aytoniaceae) ve *Targionia hypophylla* L. (Targioniaceae) eterli ekstreleri sırasıyla %43.1, %38.3 ve %24.1 oranlarında yara gerilme kuvvetinde artış oluşturdu. *Reboulia hemisphaerica*, *Plagiochasma rupestre* ve *Targionia hypophylla* ekstreleri sırasıyla %62.1, %58.0 ve %39.8 kontraksiyon değerleriyle dairesel eksizyon yara modelinde de referans örnek ile karşılaştırılabilir düzeyde ve anlamlı derecede etkili bulundu. Ciğer otlarının daha önceden belirlenmiş birçok biyolojik etkisi bulunmaktadır. Ancak, Türkiye'de yetişen ciğer otlarının yara iyileştirici etkileri daha önce araştırılmamıştır. Bu nedenle, bu çalışmada elde edilen sonuçlar gelecek araştırmlar için önem taşımaktadır. Bununla beraber, bu çalışma bryofitlerin halk arasında yara ve yanık gibi deri problemlerinde kullanımını doğrulamaktadır.

Anahtar kelimeler: Yara iyileşmesi, Ciğer otları, Bryofitler, Marchantiophyta

*Correspondence: **E-mail:** esrak@gazi.edu.tr **Phone:** +90 312 202 31 85

INTRODUCTION

The medicinal plants and their derivatives have been used for providing relief and cure of illness in traditional forms in all cultures for many years (1-4). Many articles related the biological activity of the plants have been released contemporarily, some part of these studies had been reported for wound-healing activity (5).

The use of wound-healing plants to treat external injuries as well as internal injury is a popular ethnomedicinal practice in many countries such as China, Peru, India and Nigeria (5-9).

The phytochemistry of the Bryophytes has been ignored for a long time because of their morphological small size, unobtrusive position in the nature and difficult taxonomy. Besides of all, they do not have nutritional usages for humans due to their unpleasant taste. However, some Bryophytic plants are used by Native Americans in soup, and as a flavor agent in wine (10). The Bryophytes have also been traditionally used for their medicinal properties in China, Europe and North America, to cure cuts, burns, external wounds, bacteriosis, pulmonary tuberculosis, neurasthenia, fractures, convulsions, scalds, uropathy, inflammation, fever, pneumonia, etc. (10-13).

The Bryophytes are taxonomically placed between algae and pteridophytes. They are classified into three relevant phyla known as Bryophyta (Moss), Marchantiophyta (Liverwort) and Anthocerotophyta (Hornwort). The important group as of the liverworts belongs to Marchantiophyta group are represented by approximately 8000 species in 74 families, 380 genera, and considered to be the oldest aquatic-terrestrial primitive plants in the world. The liverworts are used for remedies of cuts, fractures, burns, bruises, wounds and snake bite as mentioned in the literature. Especially during the Renaissance, the liverworts were used in herbal medicines. In China, it is still used to treat the hepatitis and as an external cure to reduce the inflammation. In fact, the most important sides of the liverworts are their structurally and biologically interesting active terpenoid compounds, which are located in oil bodies known as unique organelles of the liverworts. The components isolated from liverworts have significant biological activities such as antimicrobial, antifungal, insect antifeedant, cytotoxic, apoptosis inducing activity, some enzyme inhibitory, neurotic sprouting activity, muscle relaxing, cardiotonic activity and so on (11-13).

Plagiochasma appendiculatum Lehm. et Lind. (Aytoniaceae) distributed in India, is widely used ethnomedicinally by Gaddi tribe in Kangra valley for treating skin diseases in the form of paste, and applied externally for the treatment of burns, boils and blisters on the body. The species is also used for the treatment of skin eruption caused due to bright sun in the summer time (14). Himalayan Indians have used *Marchantia polymorpha* L. (Marchantiaceae) or *M. palmate* Nees to treat boils and abscesses because the young archegoniophore resembles an abscess as it emerges from the thallus. Moreover, in China, a mixture of the thallous of *Conocephalum conicum* L. (Dum.) (Conocephalaceae) and *Marchantia polymorpha* with vegetable oils is used on bites, boils, burns, cuts, wounds and eczema (10).

The most investigated taxa are from Angiosperms whereas limited data is currently available about Bryophytes. Particularly, there is not enough information about Turkish liverworts in *Flora of Turkey* (15). Moreover, chemical and biological studies are scarcely limited on these species except for a few studies. Thus, the aim of this study was to evaluate the wound healing activity of the Turkish liverworts by using *in vivo* models for the preliminary screening. In this frame, the ethereal extracts (Table 1) of the *Riccia fluitans* L. (Ricciaceae), *Porella cordaeana* (Huebener) Moore (Porellaceae), *Porella platyphylla* (L.) Pfeiff. (Porellaceae), *Corsinia coriandrina* (Spreng.) Lindb. (Corsiniaceae), *Mannia androgyna* (L.) A. Evans (Aytoniaceae), *Reboulia hemisphaerica* (L.) Raddi (Aytoniaceae), *Plagiochasma rupestre* (J.R. Forst et G. Forst) Steph. (Aytoniaceae), *Targionia hypophylla* L. (Targioniaceae) were debated for healing efficiency on incision and excision wounds models *in vivo.* In our ongoing research, their chemical constituents will be examined in future studies to find promising agents.

MATERIALS AND METHODS

Plant materials

Plant materials were collected from İzmir, Aydın and Muğla provinces, Turkey in 2009. Voucher specimens were identified by H. Ozenoglu Kiremit (Adnan Menderes University-Department of Biology) and deposited at the Herbarium of Adnan Menderes University in Aydın, Turkey. The list of the species with their collection places and herbarium numbers are presented in Table 1.

Preparation of plant extracts

The plant extracts were prepared according to Tosun et al., 2013. First of all, dried plant materials were macerated with ether in a dark and cool place for 3-4 weeks. The extracts were filtrated, and the ether was evaporated *in vacuo* less than 30°C. The amount of the crude extracts was exactly weighed. The extracts were kept in a freezer up to use in the activity tests (16).

Biological activity tests

Animals

Male, Sprague-Dawley rats (160-180 g) and Swiss albino mice (20-25 g) purchased from the animal breeding laboratories of from the animal breeding laboratory of Saki Yenilli (Ankara, Turkey), were used in the experiments. Before the experiments, animals were left for three days at room conditions for acclimatization. They were maintained on standard pellet diet and water *ad libitum* throughout the experiment. A minimum of six animals was used in each group.

Preparation of test samples for bioassay

Test samples of *in vivo* experimental wound models were prepared in an ointment base (vehicle) consisting of glycol stearate, 1, 2-propylene glycol, liquid paraffin (3:6:1) in 1% concentration. Immediately, after the wound was created by a surgical blade, animals of the experimental group were topically treated with 0.5 g of each test ointment. Ointment base was applied to the animals of the vehicle group. Reference group animals were treated with 0.5 g of Madecassol® (Bayer, 00001199), whereas negative control group animals were not treated with any material.

Wound healing activity

Linear incision wound model

All the animals were anaesthetized with 0.05 cc Xylazine (2% Alfazine®) and 0.15 cc Ketamine (10% Ketasol®), and the back hairs were shaved with a shaving machine. Two linear-paravertebral full-thickness skin incisions of 5 cm long were made with a sterile surgical blade at the distance of 1.5 cm from the midline of each side of the vertebral column (17). The incised wounds were sutured by three interrupted sutures of 1 cm apart. The extracts, the reference drug (Madecassol®) and the vehicle were topically applied once in a day throughout nine days. Animals of the negative control group were not treated with any material. On the 9th post wound day, all the sutures were removed. Animals were killed under anesthesia on day 10th. For the determination of tensile strength of the wound, a linear-paravertebral incised skin sample was measured using a tensiometer (Zwick/Roell Z0.5, Germany). Another skin sample underwent histopathological examination (18-20). A tensiometer measures the breaking strength in N (Newton), which is called tensile strength.

Circular excision wound model

The circular excision wound model was used for the evaluation of the wound contraction. The mice were anaesthetized with 0.02 cc Xylazine (2% Alfazine®) and 0.08 cc Ketamine (10% Ketasol®) and the back hairs were depilated by shaving. A circular wound was created on the dorsal interscapular region of each animal by excising the skin with a 5 mm biopsy punch; wounds were left open. The extracts, the reference drug (Madecassol® Bayer) and the vehicle ointments were applied topically once a day until the wounds of one group were completely healed. The progressive changes in the wound area were monitored by a camera (Fuji, S20 Pro, Japan) every other day. Later, wound area was measured by using AutoCAD program. Wound contraction was calculated as the percentage of the reduction in the wounded area. For the histopathological examination, a specimen sample of tissue was removed from the healed skin of each group of mice (20-22).

Histopathology

The cross-sectional full-thickness skin specimens from each group were collected at the end of the experiment to evaluate for the histopathological alterations. Samples were fixed in 10% buffered formalin, processed and blocked with paraffin and then sectioned into five micrometer sections and stained with hematoxylin & eosin (HE) and Van Gieson (VG) stains. The tissues were examined by the light microscope (Olympus CX41 attached Kameram® Digital Image Analyze System) and graded subjectively as mild (+), moderate (++) and severe (+++) for epidermal or dermal re-modeling. Re-epithelization or ulcus in epidermis; fibroblast proliferation, mononuclear and/or polymorph nuclear cells, neovascularization and collagen depositions in the dermis were analyzed to score the epidermal or dermal re-modeling. At the end of the examination, obtained results were combined and staged for wound healing phases as inflammation, proliferation, and re-modeling in all groups (20).

Statistical analysis of the data

The data on percentage wound healing was statistically analyzed using one-way analysis of variance (ANOVA). A p-value ≤0.05 was considered statistically significant. Histopathologic data were considered to be nonparametric (20).

RESULTS AND DISCUSSION

In the present study, the diethyl ether extracts of eight different species of the liverworts growing in Turkey (Table 1) were investigated for their *in vivo* wound healing activity. The wound healing activity was evaluated by using linear incision

Table 1. The herbarium numbers and collection sites of the liverworts growing in Turkey

Family	Plant name	Herbarium number	Collection sites
Aytoniaceae	*Mannia androgyna* (L.) A. Evans	C11/237	**Muğla;** Milas, Kapıkırı Village, Heraclea Archaic City Ruins, on the rocks and soil bank near the roadside, 35 m
	Plagiochasma rupestre (J.R. Forst et G. Forst) Steph	C11/226	**Muğla;** Milas, Kapıkırı Village, Heraclea Archaic City Ruins, on the rocks and soil ground, 70 m
	Reboulia hemisphaerica (L.) Raddi	C11/227	**Aydın;** Koçarlı, Mersin Belen road 5th km, on the road in stream bank, 696 m
Porellaceae	*Porella cordaeana* (Huebener) Moore	C11/223	**Aydın;** Koçarlı, Mersin Belen road 5th km, on the road in stream bank, 696 m
	Porella platyphylla (L.) Pfeiff	C11/222	**Aydın;** Koçarlı, Mersin Belen road 5th km, on the road in stream bank, 696 m
Ricciaceae	*Riccia fluitans* L.	C11/225	**İzmir;** Selçuk, Zeytinköy Village, Kazangöl Lake, 3 m
Targioniaceae	*Targionia hypophylla* L.	C11/236	**Muğla;** Milas, Kapıkırı Village, Heraclea Archaic City Ruins, on the rocks and soil bank near the roadside, 30 m

and circular excision wound models. The skin samples were also evaluated histopathologically.

As shown in Table 2, topical application of the ointment prepared with the ethereal extracts of the *Reboulia hemisphaerica, Plagiochasma rupestre* and *Targionia hypophylla* onto the incised wounds demonstrated the best wound tensile strength by the highest values of 43.1, 38.3, and 24.3%, respectively.

Table 2. Effects of the Liverworts extracts on linear incision wound model

Material	Statistical Mean ± S.E.M.	(Tensile strength %)
Vehicle	9.60±2.13	5.7
Negative control	10.18±2.44	-
Corsinia coriandrina	10.88±2.02	13.3
Mannia androgyna	9.15±2.82	-
Porella cordaeana	10.09±1.68	5.1
Porella platyphylla	11.39±1.79	18.7
Plagiochasma rupestre	13.28±1.64	**38.3****
Riccia fluitans	9.47±2.17	-
Reboulia hemisphaerica	13.74±1.10	**43.1*****
Targionia hypophylla	11.93±1.29	**24.3***
Madecassol®	15.24±1.06	**58.8*****

*: p<0.05, **: p<0.01, ***: p<0.001, S.E.M.: Standard error of the mean
Percentage of tensile strength values: Vehicle group was compared to Negative control group; Extracts were compared to Vehicle group

The contraction values of the wounds on the circular excision wound model for vehicle, negative control, the ethereal extracts and reference drug treated group are shown in Table 3. The ethereal extracts of *Reboulia hemisphaerica, Plagiochasma rupestre* and *Targionia hypophylla* were found to have wound healing potential with the contraction values of 35.65 and 62.13%; 27.94 and 58.04%; 31.48 and 39.78%; respectively, on day 10 and 12, while the vehicle and negative control groups and the extracts of the liverworts showed no statistically significant wound healing activity onto the incised wounds demonstrated the best wound tensile strength by the highest values of 43.1, 38.3, and 24.3%, respectively.

Histopathological analysis showed that the ethereal extracts of *Reboulia hemisphaerica, Plagiochasma rupestre* and *Targionia hypophylla* treated groups demonstrated better healing with rapid re-epithelization. The data obtained in histopathological evaluation were in accord with the outcome of wound models used in the present study. Delay in wound healing processes were observed especially in the vehicle and negative control groups compared to others (Table 4, Figure 1).

Skin sections show the hematoxylin & eosin (HE) stained epidermis and dermis in A, and the dermis stained with

Table 3. Effects of the Liverworts on circular excision wound model

Material	Wound area ± S.E.M. (Contraction %)						
	0	2	4	6	8	10	12
Vehicle	20.17±2.21	17.22±1.86 (1.37)	16.65±2.01 -	15.03±2.15 -	11.08±1.53 (11.29)	7.91±1.42 (10.01)	3.67±0.32 (8.48)
Negative control	19.67±2.18	17.46±1.99	16.59±1.95	14.88±1.83	12.49±1.85	8.79±1.42	4.01±1.19
Corsinia coriandrina	19.44±1.80	16.03±1.86 (6.91)	14.90±2.10 (10.51)	13.13±2.14 (12.64)	9.49±1.31 (14.35)	6.22±1.37 (21.37)	2.93±0.25 (20.16)
Mannia androgyna	19.40±2.77	17.03±1.73 (1.10)	17.01±1.86 -	14.19±1.92 (5.59)	10.20±1.34 (7.94)	7.77±1.39 (1.77)	3.51±0.88 (4.36)
Porella cordaeana	19.59±1.96	17.39±1.25 -	16.72±2.16 -	14.61±1.89 (2.79)	10.51±1.39 (5.14)	7.41±1.26 (6.32)	3.71±0.59 -
Porella platyphylla	19.27±1.53	15.64±1.07 (9.18)	14.05±1.48 (15.62)	13.26±2.36 (11.78)	9.70±1.47 (12.45)	6.60±1.11 (16.56)	2.96±0.34 (19.35)
Plagiochasma rupestre	20.68±2.41	15.02±1.40 (12.78)	13.44±1.96 (19.28)	11.89±2.18 (20.89)	9.79±1.15 (11.64)	5.70±1.10 (27.94)	1.54±0.09 **(58.04)****
Riccia fluitans	19.90±2.55	16.81±1.56 (2.38)	16.08±2.03 (3.42)	14.80±1.90 (1.53)	10.76±1.60 (2.89)	8.05±1.56 -	3.84±0.29 -
Reboulia hemisphaerica	20.56±2.06	15.58±1.44 (9.52)	14.07±1.65 (15.49)	12.21±2.23 (18.76)	8.84±1.17 (20.22)	5.09±1.16 **(35.65)***	1.39±0.08 **(62.13)****
Targionia hypophylla	19.78±2.23	15.41±1.85 (10.51)	14.62±1.29 (12.19)	12.19±1.76 (18.89)	8.36±1.69 (24.55)	5.42±1.31 **(31.48)***	2.21±0.14 **(39.78)***
Madecassol®	19.31±1.65	13.89±1.14 (19.34)	13.24±1.79 (20.48)	9.51±1.06 **(36.73)***	3.19±0.75 **(71.21)*****	1.17±0.43 **(85.21)*****	0.00±0.00 **(100.00)*****

*: p<0.05, **: p<0.01, ***: p<0.001, S.E.M.: Standard error of the mean
Percentage of contraction values: Vehicle group was compared to Negative control group, Extracts were compared to Vehicle group.

Van Gieson (VG) in B. The original magnification was x100 and the scale bars represent 120 µm for figures in A, and the original magnification was x400 and the scale bars represent 40 µm for B. Data are representative of 6 animal per group. 1. Vehicle; 2. Negative Control; 3. *Corsinia coriandrina;* 4. *Mannia androgyna*; 5. *Porella cordaeana*; 6. *Porella platyphylla;* 7. *Plagiochasma rupestre*, 8. *Riccia fluitans*, 9. *Reboulia hemisphaerica*, 10. *Targionia hypophylla*, 11. Madecassol®. Arrows pointing events during wound healing; s: scab, u: ulcus, re: re-epithelization, f: fibroblast, c: collagen, mnc: mononuclear cells, pmn: polymorphonuclear cells, nv: neovascularization.

A large number of people are suffered from wounds especially from chronic wounds. In spite of advances in medicine, the availability of drugs which is curative in the wound process is still limited (7). Nowadays, the natural products are potential sources for the development of the new drugs as well in the past. Wounds are physical injuries that result in an opening or breaking of the skin. Wound infections are the most common end, especially in developing countries because of poor hygienic conditions and also seriously reduce their quality of life. Thus, developing new wound healing agents are important in biological activity studies. The plant natural products can act as potent anti-inflammatory, antioxidant or anticancer agents. Antioxidant, antimicrobial and anti-inflammatory activities help to promote wound healing and contribute skin regeneration. The mechanism of antioxidant compounds is the inhibition of lipid peroxidation and by way of radical scavenging activity, which prevent cell damage. Antimicrobial activity is also important for the wound healing period, since the wound is more inclined to microbial attacks such as *Staphylococcus aureus, Streptococcus pneumonia, Klebsiella pneumonia,* which are caused infections and latency in wound area (5,23).

Wound-healing is a complex multifactorial process that results in the contraction and closure of the wound and restoration of a functional barrier (24,25). Thus, wound-healing process consists of several phases, including homeostasis, inflammation, cellular proliferation and migration of different cell types as resulting remodeling phase. The first response is inflammation as a defense mechanism of the tissue, which provides a resistance to the microbial contaminations. However, a long duration in the inflammatory phase causes a delay in healing process. Skin fibroblast proliferation is important in tissue repair as fibroblasts are involved in migration, proliferation, contractions and collagen production. The process of re-epithelialization occurs in the proliferatives phase. The final phase of the wound healing is called as maturation and remodeling phase. The completion of healing is ended by collagen coverage (3,5,6,23,26).

The liverworts have the wide range of endemic species, which include many interesting constituents with important biological activities. Principally, the liverworts contain a large amount of mono-, sesqui- and diterpenoids, and aromatic compounds with unique structures. However, the reason of the increasing interest of the liverworts is for their structurally impressive constituents exhibiting high therapeutic effects as cytotoxic, antitumor, antimicrobial, antifungal, antifeedant,

Table 4. Wound healing processes and healing phases of the experimental group animals

Groups	Wound Healing Processes								Healing Phases		
	S	U	RE	FP	CD	MNC	PMN	NV	I	P	R
Vehicle	+++	+++	-	++	++	+/++	+/++	++	++	++	-
Negative control	++	+++	-	++/+++	++/+	++	++	++	++	++/+++	-
Corsinia coriandrina	++	++/+++	-	++	++	+/++	+/++	+/++	+/++	++	-
Mannia androgyna	++	+++	-	++	++/+++	+/++	+/++	++/+++	+/++	++/+++	-
Porella cordaeana	++/+++	+++	-	++/+++	++	++	+/++	++/+++	+/++	++/+++	-
Porella platyphylla	++/+++	++/+++	-	++/+++	+/++	+/++	+/++	++	+/++	++/+++	-
Plagiochasma rupestre	++/+++	++/+++	-	++/+++	++	++	+/++	++	+/++	++/+++	-
Riccia fluitans	++/+++	+++	-	++/+++	++	++	+/++	++	+/++	++/+++	-
Reboulia hemisphaerica	++	-	+/++	++/+++	+/++	+/++	+/++	++	+/++	++	+
Targionia hypophylla	++	++/+++	-	++	++	+/++	+/++	++	+/++	++	-
Madecassol®	+/++	-	+/++	++	++	+	+	+/++	+/++	++	+/++

*HE and VG stained sections were scored as mild (+), moderate (++) and severe (+++) for epidermal and/or dermal re-modeling. S: Scab, U: Ulcus, RE: Re-epithelization, FP: Fibroblast proliferation, CD: Collagen depositions, MNC: Mononuclear cells, PMN: Polymorphonuclear cells, NV: Neovascularization, I: Inflammation phase, P: Proliferation phase, R: Re-modeling phase

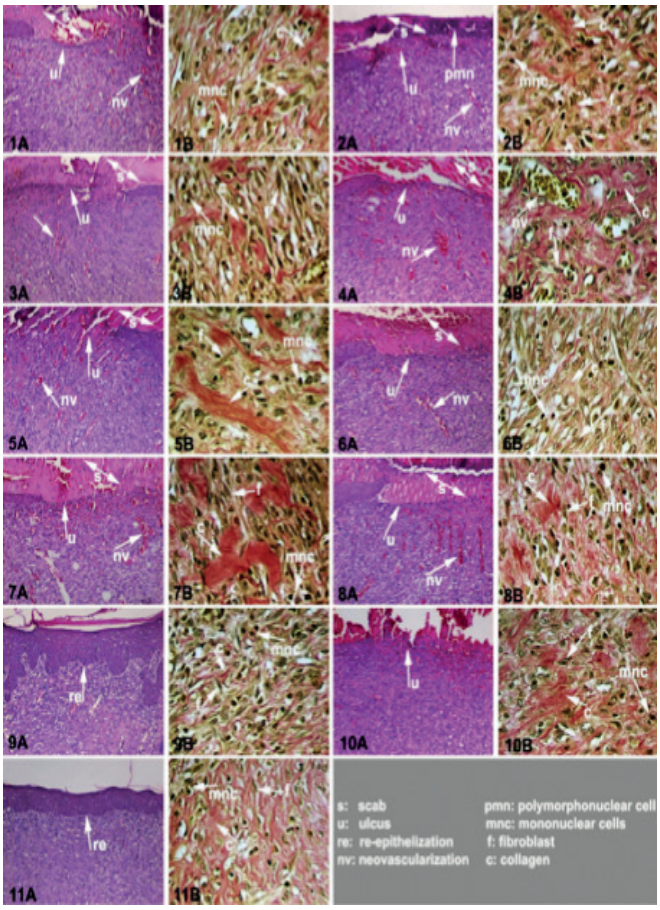

Figure 1. Histopathological view of wound healing and epidermal/dermal re-modeling in the vehicle, negative control, extracts and reference ointment Madecassol® administered animals

insecticidal, muscle relaxing, some enzyme inhibitory and apoptosis inducing activities (11-13,27).

There is not much investigation as *in vivo* biological activity studies on the most active species of *Plagiochasma rupestre* and *Reboulia haemispherica* and *Targionia hypophylla* as well as ethnomedicinal usages of these species (11). However, another species of the *Plagiochasma*, *Plagiochasma appendiculatum* (Aytoniaceae) used by Gaddi tribe in India ethnomedicinally for treating skin diseases has been found potent wound healing activity as evident from the wound contraction and increased tensile strength (14,16). It was also found that *P. appendiculatum* extract possesses potent antioxidant activity by inhibiting lipid peroxidation and increase in the super oxide dismutase (SOD) and catalase (14). Moreover, according to the records, the liverworts are used for the cure of cuts, fractures, burns, bruises, open wounds and snakebites. Especially in China, the mixture of *Marchantia polymorpha* and *Conocephalum conicum* with vegetable oils is used for bites, burns, cuts, eczema, and wounds (10).

According to the phytochemical studies on the liverworts, a wide variety of the terpenoid derivatives such as mono, sesqui- and diterpenes which are mainly accumulated in nonpolar fractions as well as aromatic and phenolic compounds have been isolated from too many liverworts collected different places of the world (11). In thin layer chromatography and qualitative analysis by using chemical reagent, these type components are detected in the ethereal extracts of the Turkish liverworts. In our previous study GC analysis was conducted on the ethereal extracts of *Reboulia hemisphaerica* and β-microbiotene (12.43%), grimaldone (8.62%), β-caryophyllene (4.91%) and cis-β-elemene (4.14%) were determined as the major components (16). In previous studies it was demonstrated that terpenic compounds possess antimicrobial, anticarcinogenic, antioxidant, anti-inflammatory, analgesic and wound healing activities (28-30). Eventually, the effect might be attributed to the mainly terpenic compounds. Moreover, it is obvious that phenolics have potent antioxidant and anti-inflammatory effects, which are the main principles in the wound healing effect (11).

CONCLUSION

The ethereal extracts of the liverwort species growing in southern part of Turkey such as *Riccia fluitans, Porella cordaeana, Porella platyphylla, Corsinia coriandrina, Mannia androgyna, Reboulia hemisphaerica, Plagiochasma rupestre, Targionia hypophylla* were evaluated comparatively for the wound-healing activity. Experimental results indicated that the ethereal extracts of *Reboulia hemisphaerica, Plagiochasma rupestre and Targionia hypophylla* has been potent wound healing capacity in this test system. The rest of the species did not show any remarkable wound healing effect. In the present study, wound-healing activity of the liverwort extracts supported the traditional use of these species. However, further studies are need to isolate the pharmacologically active compounds contributing to the wound-healing properties of the liverwort species. Moreover, wild species of the plants that have no information about their usages are also waiting to be investigated for new agents to heal the illnesses.

REFERENCES

1. Adams M, Berset C, Kessler M, Hamburger M, Medicinal herbs for the treatment of rheumatic disorders--a survey of European herbals from the 16th and 17th century, J Ethnopharmacol 121, 343-359, 2009.
2. Butler MS, The role of natural product chemistry in drug discovery, J Nat Prod 67, 2141-2153, 2004.
3. Nair HB, Sung B, Yadav VR, Kannappan R, Chaturvedi MM, Aggarwal BB, Delivery of antiinflammatory nutraceuticals by nanoparticles for the prevention and treatment of cancer, Biochem Pharmacol 80, 1833-1843, 2010.
4. Verpoorte R, Kim HK, Choi YH, In: Plants as source of medicine in medicinal and aromatic plants, Ed(s): R.J. Bogers, L.E. Craker, D. Lange, 2006.
5. Kumar B, Vijayakumar M, Govindarajan R, Pushpangadan P, Ethnopharmacological approaches to wound healing exploring medicinal plants of India, J Ethnopharmacol 114, 103-113, 2007.
6. Adetutu A, Morgan WA, Corcoran O, Ethnopharmacological survey and *in vitro* evaluation of wound-healing plants used in South-western Nigeria, J Ethnopharmacol 137, 50-56, 2011.

7. Inngjerdingen K, Nergard CS, Diallo D, Mounkoro PP, Paulsen BS, An ethonopharmacological survey of plants used for wound healing in Dogoland, Mali, West Africa, J Ethnopharmacol 92, 233-244, 2004.
8. Namsa ND, Tag H, Mandal M, Kalita P, Das AK, An ethnobotanical study of traditional anti-inflammatory plants used by the Lohit community of Arunachal Pradesh, India, J Ethnopharmacol 125, 234-245, 2009.
9. Villegas LF, Fernandez ID, Maldonado H, Torres R, Zavaleta A, Vaisberg AJ, Hammond GB, Evaluation of the wound-healing activity of selected traditional medicinal plants from Peru, J Ethnopharmacol 55, 193-200, 1997.
10. Glime JM, Bryophyte Ecology. E-book, 2006.
11. Asakawa Y, In: Progress in the Chemistry of Organic Natural Products. Ed(s): A.D. Kinghorn, H. Falk, S. Gibbons, J. Kobayashi, Springer, New York, 1995.
12. Asakawa Y, Chemosystematics of the Hepaticae, Phytochemistry 65, 623-669, 2004.
13. Asakawa Y, Potential source of medicinal plants, Curr Pharm Des 14, 3067-3088, 2008.
14. Singh M, Govindarajan R, Nath V, Rawat AK, Mehrotra S, Antimicrobial, wound healing and antioxidant activity of *Plagiochasma appendiculatum* Lehm. et Lind. J Ethnopharmacol 107, 67-72, 2006.
15. Davis PH, Flora of Turkey and the East Aegean Islands, Supplement 2. University Press, Edinburgh, 2000.
16. Tosun A, Kupeli Akkol E, Suntar I, Ozenoglu Kiremit H, Asakawa Y, Phytochemical investigations and bioactivity evaluation of liverworts as a function of anti-inflammatory and antinociceptive properties in animal models, Pharm Biol 51, 1008-1013, 2013.
17. Ehrlich HP, Hunt TK, The effect of cortisone and anabolic steroids on the tensile strength of healing wounds, Ann Surg 57, 117, 1968.
18. Lodhi S, Pawar RS, Jain AP, Singhai AK, Wound healing potential of *Tephrosia purpurea* (Linn.) Pers. in rats, J Ethnopharmacol 108, 204-210, 2006.
19. Suguna L, Singh S, Sivakumar P, Sampath P, Chandrakasan G, Influence of *Terminalia chebula* on dermal wound healing in rats, Phytother Res 16, 227-231, 2002.
20. Suntar I, Baldemir A, Coskun M, Keles H, Akkol EK, Wound healing acceleration effect of endemic *Ononis* species growing in Turkey, J Ethnopharmacol 135, 63-70, 2011.
21. Sadaf F, Saleem R, Ahmed M, Ahmad SI, Navaid ul Z, Healing potential of cream containing extract of *Sphaeranthus indicus* on dermal wounds in guinea pigs, J Ethnopharmacol 107, 161-163, 2006.
22. Tramontina VA, Machado MA, Nogueira Filho Gda R, Kim SH, Vizzioli MR, Toledo S, Effect of bismuth subgallate (local hemostatic agent) on wound healing in rats, Histological and histometric findings. Braz Dent J 13, 11-16, 2002.
23. Pattanayak SP, Sunita P, Wound healing, anti-microbial and antioxidant potential of *Dendrophthoe falcata* (L.f) Ettingsh, J Ethnopharmacol 120, 241-247, 2008.
24. Hanna JR, Giacopelli JA, A review of wound healing and wound dressing products, J Foot Ankle Surg 36, 2-14; discussion 79, 1997.
25. Karishan P, Focus on: Wound healing, chronic pain and inflammation. The scientific study of herbal wound healing therapies: Current state of play, Curr Anaesth Crit Care 17, 21-27, 2006.
26. Aravindaram K, Yang NS, Anti-inflammatory plant natural products for cancer therapy, Planta Med 76, 1103-1117, 2010.
27. Crandall-Stotler BJ, Stotler FRE, Evolutionary trends in the simple thalloid liverworts (Marchantiophyta, Jungermanniopsida subclass Metzgeriidae), Taxon 54, 299-316, 2005.
28. Adams S, Thrash TP, Methods for wound treatment and healing using limonene-based compositions. International Application Published Under the Patent Cooperation Treaty, WO2010/062933 A1, 2010.
29. Edris AE, Pharmaceutical and therapeutic potentials of essential oils and their individual volatile constituents: A review, Phytother Res 21, 308-323, 2007.
30. Takayama C, de-Faria FM, de Almeida AC, Valim-Araujo Dde A, Rehen CS, Dunder RJ, Socca EA, Manzo LP, Rozza AL, Salvador MJ, Pellizzon CH, Hiruma-Lima CA, Luiz-Ferreira A, Souza-Brito AR, Gastroprotective and ulcer healing effects of essential oil from *Hyptis spicigera* Lam. (Lamiaceae), J Ethnopharmacol 135, 147-155, 2011.

Received: 07.01.2016
Accepted: 25.02.2016

Turk J Pharm Sci 13(3), 292-299, 2016
DOI: 10.4274/tjps.2016.02

ORIGINAL ARTICLE

Development and Validation of HPLC-UV Method for the Determination of Diclofenac in Human Plasma with Application to a Pharmacokinetic Study

Diklofenak'ın İnsan Plazmasından HPLC-UV ile Tayin Yöntemi Geliştirilmesi ve Validasyonu ile Farmakokinetik Çalışmaya Uygulanması

Gülsüm Gül ARISOY[1], Emrah DURAL[1,2*], Görkem MERGEN[1,3], Mustafa ARISOY[4], Gülin GÜVENDİK[5], Tülin SÖYLEMEZOĞLU[1]

[1]Ankara University, Institute of Forensic Sciences, Department of Forensic Toxicology, Ankara, TURKEY
[2]Cumhuriyet University, Faculty of Pharmacy, Department of Pharmaceutical Toxicology, Ankara, TURKEY
[3]TechKnowledge FZ LLC
[4]Ankara University, Faculty of Pharmacy, Department of Pharmaceutical Chemistry, Ankara, TURKEY
[5]Ankara University, Faculty of Pharmacy, Department of Pharmaceutical Toxicology, Ankara, TURKEY

ABSTRACT

A simple, rapid and reliable high performance liquid chromatography method (HPLC) with ultraviolet detection (UV) was developed and validated according to ICH guidelines, for quantitative analysis and therapeutic drug monitoring of diclofenac sodium (DS) in human plasma. Plasma samples (0.7 mL) were acid hydrolysis by 100 µL, 1 M hydrochloric acid. Analytes were concentrated from plasma by liquid–liquid extraction with 2 mL ethyl acetate by repeated twice, which allows to obtain good extraction yields (98.75%-99.32%). The separation was achieved by employing C18 analytical column (3.5 µm particle size, 150 mmx3.9 mm I.D.) under isocratic conditions using acetonitrile and NaH_2PO_4 mixture (42.5:57.5, v/v) as mobile phase (pH: 3.16) flow rate of 1.5 mL/min. Naproxen (3 µg/mL) was used as an internal standard (IS). The DS and IS were detected at 281 nm and eluted at 2.6 and 6.2 min, respectively. Total run time was 7 min. Method showed linearity with very good determination coefficients (r^2=0.999), over the concentration range of 50 - 1600 ng/mL. Limits of detection (LOD) and quantification (LOQ) were 8.95 ng/mL and 27.12 ng/mL, respectively. Intra-day precision and accuracy were between 0.93-5.27; 1.74-9.81, respectively. Inter-day precision and accuracy were between 2.71-6.64; 2.03-9.16, respectively. This method was successfully applied for determination of DS plasma concentrations during a pharmacokinetic study in healthy volunteers (n=12) after an oral administration of Voltaren® 75 mg/tablet and remarkable variations in DS levels were observed. In our study, on the contrary to equivalent doses of DS, the observed significant differences in plasma levels of DS, on 2nd, 4th and 6th hours, can be explained by pharmacokinetic differences, that arise from mainly polymorphisms of CYP2C9 and CYP3A4, which are major enzymes responsible for DS metabolism.

Key words: Diclofenac sodium, Validation, Plasma, High performance liquid chromatography, Ultraviolet detection

ÖZ

Diklofenak sodyumun (DS) insan plazmasında kantitatif analizleri ve terapötik ilaç izlemi için, basit, hızlı ve güvenilir bir ultraviyole dedektörlü yüksek performanslı sıvı kromatografisi (YPSK-UV) metodu geliştirildi ve ICH kurallarına göre valide edildi. Plazma örnekleri (0.7 mL) 100 µL, 1 M hidroklorik asitle hidroliz edildi. Analitler plazmadan iyi ekstraksiyon verimi (%98.75-%99.32) sağlayan sıvı-sıvı ekstraksiyonu metodu ile 2 mL etil asetatla iki tekrar ile elde edildi. Ayrım izokratik şartlar altında C18 analitik kolon (3.5 µm partikül büyüklüğü, 150 mmx3.9 mm I.D.), mobil faz asetonitril ve NaH2PO4 (42.5:57.5, v/v) karışımı (pH 3.16), akış hızı 1.5 mL/dk ile gerçekleştirildi. Naproksen (3 µg/mL) iç standart (İS) olarak kullanıldı. DS ve İS 281 nm'de ve sırasıyla 2.6 ve 6.2 dakikalarda tespit edildi. Toplam analiz süresi 7 dakika idi. Metot 50 - 1600 ng/mL konsantrasyon aralığında çok iyi bir belirlenme katsayısı ile (r^2=0.999) doğrusallık gösterdi. Gözlenebilme sınırı ve tayin sınırı sırasıyla 8.95 ng/mL ve 27.12 ng/mL idi. Gün içi kesinlik ve doğruluk sırasıyla 0.93-5.27; 1.74-9.81 aralığında idi. Günler arası kesinlik ve doğruluk ise sırasıyla 2.71-6.64; 2.03-9.16 aralığında idi. Bu metot sağlıklı gönüllülerin (n=12) tek doz oral Voltaren® 75 mg/tablet alımı ile farmakokinetik çalışma süresince DS plazma konsantrasyonlarının belirlenmesi için başarıyla uygulandı ve DS düzeylerinde dikkate değer varyasyonlar gözlendi. Çalışmamızda DS'nin eşit dozlarına karşın, 2., 4. ve 6. saatlerdeki plazma düzeylerinde gözlenen anlamlı farklılıklar, özellikle DS metabolizmasından sorumlu majör enzimler olan CYP2C9 ve CYP3A4 polimorfizmlerinden kaynaklanabilecek farmakokinetik farklılıklarla açıklanabilir.

Anahtar kelimeler: Diklofenak sodyum, Validasyon, Plazma, Yüksek performanslı sıvı kromatografisi, Ultraviyole deteksiyon

*Correspondence: E-mail: emrahdural@cumhuriyet.edu.tr Phone: +90 346 219 10 10-3920

INTRODUCTION

Diclofenac sodium (DS), 2-*[(2,6-dichlorophenyl)amino]phenyl-acetic acid,* (Figure 1a) is non-steroidal anti-inflammatory analgesic (NSAID) with potent cyclooxygenase (COX) inhibition activity (1,2). DS has a well documented safety profile, which is comparable to those of other NSAIDs. It inhibits prostaglandin synthesis by inhibition of enzymatic transformation of arachidonic acid into prostaglandins (3,4). This drug is widely used in clinical medicine for the pain control and treatment of rheumatoid arthritis, osteoarthritis, ankylosing spondylitis also acute injury (1). In addition to, it is used to treat chronic pain associated with cancer (2,5). DS has anti-uricosuric feature. The development of Alzheimer disease may be prevent if use of DS which low-dose in long-term (5).

DS is well-absorbed after oral administration with expensive hepatic metabolism. It is extensively (>99.7%) protein bound (albumin) in plasma and serum at therapeutic concentrations. Terminal half life is 1-2 hours. Food can cause a delay in the onset of absorption and a reduction in plasma levels of approximately 30%. After absorption, approximately half of the absorbed dose is metabolized immediately by the liver, due to first pass metabolism. 35% of absorbed DS enters enterohepatic circulation. The distribution volume (V_d) of DS is 1.4 L/Kg. C_{max} is reached at approximately 4 hours. T_{max} is approximately 0.5-1 h. Elimination is rapid with 90% of the drug clearance taking between 3 to 4 hours. The DS metabolism products, which are mainly 4'- hydroxy (OH) diclofenac and minor monohydroxy metabolites are 3'-OH diclofenac and 5'-OH diclofenac, are excreted by the urine (65%) and biliary (35%) (2,5-7).

The use of DS has been associated with occasional hepatic toxicity (8,9). Although the etiology of this toxicity is not known, clinical evidence suggests that it may be due to an immune (10,11) or a non-immune mechanism (9,12,13). In both cases, covalent modification of liver proteins may play an important role in the etiology of DS hepatotoxicity (14). The fact that, CYP2C9 was known to have a major role in the oxidative metabolism of DS (15,16). It seemed possible that CYP2C9 might metabolically activate DS into a reactive metabolite(s), which may have a role in DS hepatitis in humans. Naproxen which was used as an internal standart in our study, is a proprionic acid derivate related to the arylacetic acid group of nonsteroidal anti-inflammatory drugs. Naproxen is chemically, *(S)-6-methoxy-α-methyl-2-naphthaleneacetic acid* (Figure 1b) is commonly used for the reduction of moderate

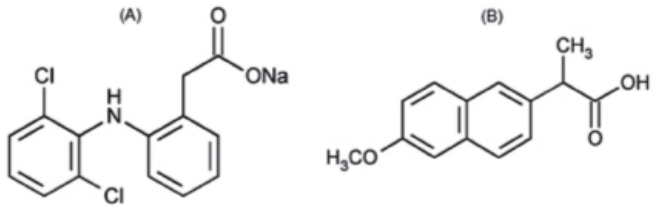

Figure 1. The chemical structure of diclofenac sodium (A) and naproxen (B)

to severe pain, fever, inflammation, and stiffness. It works by inhibiting both the COX-1 and COX-2 enzymes. It is antipyretic and analgesic effects were related to inhibition of both the COX-1 and COX-2 (17).

Bioavailability, bioequivalence and therapeutic drug monitoring studies have received major attention from the pharmaceutical industry, health authorities and clinic. These studies are performed to evaluate the safety and efficacy of a genetic structure. Which studies as well as drug product development studies require rapid, simple, sensitive and reliable bioanalytical methods to monitoring the target drug in human plasma sample. Also for clinical studies, it is essential to establish accurate, sensitive and selective analytical techniques that permit detection and quantitative measurement of drug entities in biological and pharmaceutical samples (1). Several methods have been reported for determination of DS including spectrophotometric (18,19), spectrofluorimetric (20,21), polarographic (22), conductometric (23), high-performance liquid chromatography (HPLC) (1,24-29), gas chromatography mass spectrometry (GC-MS) (30,31) and capillary electrophoresis (32) in human plasma and other biological fluids. Some of these methods are not suitable for routine analysis because they need sophisticated instruments, not yet available in many routine control laboratories. Since, HPLC-UV assays are reliable, inexpensive and widely utilized; it has appeared to fit best for performing simultaneous separation, quantification and clinical monitoring of DS as a primary concern of this paper.

Compared with other studies the advantages of present method are short run time (total run time 7 min) (26,28), using low biological sample volume (0.7 mL plasma) (26,27), high sensitivity (LOD 8,95 µg/mL) with small volume samples (1,2), include simple, efficient and inexpensive extraction procedure, high recovery value (98.75-99.32%) (26-28) and using inexpensive chemicals in analytical processes (27). Also this method is used to determine the DS in human plasma samples obtained from twelve healthy volunteers. The originality of this DS pharmacokinetic study is being the only research has ever been done with the contribution of the largest volunteers in Turkey. In addition to this, the method is efficient in analyzing large numbers of plasma obtained for pharmacokinetic study after therapeutic dose of diclophenac. In the present study, our objective is to develop and validate a reliable, simple, fast, and inexpensive HPLC method using UV detection for determination of DS in human plasma with the lower volume sample preparation according to ICH guidelines (33,34) and also to emphasize interpersonal differences in metabolization of DS for correct dosage of by simultaneously monitoring its levels in plasma. The developed method is validated by using linearity, precision, accuracy and sensitivity parameters according to ICH guidelines. For this purpose a group of volunteers, who are the employees of Gülhane Military Medical Academy, were contributed and DS levels in the plasma samples from volunteers were investigated.

EXPERIMENTAL

Chemicals and reagents

Ethyl acetate (EtOAc), acetonitrile (ACN), sodium dihydrogen phosphate dehydrate (NaH_2PO_4), hydrochloric acid (HCl), ortophosphoric acid (H_3PO_4) and methanol (MeOH) were purchased from Merck (Darmstadt, Germany). The standards of pharmaceuticals, diclofenac sodium (DS) and naproxen, which is internal standard (IS), were obtained from Sigma-Aldrich (St. Louis, MO, USA). Ultrapure water, which is prepared daily fresh, was used. Prescribed DS tablets, for volunteers, were obtained from pharmaceutical firm Novartis Medical Company (Istanbul, Turkey). All chemicals used in this study were of analytical-grade in the highest purity available, except MeOH and ACN that were HPLC grade.

Instrumentation and optimized chromatographic conditions

The separation and quantification were performed by HP Agilent 1100 (Santa Clara, CA, USA) high-performance liquid chromatography (HPLC) system, equipped with a UV detector.

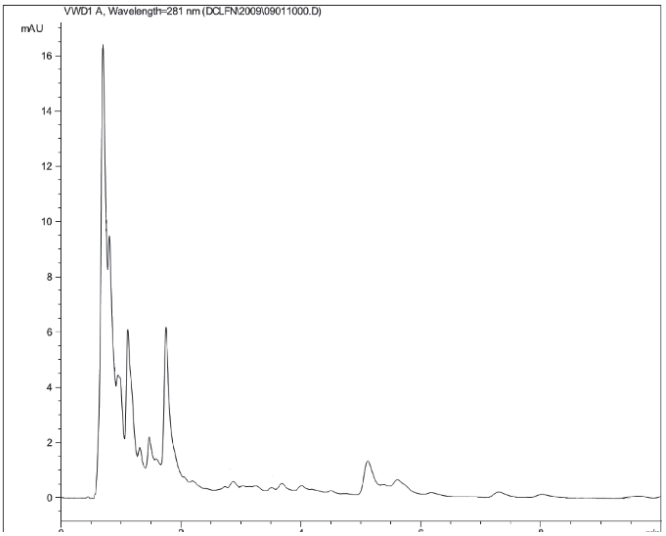

Figure 2. HPLC chromatogram of the blank human plasma

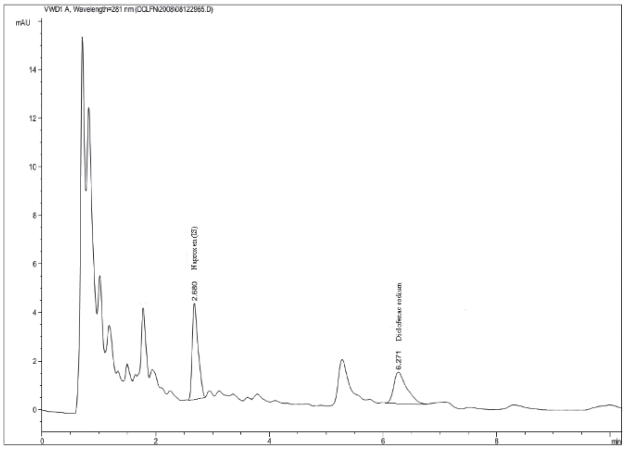

Figure 3. The HPLC chromatogram of DS (and internal standard) in human plasma spiked with 0.8 µg/mL DS (t_R=2.680) and 3 µg/mL naproxen (t_R=6.271) as an internal standard

Optimum analytic conditions were set after an optimization procedure was performed for column selection, content of mobile phase (MP) and wavelength. Prior to optimization, a standard assay for DS determination offered by the manufacturer was used and each parameter was adjusted while others were fixed.

The system consisted of isocratic pump, manual injector with a loop volume of 20 µL, and a Waters C18 column (3.5 µm, 150x4.6 mm I.D.) The wavelength at 281 nm was chosen for UV detection. The mobile phase, which consists of acetonitrile and Na_2HPO_4 buffer (42.5:57.5, v/v) adjusted to pH 3.16 by 0.1 M orthophosphoric acid. It was filtered through a 0.45 µm membrane (Alltech, IL, USA) and degassed in ultrasonic bath for 30 min. An isocratic solution was performed at a flow rate of 1.5 mL/min and at room temperature. Peak areas were measured and calculations were carried out considering the internal standard (IS) peak ratios.

Preparation of stock and working standard solutions

Stock solutions of DS and naproxen (IS) were prepared in methanol solution at the concentrations of 200 µg/mL and 30 µg/mL respectively. Working standards of DS, used for spiked plasma samples, were prepared weekly in the concentrations of 0.5, 1, 2, 4, 8 and 16 µg/mL and made by dilution of the stock solutions with methanol. Blank human blood samples, which were obtained from *Ankara University Serpil Akdağ Blood Center*, centrifuged at 3000 g for 5 min to separate the plasma. Human plasma samples and all working solutions were stored at -20°C until the analysis were carried out. These were checked chromatographically for purity before experiments and utilized (Figure 2) as quality control specimens for validation and optimization process. Their stability was checked before and after the injections of every sample set.

Preparation of sample

Blank plasma samples (0.7 mL) were placed into clean glass tubes which is containing 1 mL HCl (1 M). After that each of these tubes, 100 µL IS (30 µg/mL) and 100 µL of diclofenac sodium solutions, which were the concentrations of 0.5, 1, 2, 4, 8 and 16 µg/mL, were spiked. Reaching the total volume to 1.1 mL and achieving 10 times diluted mixtures; yielding analyte concentrations as calibration samples namely 50, 100, 200, 400, 800, 1600 ng/mL diclofenac sodium and 3000 ng/mL naproxen. Different from the calibration solutions, 100 µL MeOH was added instead of DS solution for the samples from patient's plasma.

Extraction procedure

Liquid-liquid extraction was applied for human plasma samples with acidic hydrolysis (35,36). A volume of 0.1 mL of 1 M hydrochloric acid was added to the samples and mixed at 900 g for 30 second. A volume of 2 mL of ethyl acetate was added to sample tubes and mixed at 900 g for 2 min and then centrifuged at 3000 g for 5 min. This extraction procedure

was repeated twice. Supernatant was collected to another sample tube and dried under nitrogen at 40 ˚C. Residue was dissolved in 50 µL volume of mobile phase, in order to be ready for injection, and then loaded into HPLC, by 20 µL which is loop volume.

Volunteers

Volunteers, who were consist of 12 healthy Gülhane Military Medical Academy employees, participated in this study. The average age of participants was 32±8.12. After ingestion of tablets, which including 75 mg DS, bloodletting was performed at 2nd, 4th and 6th hours. The plasma samples were collected severally and samples were stored at -20˚C. This study was approved by *Local Ethical Committee of Gülhane Military Medical Academy* in 12/11/2008 and decision number is 90.

RESULTS AND DISCUSSION

Selection of internal standard

Naproxen, which was developed in the 1970s, is a non-selective COX inhibitor is a nonsteroidal anti-inflammatory drug (NSAID) of the propionic acid class and is commonly used for relief of a wide variety of pain, fever, swelling and stiffness (17). Naproxen was chosen as internal standard due to its similar physico-chemical properties with diclofenac sodium (DS). On the other hand, the chromatographic pre-study have demonstrated that, naproxen might used as a reliable internal standard (Figure 1-3).

Validation of method

The analytical method was validated to demonstrate the selectivity, specificity, linearity, recovery, limit of

Table 1. Recovery of DS in human plasma (n=3)

Theoretical concentration ng/mL		Mean areas of diclofenac sodium (DS) and internal standard (IS)						
		First group extraction			Second group extraction			
		DS added before extraction	IS added before extraction	Areas (DS/IS)	DS added after extraction	IS added before extraction	Areas (DS/IS)	Mean Recovery (%)
200	1	4.59	33.78		4.87	33.34	0.146	
	2	4.64	30.40		4.99	33.35	0.150	
	3	4.83	31.92		4.72	32.29	0.146	
	Mean	4.69	32.03	0.146	4.86	32.99	0.147	99.32
400	1	10.3	31.7		10.99	33.33	0.330	
	2	10.02	33.47		10.01	32.35	0.309	
	3	10.72	33.25		10.65	33.65	0.317	
	Mean	10.35	32.81	0.315	10.55	33.11	0.319	98.75
800	1	21.12	31.92		20.4	32.28	0.632	
	2	20.11	31.53		21.78	32.23	0.676	
	3	20.58	32.36		20.62	32.11	0.642	
	Mean	20.60	31.94	0.645	20.93	32.21	0.650	99.23

DS: Diclofenac sodium, IS: Internal standard

Table 2. Precision and accuracy of the assay for DS (n=5)

Theoretical Conc. ng/mL	Intra-day				Inter-day			
	DS/IS				DS/IS			
	Estimated DS Conc.	SD	RSD%	RE%	Estimated Conc.	SD	RSD%	RE%
50	54.91	2.20	4.01	9.81	54.58	1.82	3.33	9.16
100	97.29	0.91	0.93	2.71	93.86	6.13	6.53	6.14
200	184.66	6.90	3.74	7.67	182.18	5.10	2.80	8.91
400	429.06	13.02	3.035	7.27	430.96	28.60	6.64	7.74
800	755.60	21.68	2.87	5.55	775.96	21.59	2.78	3.01
1600	1572.20	82.90	5.27	1.74	1567.60	42.44	2.71	2.03

DS: Diclofenac sodium, IS: Internal standard, SD: Standard deviation, RSD%: Percent relative standard deviation, RE%: Percent relative error

detection (LOD) and limit of quantification (LOQ). Intra- and inter-day validation protocol was applied considering reproducibility of method and instrument to obtain accurate and precise measurements in agreement with Conference on Harmonization Guidelines (33,34).

Recovery

The recovery of extraction procedures from human plasma is determined by comparing areas of DS and IS. DS and the IS first joined together in the plasma samples before extraction was performed three different extractions (200, 400, 800 ng/mL diclofenac sodium and 3000 ng/mL naproxen). Also DS and the IS joined together in the plasma samples after extraction in three different plasma samples. The areas of DS and IS are calculated and compared then % efficiency is obtained. Three individual replicates of spiked samples at mid-concentrations (200, 400, 800 ng/mL DS) were prepared with internal standard (n=3). The extraction procedure was conducted as described previously. Peak area ratios were compared and recoveries were calculated as 98.75%-99.32% for plasma (Table 1).

Precision

Precision, defined as relative standard deviation (RSD%), was determined by five individual replicates at six different concentrations (50, 100, 200, 400, 800 and 1600 ng/mL) (n=5). Interday and intraday precisions of method and the instrument were calculated. Results were showed that, RSD% were less than 6.7% both for intra- and interday precisions (Table 2). Analytical instrument precision was also displayed higher precisions namely less than 6.3% considering intra- and interday performances (Table 3).

Accuracy

Accuracy defines as the measure of how close the experimental value is to the true value. Accuracy is the degree of veracity while precision is the degree of reproducibility and accuracy expressed as the relative error (RE%) of the estimated concentrations. Table 2 shows RE% of estimated concentrations for intra- and interday accuracy of assays. The instrument was as accurate as assay which is displayed in Table 3. The accurate and precise measurements pointed at good reproducibility for the method and the instrument.

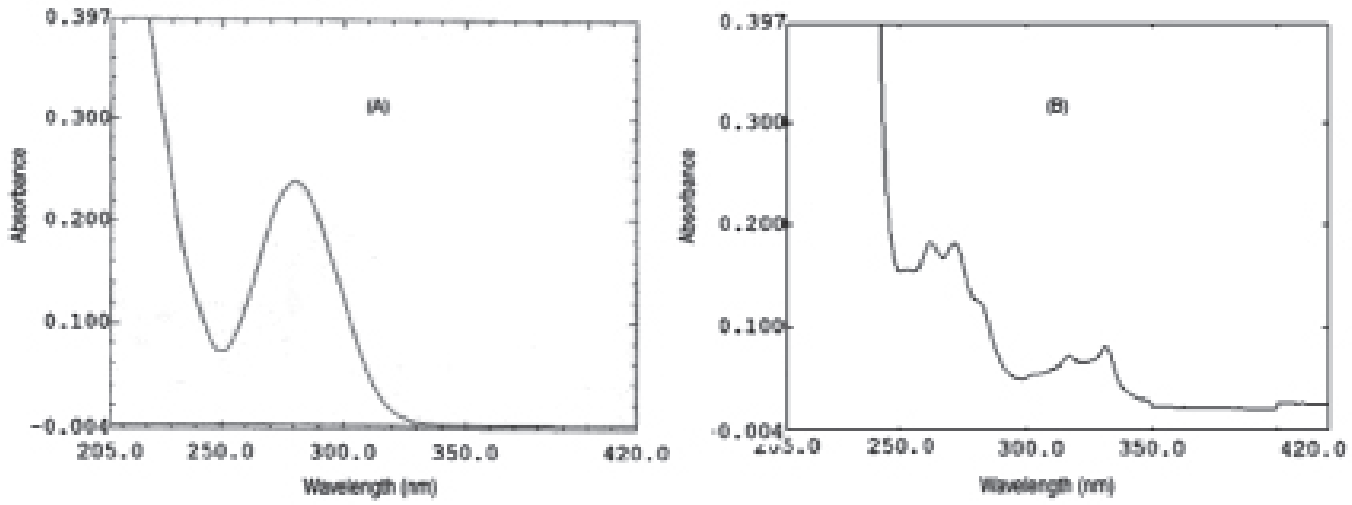

Figure 4. The obtained UV spectrums and maximum absorption wavelengths of DS (A) and Naproxen (B)

Table 3. Precision and accuracy of analytical instrument, HPLC – UV, for determination of DS (n=5)

Theoretical Conc. ng/mL	Intra-day DS/IS				Inter-day DS/IS			
	Estimated Conc.	SD	RSD%	RE%	Estimated Conc.	SD	RSD%	RE%
50	60.16	1.12	1.86	20.32	55.65	2.71	4.87	11.30
100	112.55	5.68	5.05	12.55	95.17	4.81	5.06	4.83
200	223.23	11.16	5.00	11.61	184.99	11.52	6.23	7.51
400	443.71	12.066	2.72	10.93	418.57	14.90	3.56	4.64
800	915.36	15.39	1.68	14.42	756.65	11.27	1.49	5.42
1600	1829.62	78.19	4.27	14.35	1577.49	40.15	2.55	1.41

DS: Diclofenac sodium, IS: Internal standard, SD: Standard deviation, RSD%: Percent relative standard deviation, RE%: Percent relative error

Specificity and selectivity

Method for plasma demonstrated excellent chromatographic specificity with no endogenous interference at the retention times of the IS and DS (2.6 and 6.2 min, respectively). Representative chromatograms for human plasma spiked with DS (800 ng/mL) and the IS (3000 ng/mL) are shown in Figure 2 and Figure 3. The most appropriate wavelength at 281 nm was chosen for UV detection of DS and IS (Figure 4).

Limit of detection and quantification

Limit of detection (LOD) and limit of quantification (LOQ) were determined based on the standard deviation of the response and the slope of the calibration curve, according to ICH guidelines (LOD= 3.3 σ/S, LOQ= 10 σ/S where σ is the standard deviation of the response and S is the slope of the calibration curve) (33,34). LOD and LOQ values were calculated from plasma samples and found as 8.95 ng/mL and 27.12 ng/mL respectively.

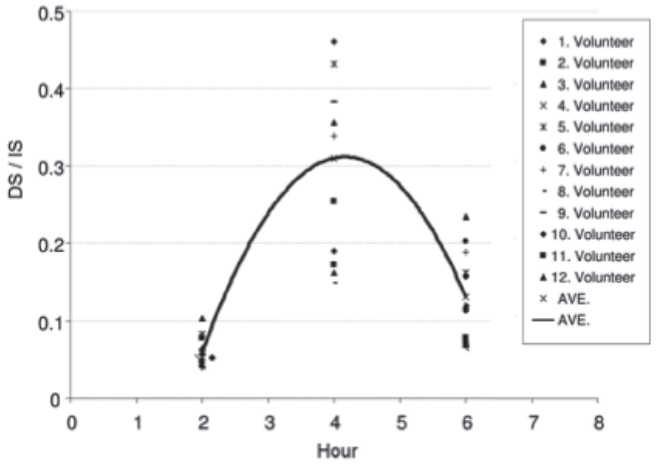

Figure 5. DS levels in plasma of volunteers after administration of Voltaren® SR 75 mg single oral dose

Table 4. Diclofenac sodium levels in 2nd, 4th and 6th times of volunteers plasma (ng/mL)

Number of volunteers	2nd hour	4th hour	6th hour
1	82.28	248.82	153.40
2	70.95	329.18	104.95
3	92.27	213.86	160.60
4	86.10	398.09	92.49
5	114.78	550.89	214.11
6	63.22	658.37	264.44
7	61.74	435.47	246.66
8	60.67	196.24	161.02
9	80.14	490.15	92.74
10	73.99	586.69	208.64
11	109.60	227.44	109.07
12	139.68	456.46	295.23
Mean	86.29	399.31	175.28

Linearity

After establishing the chromatographic conditions, separate calibration curves were prepared for plasma over a DS concentration range of 50-1600 ng/mL. For each concentration 5 individual replicates were injected and linearity was obtained for both methods with the determination coefficients (r^2) over 0.999.

CONCLUSIONS

In this study, simultaneous procedure of HPLC-UV method was proposed with simple extraction of sample yielding good recovery, selective chromatographic separation, and sensitive UV detection with enhanced sensitivity and accuracy of determination for analysis of DS. Therefore, to achieve quality separation of analyte in a reasonable analysis time, acceptable chromatographic factors were adjusted. The mobile phase composition and the pH were optimized. The mobile phase was a phosphate buffer adjusted to acidic pH and containing ACN as the organic modifier. Baseline separation of the analyte (and the IS) was achieved in less than 7 min. The method was validated in terms of linearity, accuracy, precision, reproducibility, quantification and detection limits in accordance with internationally accepted guidelines which are ICH. Analysis for all analytes demonstrates very precise and accurate results, even for inter-day assays which allow determining therapeutic and toxic concentration levels.

The study results showed that, established HPLC-UV method is applicable for the therapeutic drug monitoring bioavailability, bioequivalence study and applicable as a reference method in routine monitoring for toxicological and/or analytic purposes in research laboratories.

Diclofenac sodium levels of volunteers

Although considerable individual differences were observed, representative curves plotted by drug levels of each volunteer were similar. Variations in the DS levels detected in the volunteers were graphed and tabled (Table 4, Figure 5). After ingestion of DS, reaches the maximum level in plasma, at 4th hour. Even though, each volunteer was medicated with equivalent single oral dose, DS levels in plasma were quite dissimilar. Variations may arise from because of enzyme differences which are CYP2C9 and CYP3A4, mainly enzymes responsible for DS metabolism. In this respect, for an application of an effective dosage, the enzyme polymorphism should be taken under consideration in medical therapies.

According to monitored drug levels, differences in concentration rates of DS in human plasma can be expressed and the variation of plasma concentration can be based on hepatic enzyme polymorphism. DS is metabolized mainly by CYP2C9 and CYP3A4. The resulting data may also be considered as a pre-research for pharmacogenetic

polymorphismin this group of volunteers. The analytes were then quantified using HPLC technique, which provided good sensitivity and selectivity. The method has been shown to provide good reproducible recoveries and low limits of detection that allow the accurate quantification of the DS in plasma samples. As the DS level increases in biological material, the expected medical effects also increase. Since, the optimum drug use and maximum resultant effect is the main objective, this report offers clinical application of proposed method for monitorizations of DS in human plasma.

ACKNOWLEDGEMENTS

Authors would like to thank to Ankara University Institute of Forensic Science all personnel for the excellent and open collaboration.

REFERENCES

1. Emara LH, Taha NF, El-Ashmawy AA, Raslan HM, Mursi NM. A rapid and sensitive bioanalytical hplc method for determining diclofenac sodium in human plasma for bioequivalence studies. J Liq Chromatogr Related Technol 35, 2203-2216, 2012.
2. Davies NM, Anderson KE. Clinical pharmacokinetics of diclofenac. Clin Pharmacokinet 3, 184-213, 1997.
3. Menasse R, Hedwall PR, Kraetz J, Pesicinand C, Riesterer L. Pharmacological properties of diclofenac sodium and its metabolites. J Rheumatol Suppl 22, 5-16, 1978.
4. Maier R, Menasse R, Riesterer L, Pericinand C, Ruegg M. The pharmacology of diclofenac sodium (Voltarol). Rheumatol Rehab Suppl 2, 11-21, 1979.
5. Hassan SS, Yunus SH, Latif A. Study and improvement of methods for the determination of diclofenac sodium in pharmaceutical preparations. Pak J Pharm Sci 20-23, 7-10, 2010.
6. Metabolism of Drugs and Other Xenobiotics. P. Anzenbacher and U.M. Zanger. pp. 408, Wiley-VCH, Weinheim, 2012.
7. Dorado P, Berecz R, Caceres MC, LLerena A. Analysis of diclofenac and its metabolites by high-performance liquid chromatography: relevance of CYP2C9 genotypes in diclofenac urinary metabolic ratios. J Chromatogr B 789, 437–442, 2003.
8. Ouellette GS, Slitzky BE, Gates JA, Lagardeand S, West AB. Reversible hepatitis associated with diclofenac. J Clin Gastroenterol 13, 205-210, 1991.
9. Banks AT, Zimmerman HJ, Ishakand KG, Harter JG. Diclofenac-associated hepatotoxicity: Analysis of 180 cases reported to the food and drug administration as adverse reactions. Hepatol 22, 820-827, 1995.
10. Breen EG, McNicholl J, Cosgrove E, McCabeand J, Stevens FM. Fatal hepatitis associated with diclofenac. Gut 27, 1390-1393, 1986.
11. Schapira D, Bassan L, Nahirand AM, Scharf Y. Diclofenac-induced hepatotoxicity. Postgrad Med J 62, 63-65, 1986.
12. Dunk AA, Walt RP, Jenkinsand WJ, Sherlock SS. Diclofenac hepatisis. Br Med J (Clin Res Ed) 284, 1605-1606, 1982.
13. Iveson TJ, Ryley NG, Kelly PM, Trowell JM, McGeeand JO, Chapman RW. Diclofenac associated hepatitis. J Hepatol 10, 85-89, 1990.
14. Boelsterli UA, Zimmerman HJ, Kretz-Rommel A. Idiosyncratic liver toxicity of nonsteroidal antiinflammatory drugs: Molecular mechanisms and pathology. Crit Rev Toxicol 25, 207-235, 1995.
15. Yamazaki H, Inoue K, Chiba K, Ozawa N, Kawai T, Suzuki Y, Goldstein JA, Guengerichand FP, Shimada T. Comparative studies on the catalytic roles of cytochrome P450 2C9 and its cys- and leu-variants in the oxidation of warfarin, flurbiprofen, and diclofenac by human liver microsomes. Biochem Pharmacol 56, 243-251, 1998.
16. Omura T, Sato R. The Carbon monoxide-binding pigment of liver microsomes. J Biol Chem 239, 2379-2385, 1964.
17. Davies NM, Anderson KE. Clinical Pharmacokinetics of Naproxen. Drug Disposition. 32, 268-293,1997
18. Micalizzi YC, Pappano NB, Debattista NB. First and second order derivative spectrophotometric determination of benzyl alcohol and diclofenac in pharmaceutical forms. Talanta 47, 525-530, 1998.
19. Kustrin A, Zivanovic L, Zecevic M, Radulovic D. Spectrophotometric study of diclofenac-Fe(III) complex. J Pharm Biomed 16, 147-153, 1997.
20. Kubo H, Umiguchi Y, Kinoshita T. Fluorometric determination of methotrexate in serum by high performance liquid chromatography using in-line oxidation with hydrogen peroxide. J Liq Chromatogr 16, 465-474, 1993.
21. Carreira L.A, Rizk M, El-Shabrawy M, Zakhari NA, Toubar S. Europium (III) ion probe spectrofluorometric determination of diclofenac sodium. J Pharm Biomed 13, 1331-1337, 1995.
22. Ali A.M.M. Cathodic adsorptive stripping voltammetric determination of the anti-inflammatory drug indomethacin. J Pharm Biomed Anal 18, 1005-1012, 1999.
23. Aly F, Belal F. Conductimetric determination of some nonsteroidal anti-inflammatory drugs in dosage forms. Pharmazie 49, 454-455, 1994.
24. Martin MJ, Pablos F, Gonzalez AG. Simultaneous determination of caffeine and non-steroidal anti-inflammatory drugs in pharmaceutical formulations and blood plasma by reversed-phase HPLC from linear gradient elution. Talanta 49, 453-459, 1999.
25. Haque A, Stewart JT. Direct injection HPLC analysis of some non-steroidal antiinfammatory drugs on restricted access media columns. Chromatogr 13, 51-56, 1999.
26. Yilmaz B, Asci A, Palabiyik SS. HPLC method for determination of diclofenac in human plasma and its application to a pharmacokinetic study in Turkey. J Chromatogr Sci. 49, 422-427, 2011.
27. Arcelloni C, Lanzi R, Pedercini S, Molteni G, Fermo I, Pontiroli A, Paroni R. High-performance liquid chromatographic determination of diclofenac in human plasma after solid-phase extraction. J Chromatogr B, 763, 195-200, 2001
28. Lee HS, Jeong CK, Choi SJ, Kim SB, Lee MH, Ko GI, Sohn DH. Simultaneous determination of aceclofenac and diclofenac in human plasma by narrowbore HPLC using column-switching. J Pharm Biomed Anal, 23, 775–781, 2000.
29. Chawla JL, Sodhi RA, Sane RT. Simultaneous determination of chlorzoxazone, paracetamol and diclofenac sodium by different chromatographic techniques. Indian Drugs 33, 171-178, 1996.
30. Leis HJ, Auler GF, Gleispach H, Windischofer W. Preparation of deuterated diclofenac for use as an internal standard in quantitative measurement by gas chromatography negative-ion chemical ionization mass spectrometry. Rapid Commun Mass Spectrom 10, 1605–1606, 1996.
31. Borenstein MR, Xue Y, Cooper S, Tzeng TB. Sensitive capillary gas chromatographic-mass spectrometric-selected-ion monitoring

method for the determination of diclofenac concentrations in human plasma. J Chromatogr B Biomed Appl 11, 59-66, 1996.

32. Donato MG, Baeyens W, Van-den-Bossche W, Sandra P. The determination of non-steroidal antiinflammatory drugs in pharmaceuticals by capillary zone electrophoresis and micellar electrokinetic capillary chromatography. J Pharm Biomed 12, 21-26, 1994.
33. International Conference on Harmonization (ICH). Guidance for Industry Q2B Validation of analytical procedures: Methodology. November 1996.
34. International Conference on Harmonization (ICH). International Conference on Harmonization of Technical Requirements for Registration of Pharmaceuticals for Human Use. ICH Harmonised Tripartite Guideline. Validation of Analytical Procedures: Text And Methodology Q2(R1). November 2005.
35. Lala LG, D'Mello PM, Naile SR. J. HPTLC determination of diclofenac sodium from serum. Pharmaceut Biomed 29, 539-544, 2002.
36. Choi MH, Choi YK. Rapid and sensitive analysis of diclofenac in human plasma by GC/SIM/MS. Anal Lett 32, 2245-2253, 1999.

Received : 07.01.2016

Accepted : 28.04.2016

Turk J Pharm Sci 13(3), 300-303, 2016
DOI: 10.4274/tjps.2016.03

ORIGINAL ARTICLE

Composition of the Essential Oils of *Juniperus oxycedrus L.* subsp. *oxycedrus* Growing in Turkey

Türkiye'de Yetişen *Juniperus oxycedrus* L. subsp. *oxycedrus*'un Uçucu Yağ Bileşikleri

Sevim ALAN[1*], Mine KÜRKÇÜOĞLU[2], Görkem ŞENER[1,2]

[1]Anadolu University, Faculty of Pharmacy, Pharmaceutical Botany, 26470 Eskişehir, TURKEY
[2]Anadolu University, Faculty of Pharmacy, Department of Pharmacognosy, 26470 Eskişehir, TURKEY

ABSTRACT

In this study, the chemical compositions of the leaves, berries and twigs essential oils of *J. oxycedrus* L. subsp. *oxycedrus*, collected in Turkey, were determined. The oils were analyzed by GC and GC-MS. 15-21 volatile compounds were identified of the leaves, berries and twigs essential oils representing 82.4-98.0% of the total oils. The essential oils were obtained from leaves, berries and twigs by yielding 0.02%, 2.12% and 0.01%, resp. The major compounds were determined manoyl oxide (32.8%) and caryophyllene oxide (11.9%) in leaf oil, myrcene (44.6%), α-pinene (19.9%) and germacrene D (15.5%) in berry oil, manoyl oxide (35.4%) and caryophyllene oxide (16.8%) in twig oil.

Key words: *Juniperus oxycedrus*, GC and GC/MS, Essential oil

ÖZ

Bu çalışmada, Türkiye'den toplanan *J. oxycedrus* subsp. *oxycedrus* türünün yaprak, meyve ve ince dallarından elde edilen uçucu yağlarının kimyasal içerikleri belirlenmiştir. Uçucu yağlar GC ve GC/MS cihazları aracılığıyla analiz edilip, toplam yağın %82.4-98.0 içeriği 15-21 arasında değişen uçucu bileşen ile yaprak, meyve ve ince dal üzerinde tespit edilmiştir. Uçucu yağlar yaprak, meyve ve ince daldan sırasıyla %0.02, %2.12 ve %0.01 verimleri ile elde edilmiştir. Ana bileşenler yaprak yağında %32.8 manoil oksit ve %11.9 karyofillen oksit, meyve yağında %44.6 mirsen, %19.9 α-pinen ve %15.5 germakren D, ince dal yağında %35.4 manoil oksit ve %16.8 karyofillen oksit belirlenmiştir.

Anahtar kelimeler: *Juniperus oxycedrus*, GC and GC/MS, Uçucu Yağ

INTRODUCTION

The genus *Juniperus* L. belongs to the Cupressaceae family, representing about 70 species all over the world, and widely distributed throughout the forests of the temperate and cold regions of the northern Hemisphere, from the far north to the Mediterranean. *Juniperus* L. is represented in Turkey by 7 species and 14 taxa. *Juniperus oxycedrus* has two subspecies – subsp. *oxycedrus* and subsp. *macrocarpa* – in Turkey (1,2).

Several studies have reported the chemical composition of leaves, berries and twigs and their the essential oils (EOs) of *J. oxycedrus* L. subsp. *oxycedrus* (Table 1) (3-16).

In the present work, leaves, berries and twigs EOs of *J. oxycedrus* subsp. *oxycedrus* were investigated to chemical compositions of plants collected from Eskişehir: Hekimdağ in Turkey. In the study, the oils were obtained by hydrodistillation. The oils were analyzed by gas chromatography (GC) and gas chromatography/ mass spectrometry (GC/MS).

EXPERIMENTAL

Plant material

J. oxycedrus subsp. *oxycedrus* was collected from Eskişehir: Hekimdağ, in Turkey on 15 March 2015. Voucher specimens are kept at the Herbarium of Pharmacy Faculty, Anadolu University, Turkey (ESSE 14987).

Isolation of essential oils

The oils were obtained by hydrodistillation for 3 hours using Clevenger apparatus. The essential oils were stored at 4°C in the dark until analyzed. The oils were analyzed by capillary GC and GC/MS using a Agillent GC-MSD system.

*Correspondence: E-mail: salan@anadolu.edu.tr Phone: +90 545 299 72 14

Table 1. EO yield and chemical composition of *Juniperus oxycedrus* L. subsp. *oxycedrus* (3-16)

Part of plant	Yield %	Major compounds %	Ref.
Leaf	0.7 HD	α-Pinene (42.9%) Limonene (17.8%) Caryophyllene oxide (5.1%) β-Myrcene (3.9%) β-Pinene (3.8%)	3
Leaf	0.01 HD	α-Pinene (17.1%) 13-*epi*-Manoyl oxide (12.5%) (*Z*)-6-pentadecen-2-one (11.5%)	4
Leaf	0.1 HD	*trans*-Pinocarveol (7.0%) *cis*-Verbenol (6.3%) Manoyl oxide (6.0%)	5
Leaf	1.66 HD	α-Pinene (31.25%) Sabinene (5.21%) Limonene (5.02%)	6
Leaf	0.2 HD	Limonene (30.0%) α-Pinene (26.3%) (*Z, E*)-Farnesol (5.1%) Salvial-4 (14)-en-1-one (4.9%)	7
Leaf	0.4±0.14 HD	α-Pinene (49.46%) Germacrene D (8.96%) 13-*epi*-Manoyl oxide (3.62%)	8
Leaf	0.2-0.5 HD	α-Pinene (41.3%) α-Phellandrene (8.2%) *p*-Cymene (6.2%) Manoyl oxide (5.3%)	9
Berry	- SPME	α-Pinene (88.44%) β-Myrcene (6.71%) β-Pinene (2.07%)	10
Berry	0.97 HD	α-Myrcene (23.4%) α-Pinene (16.7%) Citronellol (16.3%) β-Caryophyllene (6.3%)	11
Berry	2.21 HD	Citronellol (26.8%) α-Myrcene (24.3%) α-Pinene (14.4%) Limonene (9.3%)	11
Berry	0.7-1.2 HD	β-Myrcene (56.87±4.6%) α-Pinene (14.84±2.9%) DL-Limonene (5.96±0.6%)	12
Berry	0.4-0.7 HD	β-Myrcene (54.06±6.1%) α-Pinene (10.22±2.7%) DL-Limonene (9.20±1.7%) Germacrene D (8.56±1.7%) (*E*)-Nerolidol (5.94±1.6%)	12
Berry	0.8-1.5 HD	β-Myrcene (49.75±3.8%) α-Pinene (16.50±2.3%) DL-limonene (13.82±2.7%)	12
Berry	0.9-1.5 HD	β-Myrcene (56.97±3.7%) α-Pinene (19.55±3.7%) α-Cadinol (3.92±1.6%) Germacrene D (3.74±0.2%)	12

Table 1 continued

Berry	1.2-1.8 HD	β-Myrcene (45.50±3.0%) α-Pinene (36.64±2.0%) DL-Limonene (5.75±2.1%) Germacrene D (3.65±0.6%)	12
Berry	0.72 HD	α-Pinene (27.4%) β-Myrcene (18.9%) α-Phellandrene (7.1%) Limonene (6.7%)	13
Berry	2.5 HD	α-Pinene (27.4%) β-Myrcene (18.9%)	14
Berry	0.5 HD	α-Pinene (60.60±3.33%) β-Myrcene (24.97±1.76%) γ-Muurolene (5.19%).	15
Berry	0.45 SFE	Germacrene D (13.8%) α-Pinene (10.5%) β-Myrcene (8.1%)	16
Needles	- HD	α-Pinene (92.22%) β-Myrcene (2.46%) β-Pinene (1.79%)	10
Wood	0.68 HD	δ-Cadinene (14.5%) *cis*-Thujopsene (9.2%) α-Muurolene (4.9%) Cadalene (3.7%) Eremophilene (2.5%) α-Cedrol (2.2%)	13

HD: Hidrodistillation, SFE: Supercritical carbon dioxide extraction, SPME: Solid Phase Micro Extraction

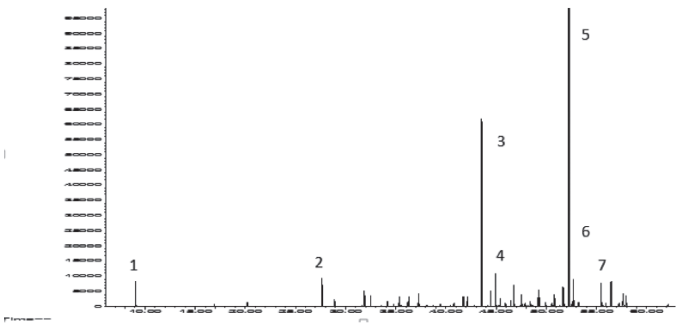

Figure 1. Chromatogram of the twigs essential oil of J. oxycedrus L. subsp. oxycedrus
1. α- Pinene, 2. α- Cubebene, 3. Caryophyllene oxide, 4. Humulene epoxide-II, 5. Manoyl oxide, 6. Caryophyllenol II, 7. Dodecanoic acid

Gas Chromatography (GC) and Gas Chromatography - Mass Spectrometry (GC/MS) analysis

The GC/MS analysis was carried out with an Agilent 5975 GC-MSD system. Innowax FSC column (60 m x 0.25 mm, 0.25 mm film thickness) was used with helium as carrier gas (0.8 mL/min). GC oven temperature was kept at 60˚C for 10 minutes and programmed to 220˚C at a rate of 4˚C/min, and

kept constant at 220˚C for 10 minutes and then programmed to 240˚C at a rate of 1˚C/minutes. Split ratio was adjusted 40:1. The injector temperature was at 250˚C. MS were taken at 70 eV. Mass range was from m/z 35 to 450.

Table 2. Composition of the EOs of *Juniperus oxycedrus* L. subsp. *oxycedrus*

RRI	Compounds	Twigs %	Berries %	Leaves %
1032	α-Pinene	2.4	19.9	1.4
1132	Sabinene	-	1.4	-
1174	Myrcene	-	44.6	-
1190	Sylvestrene	0.7	-	-
1203	Limonene	-	2.7	-
1213	1,8-Cineole	-	-	-
1218	β -Phellandrene	-	0.7	-
1280	*p*-Cymene	0.5	-	-
1290	Terpinolene	-	0.5	-
1466	α-Cubebene	2.0	0.3	-
1604	Isobornyl acetate	1.6	0.3	1.2
1612	β-Caryophyllene	1.5	4.6	3.7
1668	(*Z*)-β-Farnesene	-	0.5	-
1687	α-Humulene	-	3.1	-
1704	*g*-Muurolene	-	0.3	-
1706	α-Terpineol	1.9	-	-
1726	Germacrene D	-	15.5	5.7
1740	α-Muurolene	1.3	0.7	3.2
1773	*d*-Cadinene	1.4	1.8	4.1
1776	*g*-Cadinene	-	-	1.6
1941	α-Calacorene	0.7	-	1.8
2008	Caryophyllene oxide	16.8	-	11.9
2050	(*E*)-Nerolidol	1.4	-	-
2071	Humulene epoxide-II	3.4	-	4.7
2148	Cedrol	2.9	-	-
2243	Torilenol	1.2	-	2.5
2255	α-Cadinol	-	1.1	-
2256	Cadalene	2.8	-	2.2
2316	Caryophylladienol I	1.8	-	-
2376	Manoyl oxide	35.4	-	32.8
2392	Caryophyllenol II (=*Caryophylla-2(12),6-dien-5b-ol*)	4.5	-	-
2503	Dodecanoic acid *(=lauric acid)*	4.2	-	3.1
2524	Abietatriene	2.5	-	2.5

RRI: Relative Retention Indices calculated against n-alkanes

The GC analysis was carried out using an Agilent 6890 N GC system. In order to obtain the same elution order with GC/MS, simultaneous injection was done by using the same column and appropriate operational conditions. FID temperature was 300˚C.

Identification of compounds

The components of essential oils were identified by comparison of their mass spectra with those in the Baser Library of Essential Oil Constituents, Wiley GC/MS Library, Adams Library, MassFinder Library and confirmed by comparison of their retention indices. Alkanes were used as reference points in the calculation of relative retention indices (RRI). Relative percentage amounts of the separated compounds were calculated from FID chromatograms.

RESULTS AND DISCUSSION

The EOs were obtained from leaves, berries and twigs by yielding 0.02%, 2.12% and 0.01%, respectively. The list of compounds identified in the hydrodistilled leaves, berries and twigs of *J. oxycedrus* L. subsp. *oxycedrus* with their relative percentages and retention indices are given in Table 2.

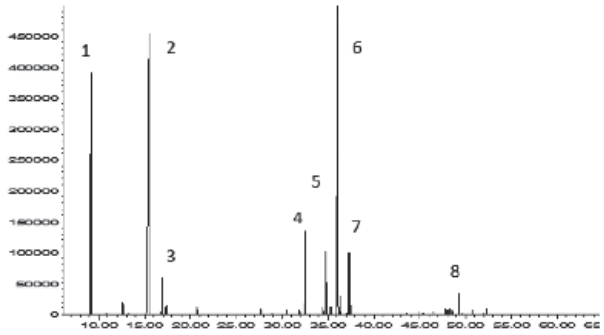

Figure 2. Chromatogram of the berries essential oil of J. oxycedrus L. subsp. oxycedrus

1. α- Pinene, 2. Myrcene, 3. Limonene, 4. β- Caryophyllene, 5. α- Humulene, 6. Germacrene D, 7. d- Cadinene, 8. α- Cadinol

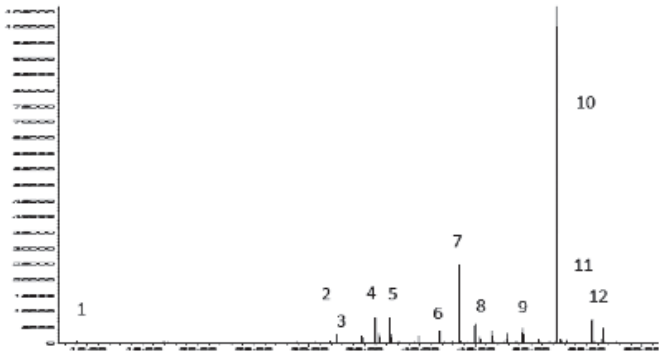

Figure 3. Chromatogram of the leaves essential oil of J. oxycedrus L. subsp. oxycedrus

1. α- Pinene, 2. Bornyl acetate, 3. β- Caryophyllene, 4. Germacrene D, 5. d-Cadinene, 6. α- Calacorene, 7. Caryophyllene oxide, 8. Humulene epoxide-II , 9. Cadalene, 10. Manoyl oxide, 11. Dodecanoic acid, 12. Abietatriene

In our study, 15-21 volatile compounds were identified of the leaves, berries and twigs EOs representing 82.4-98.0% of the total oils. Twig oil composition was not found in previous studies. Manoyl oxide (35.4%) and caryophyllene oxide (16.8%) were identified as major contituents in twig oil (Figure 1), myrcene (44.6%), α-pinene (19.9%) and germacrene D (15.5%) in berry oil (Figure 2), manoyl oxide (32.8%) and caryophyllene oxide (11.9%) in leaf oil (Figure 3).

As seen in previous studies Table 1, the leaf oils were characterized by the presence of α-pinene, t-pinocarveol and limonene as main contituents (3-10). But, in our study, the occurrence of manoyl oxide and caryophyllene oxide was interesting. While some contituents like α-pinene and myrcene were found in berry oil samples (11-15), germacrene D was only in one sample (16).

Medini *et al.* have reported α-pinene, germacrene D, myrcene, abietadiene and *cis*-calamenene as main constituents of the EOs of the berries of *Juniperus oxycedrus* L. subsp. *rufescens* (L.K.) and *Juniperus oxycedrus* L. subsp. *macrocarpa* (S. & M.) Ball. (17).

Sezik et al. have reported manoyl oxide (21.9%) and α-pinene (11.3%) as main constituents in leaf oil of *J. oxycedrus* subsp. *macrocarpa* from Eskişehir (18).

Variability of the oil composition in different populations of the same plant species might be attributed mainly to genetic diversity (19). Chemical composition and the main components of EOs *J. oxycedrus* have differentiate chemotype due to containing different climatic conditions of a large geographical diversity.

ACKNOWLEDGEMENTS

The author is grateful to Prof. Dr. K.H.C. Başer for allowing us to use the Başer Library of Essential Oil Constituents during the GC/MS Analyses.

REFERENCES

1. Coode MJE, Cullen J, *Juniperus* L.; P. H. Davis, Flora of Turkey and the East Aegean Islands, 1, pp. 78-84, Edinburgh at the University Press, Edinburgh, 1965.
2. Guner A, Aslan S, Ekim T, Vural M, Babac MT, A checklist of the Flora of Turkey (vascular plants), Ed(s), Flora Series 1, 12-14, Nezahat Gökyiğit Botanik Bahçesi Yayınları, 2012.
3. Hayta S, Bagci E. Essential oil constituents of the leaves, bark and cones of *Juniperus oxycedrus* subsp *oxycedrus* L. from Turkey. Acta Botanica Gallica: Botany Lett 161(2), 201–207, 2014.
4. Nadia A, Abderrahmane R, Mohamed A, Adams PR. Chemical studies of leaf essential oils of three species of *Juniperus* From Tensift Al Haouz-Marrakech Region (Morocco). J Essent Oil Res 21(4), 337-341, 2009.
5. Dob T, Dahmane D, Chelghoum C. Essential oil composition of *Juniperus oxycedrus* growing in Algeria. Pharm Biol 44(1), 1–6, 2006.
6. Elhoussine D, Rachida C. Identification of the volatile constituents of the essential oil of *Juniperus oxycedrus* L. (Cupressaceae) from the North Centre Region of Morocco. Asian J Pharm Clin Res, Suppl. 1, 2011.
7. Giuseppa V, Bice B, Filippo M, Aurelio M. The leaf and female cone oils of *Juniperus oxycedrus* L. subsp. *oxycedrus* and *J. oxycedrus* subsp. *macrocarpa* (Sibth. et Sm.) Ball. from Abruzzo. J Essent Oil Res 15, 418-421, 2003.
8. Medini H, Manongiu B, Aicha N, Chekir-Ghedira L, Harzalla-Skhiri F, Khouja ML. Chemical and antibacterial polymorphism of *Juniperus oxycedrus* ssp. *oxycedrus* and *Juniperus oxycedrus* ssp. *macrocarpa* (Cupressaceae) leaf essential oils from Tunisia. J Chem 2013, 1-9, 2013.
9. Adams RP. The leaf essential oils and chemotaxonomy of *Juniperus* sect. *Juniperus*. Biochem System Ecol 26, 637-645, 1998.
10. Yazid FC, Noureddine Y. Enantiomeric and non-enantiomeric monoterpenes of *Juniperus communis* L. and *Juniperus oxycedrus* needles and berries determined by HS-SPME and enantioselective GC/MS. Food Chem 135, 1796-1800, 2012.
11. Koukos PK, Papadopoulous KI, Papagiannopoulos AD. Variation in the chemical composition of the berry oil of *Juniperus oxycedrus* L. grown in North and West Greece. Eur J Wood Wood Prod 60, 152-153, 2002.
12. Hajdari A, Mustafa B, Gashi V, Nebija D, Ibraliu A, Novak J. Chemical composition of the essential oils of ripe berries of *Juniperus oxycedrus* L., growing wild in Kosovo. Biochem System Ecol 57, 90-94, 2014.
13. Monica RL, Rosa T, Filomena C, Antoine MS, Giancarlo AS, Francesco M. Comparative chemical composition, antioxidant and hypoglycaemic activities of *Juniperus oxycedrus* ssp. *oxycedrus* L. berry and wood oils from Lebanon. Food Chem 105, 572–578, 2007.
14. Monica RL, Antoine MS, Rosa T, Giancarlo AS, Francesco M, Ilaria L, Roberto G, Jindrich C, Hans WD. Phytochemical analysis and *in vitro* antiviral activities of the essential oils of seven Lebanon species. Chem Biodivers 5, 461-470, 2008.
15. Eduardo GH, Del Carmen R, Rafael GV. Determination by gas chromatography of terpenes in the berries of the species *Juniperus oxycedrus* L., *J. thurifera* L., and *J. sabina* L. J Chromatogr 396, 416-420, 1987.
16. Marongiu B, Porcedda S, Caredda A, De Gioannis B, Vargiu L, La Colla P. Extraction of *Juniperus oxycedrus* ssp. *oxycedrus* essential oil by supercritical carbon dioxide, influence of some process parameters and biological activity. Flavour Fragr J 18(5), 390-397, 2003.
17. Medini H, Ameur E, Khouja ML, Piras A, Porcedda S, Falconieri D, Marongiuc B, Farhat F, Chemli R. Chemical composition of the essential oils of the berries of *Juniperus oxycedrus* L. ssp. *rufescens* (L. K.) and *Juniperus oxycedrus* L. ssp. *macrocarpa* (S. & m.) Ball. and their antioxidant activities, Nat Prod Res 26(9), 810–820, 2012.
18. Sezik E, Kocakulak E, Baser KHC, Ozek T. Composition of the essential oils of *Juniperus oxycedrus* subsp. *macrocarpa* from Turkey. Chem Nat Compound 41(3), 352-354, (2005).
19. Skoula, M., Abbes, J. E., Johnson, C. B. Genetic variation of volatiles and rosmarinic acid in populations of *Salvia fruticosa* Mill. growing in Crete. Bichem Systemt Ecol 28, 551-561, (2000).

Received : 07.01.2016
Accepted : 26.05.2016

Turk J Pharm Sci 13(3), 304-310, 2016
DOI: 10.4274/tjps.2016.04

ORIGINAL ARTICLE

Formulation and Evaluation of Lansoprazole Loaded Nanosponges

Lasoprazol Yüklü Nanosüngerlerin Formülasyonu ve Değerlendirilmesi

Subhash Chandra Bose PENJURI[1*], Nagaraju RAVOURU[2], Saritha DAMINENI[3], Sailakshmi BNS[2], Srikanth Reddy POREDDY[1]

[1]Department of Pharmaceutics, MNR College of Pharmacy, Sangareddy, Telangana, INDIA
[2]Sri Padmavathi Mahila Visvavidyalayam (Women's University), Institute of Pharmaceutical Technology,Tirupati, Andhra Pradesh, INDIA
[3]Department of Pharmaceutics, Sultan-ul-Uloom College of Pharmacy, Hyderabad, Telangana, INDIA

ABSTRACT

Lansoprazole is proton pump inhibitor which extensively degraded in acidic pH conditions. Lansoprazole loaded nanosponges were prepared by Emulsion solvent diffusion method using ethylcellulose, PVA and pluronic F-68 and dichloromethane as a solvent. The prepared nanosponges were evaluated for percentage yield, incorporation efficiency, particle size, drug polymer compatibility, scanning electron microscopy and *in-vitro* drug release. SEM studies confirmed their porous structure with number of nanochannels. The FTIR spectra showed stable character of lansoprazole in mixture of polymers and revealed the absence of drug polymer interactions. DSC study revealed that drug was involved in complexation with nanosponges. The average particle size of lansoprazole nanoparticles was found to be in the range of 83.4 nm to 190.69 nm. The negative zeta potential values were attained to ensure a good stability of nanosponges. The drug release from nanosponges was found to extended upto 12 h. The optimized nanosponges were formulated in to enteric coated tablet and evaluated for weight variation, hardness, friability and dissolution studies. *In-vitro* release of drug from enteric coated tablet follows zero order and showed controlled release behavior for a period of 24 h. The data obtained in this study suggests that nanosponges of lansoprazole are promising for controlled drug delivery, which can reduce dosing frequency.

Key words: Lansoprazole, Ethylcellulose, Pluronic F-68, Zero order, Nanosponges, Fickian release

ÖZ

Lansoprazol asidik pH koşullarında yoğun şekilde bozulan proton pompası inhibitörüdür. Lansoprazol yüklü nanosüngerler etilselüloz, PVA ve pluronic F68 ve solvan olarak da diklorometan kullanılarak emülsiyon çözücü difüzyon metodu ile hazırlandı. Hazırlanan nanosüngerler yüzde verim, yükleme etkinliği, partikül büyüklüğü, etkin madde polimer geçimliliği, taramalı elektron mikroskobu ve *in vitro* ekin madde salımı açısından değerlendirildi. SEM çalışmaları çok sayıda nanokanallar ile poröz yapılarını doğruladı. FTIR spektrumu polimer karışımı içinde lansoprazolün stabilitesini ve etkin madde polimer etkileşimi olmadığını gösterdi. DSC çalışması etkin maddenin nanosüngerle kompleks halinde olduğu ortaya çıkardı. Lansoprazol nanopartiküllerin ortalama partikül büyüklüğü 83.4 nm ile 190.69 nm aralığında bulundu. Negatif zeta potansiyel değerlerine ulaşılması nanosüngerlerin iyi stabilite göstermelerini sağladı. Etkin maddenin nanosüngerlerden salımının 12 saate kadar uzatıldığı bulundu. Optimize edilmiş nanosüngerler enterik kaplı tabletler halinde formüle edildi ve ağırlık sapması, sertlik, friabilite ve çözünme çalışmaları değerlendirildi. Enterik kaplı tabletlerden etkin maddenin *in vitro* salımı sıfır dereceye uyumlu ve 24 saatlik periyotda kontrollü salım davranışı gösterdi. Bu çalışmadan elde edilen veriler gösterdi ki lansoprazol nanosüngerleri doz sıklığını azaltabilecek kontrollü salım için gelecek vaad etmektedir.

Anahtar kelimeler: Lansoprazol, Etilselüloz, Pluronic F68, Sıfır derece, Nanosünger, Fick salımı

INTRODUCTION

The drug delivery technology has certainly a new interest for drugs by providing them new life through their therapeutic targets. Nowadays, targeting drug delivery is the major problem which is being faced by the researchers. Target oriented drug administration with improvements in therapeutic efficacy, reduction in side effects and optimized dosing regimen, shall be the leading trends in the area of therapeutics. Targeted drug delivery implies for selective and effective localization of pharmacologically active moiety at pre identified target in therapeutic concentration, while restricting its access to non-target normal cellular linings and thus minimizing toxic effects and maximizing therapeutic index of the drug (1).

*Correspondence: **E-mail:** penjurisubhash@gmail.com **Phone:** +91-8455-230690

Nanosponges have emerged as one of the most promising fields of science because of their perceived application in controlled drug delivery. Nanosponge delivery system can precisely control the release rates or target drugs to a specific body site and have an enormous impact on the health care system. This nanosized delivery system has definite advantages for the purpose of drug delivery because of its high stability, high carrier capacity and feasibility of incorporation of both hydrophilic and hydrophobic substances. The application of nanosponges for targeted and localized delivery of therapeutic agents is the driving force for the research in this area (2).

The sponge acts as a three-dimensional network or scaffold. The backbone is long-length polyester. It is mixed in solution with cross-linkers to form the polymer. The net effect is to form spherically shaped particles filled with cavities where drug molecules can be stored. The polyester is biodegradable, so it breaks down gradually in the body. As it breaks down, it releases its drug payload in a predictable fashion. The nanosponges can be synthesized to be specific size and to release drugs over time by varying proportions of cross-linker to polymer. The main limitation of nanosponges is their ability to include only small molecules (3).

Nanosponges are solid in nature and are small particles with porous surface can be formulated as oral, parenteral, topical or inhalational dosage forms. For oral administration, these may be dispersed in a matrix of excipients, diluents, lubricants and anti caking agents which is suitable for the preparation of tablets or capsules and the major benefits of these capsules or tablets are reduction of total dose, retention of dosage form, reduction in toxicity and improving patient compliance by prolonged release (3,4). For parenteral administration, these can be simply mixed with sterile water, saline or other aqueous solutions (4). For topical administration, they can be effectively incorporated into topical hydrogel (5).

Lansoprazole is a proton pump inhibitor commonly used in the treatment of gastric ulcer, gastro oesophageal reflux disease (GERD), duodenal ulcer, ulcers associated with usage of Nonsteroidal anti-inflammatory drug (NSAID) and long term management Zollinger-Ellison syndrome (6). Lansoprazole is primarily metabolized by liver. Hence it is a need to reduce the dose to the hepatic failure patients. But reduction of dose in conventional dosage systems may not show sufficient pharmacological effect (7). Regular usage of lansoprazole causes various adverse effects like abdominal pain, diarrhoea, skin rashes, thrombocytopenia, impotence etc. So, controlled delivery of lansoprazole at optimal concentration may be required (8). Oral route is preferable than other routes with respect to safety, comfort and reliability. Hence controlled delivery of lansoprazole by oral route is ideal. Controlled release of lansoprazole will reduce the frequency of dosing and dose size and may increase patient convenience (7,8). More over lansoprazole is highly acid labile and represents many formulation challenges to protect it from acidic environment of the stomach (9). So the aim of the present investigation was to formulate enteric coated tablets of lansoprazole nanosponges to protect it from acidic environment and deliver at controlled rate to its absorptive site so that its oral bioavailability can be enhanced (8,9).

MATERIAL AND METHOD

Lansoprazole was gift sample from Dr. Reddy's Labs limited, Hyderabad. Ethyl Cellulose, Polyvinyl Alcohol and Pluronic F68 were purchased from Qualigens Fine chemicals, New Delhi. All other ingredients used were analytical grade.

Methodology

Preparation of lansoprazole nanosponges (5,10)

Lansoprazole nanosponges were prepared by different proportions of ethyl cellulose, polyvinyl alcohol and Pluronic F68 by emulsion solvent diffusion technique. The disperse phase consisting of 100 mg lansoprazole and specified quantity of ethylcellulose (Table 1) dissolved in 30 mL of dichloromethane was slowly added to a definite amount of PVA in 100 mL of aqueous continuous phase. The mixture was stirred at 1000 rpm on a magnetic stirrer for two hours. The formed lansoprazole nanosponges were collected by vacuum filtration and dried in an oven at 40ºC for 24 h.

Percentage yield

The lansoprazole nanosponges obtained after drying was weighed. Percentage yield value was calculated as follows (11):

% yield = Weight of nanosponges×100/Total solids weight

Entrapment efficiency (11)

UV spectrophotometric method was used to estimate entrapment efficiency of lansoprazole nanosponges. A calibration curve was plotted for lansoprazole in methanolic HCl in the range of 3-18 µg/mL (Beer's Lambert's range) at 293 nm. A good linear relationship was observed between the concentration of lansoprazole and its absorbance (r^2=0.9993, m=0.0469, n=3). 100 mg of lansoprazole nanosponges of each batch were selected, powdered in a mortar and placed in 100 mL of methanolic HCl. Lansoprazole was extracted by centrifuging at 1000 rpm for 30 min, filtered and analyzed concentration from calibration curve data after necessary dilution. Percentage entrapment was calculated as follows:

% Entrapment efficiency= Actual drug content in the nanosponge×100/Theoritical drug content

Particle size measurement (5,11)

The average particle size of lansoprazole nanosponges were determined by photon correlation spectroscopy (PCS) using a Nano ZS-90 (Malvern Instruments limited, UK) at a fixed angle at 25º. Sample was diluted 10 times with distilled water and then it was analyzed for particle size.

Zeta potential (5,11)

The zeta potential was measured for the determination of the movement velocity of the particles in an electric field and the particle charge. In the present work, the nanosponges was diluted 10 times with distilled water and analyzed by Zetasizer using Laser Doppler Micro electrophoresis (Zetasizer nano ZS, Malvern instruments Ltd., UK).

Table 1. Composition of lansoprazole nanosponges

	F1	F2	F3	F4	F5	F6
Lansoprazole (mg)	100	100	100	100	100	100
Polyvinyl alcohol (mg)	600	800	900	1000	1100	1200
Ethyl cellulose (mg)	400	600	800	1000	800	600
Pluronic F68 (mg)	200	200	200	200	200	200
Dichloromethane (mL)	30	30	30	30	30	30
Distilled water (mL)	100	100	100	100	100	100

Table 2. Formulation of lansoprazole tablets

Ingredient	Quantity (mg)
Nanosponges (F2)	35 (equivalent to 30 mg of lansoprazole)
Microcrystalline cellulose	60
Magnesium stearate	5

Table 3. Evaluation parameters of lansoprazole nanosponges

	Percentage Yield	Entrapment efficiency	Particle size (nm)	Zeta Potential (mV)
F1	38.35±1.27	50.71±0.73	190.69	-4.9
F2	59.57±1.09	86.93±0.65	83.4	-5.2
F3	34.68±1.17	79.57±1.01	103.26	-5.6
F4	28.24±0.97	78.04±1.62	114.91	-6.1
F5	33.31±2.1	70.31±0.94	135.33	-5.3
F6	24.8±1.73	69.47±1.2	173.27	-5.2

(Mean ± SD, n=3)

Table 4. Evaluation of lansoprazole tablets

Formulation	Weight variation	Thickness (mm)	Hardness (kg/cm^2)	Friability (%)	Assay (%)
F1	Complies	3.18±0.14	5.66±0.29	0.886	99.93±1.16
F2	Complies	3.23±0.11	5.65±0.2	0.752	99.47±1.81
F3	Complies	3.09±0.17	5.72±0.15	0.892	98.18±1.43
F4	Complies	3.21±0.09	5.81±0.1	0.836	99.97±1.97
F5	Complies	3.27±0.21	5.9±0.21	0.811	99.01±2.13
F6	Complies	3.15±0.12	5.83±0.07	0.798	98.43±1.73

Particle shape and morphology (12)

The shape and morphology of nanosponges was examined using Scanning Electron Microscopy (LEO 440I). Sample was deposited on a glass slide, and was kept under vacuum. The samples were coated with a thin gold/palladium layer using a sputter coater unit. The scanning electron microscope was operated at an acceleration voltage of 15 kV.

Fourier transform infrared spectroscopy studies (12)

The FTIR spectral measurements were taken at ambient temperature using a Perkin Elmer Model 1600 (USA). Samples were dispersed in KBr powder and the pellets were made by applying 5 ton pressure. FTIR spectra were obtained by powder diffuse reflectance on FTIR spectrophotometer.

Differential scanning calorimetric studies (12)

Differential scanning calorimetry (DSC-60, Shimadzu Corporation, Japan) studies were carried out to check compatibility between drug and polymers. DSC was used after calibration with Indium and lead standards, samples (3-5 mg) were heated (range 50-400 ºC, 10 ºC/min) in crimped aluminium pans under a nitrogen atmosphere. The enthalpy of fusion and melting point were automatically calculated.

Porosity

Bulk volume was obtained by pouring the nanosponges in to a grated cylinder and is noted. It is then under gone for 100 tappings and the volume is noted as true volume.

% Porosity= (Bulk Volume-True Volume/Bulk volume)×100

Determination of residual solvents concentration (13)

Gas chromatography (Shimadzu GC-14B chromatograph, Japan) was used to estimate residual dichloromethane in lansoprazole nanosponges. Dichloromethane content in nanosponges was determined by gas chromatography on an Agilent 7890 Gas Chromatograph, USA fitted with a flame ionization detector. For estimation of residual solvents, 100 mg of nanosponges were dissolved in little amount of DMSO in a 10 mL volumetric flask and volume was made up to 10 mL with DMSO. The solution was filtered through 0.45 µm filter and degassed using sonicator. From the sample, 1 µl was injected into injection port, the chromatogram was recorded and the peak area of solvent was measured. A calibration curve was plotted for dichloromethane in the range of 10-50 ppm. A good linear relationship was observed between the concentration of dichloromethane and its peak area (r^2=0.9989). The concentration of residual solvent was calculated from calibration curve data.

Preparation of lansoprazole tablets

Lansoprazole tablets were prepared by direct compression method. The prescribed quantity of lansoprazole nanosponges, polymers and excipients (Table 2) were mixed homogeneously and the mixture was then compressed into tablets (100 mg) using an 8 mm, biconcave punches on a 'Rimek mini press 16 station rotary compression machine.

Evaluation of lansoprazole tablets

Weight variation

The weight variation test was performed according to specifications given in the Indian Pharmacopoeia on 20 tablets. The maximum acceptable limit is ±7.5% deviation of an individual weight from average weight.

Thickness

The thickness of 20 randomly selected tablets from each formulation was determined in mm using a vernier caliper (Pico India).

Hardness

Twenty tablets were randomly selected from each formulation and measured hardness in kg/cm^2 using Monsanto type hardness tester.

Friability

Tablet friability was measured using the Roche Friabilator. Randomly selected twenty pre-weighed tablets were placed in the apparatus and operated for 100 revolutions and then the tablets were reweighed. The friability was determined as the mass loss in percent according to following to Equation

F= (WA-WB/WA)×100

Where F: Friability, WA: Initial weight (gm), WB: Final weight (gm); the acceptable limits of the weight loss should not be more than 1%.

Assay

Ten tablets were randomly selected from each formulation and crushed to a fine powder in mortar with pestle. Weigh accurately equivalent to 10 mg of lansoprazole from fine powder then transfer in 100 mL volumetric flask, 100 mL of methanolic HCL was added to dissolve and sonicated for 20 minutes. Lansoprazole was extracted by centrifuging at 1000 rpm for 30 min. The samples were filtered, diluted and analyzed UV spectrophotometrically at 239 nm.

Enteric coating of lansoprazole tablets (14)

Enteric coating of optimized lansoprazole tablets was done to protect the drug in acidic environment. Coating solution was prepared by dissolving 5% w/v of cellulose acetate phthalate and 1.5% w/v of propylene glycol 400 in acetone. Coating solution was applied by dip coating technique using pipette (10 mL) attached to vacuum pump. Vacuum pump produced suction force that allowed tablet to adhere to pipette mouth. This adhered tablet was then partially dipped in coating solution to allow coat formation at one side of tablet. The other side was coated when other side dried.

In vitro release studies (15,16)

A calibration curve was plotted for lansoprazole in pH 1.2 and pH 6.8 buffers in the range of 3-18 µg/mL (Beer's Lambert's range) at 306 nm and 285 nm respectively. A good linear relationship was observed between the concentration of lansoprazole and its absorbance in pH 1.2 buffer (r^2=0.9987,

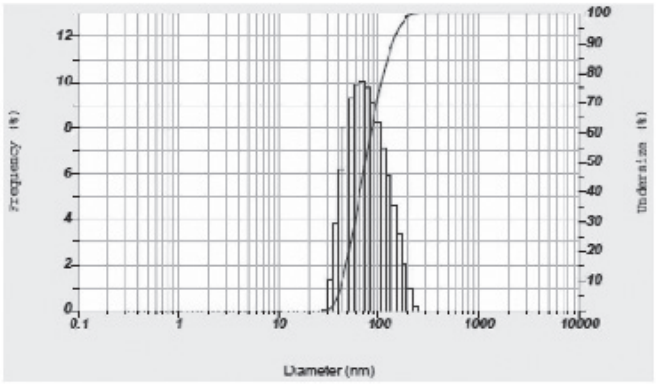

Figure 1. Particle size of lansoprazole nanosponges (F2)

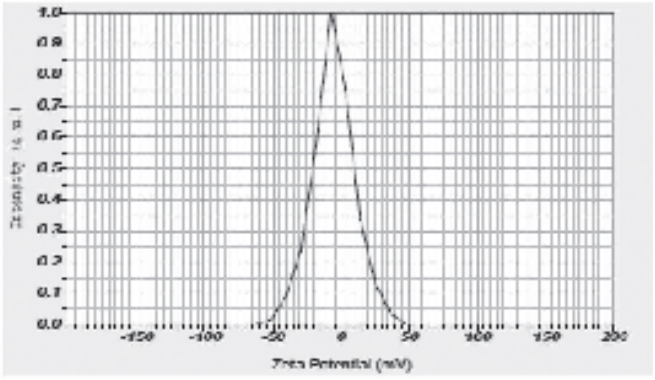

Figure 2. Zeta potential of lansoprazole nanosponges (F2)

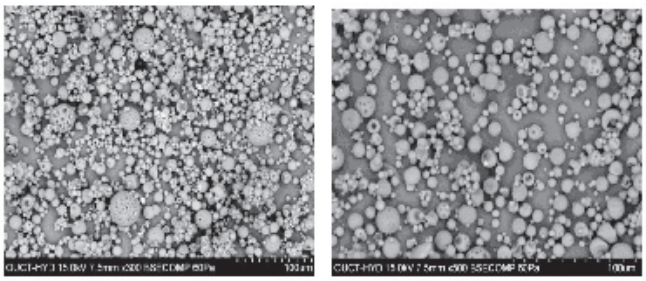

Figure 3. Scanning electron micrograph of lansoprazole nanosponges

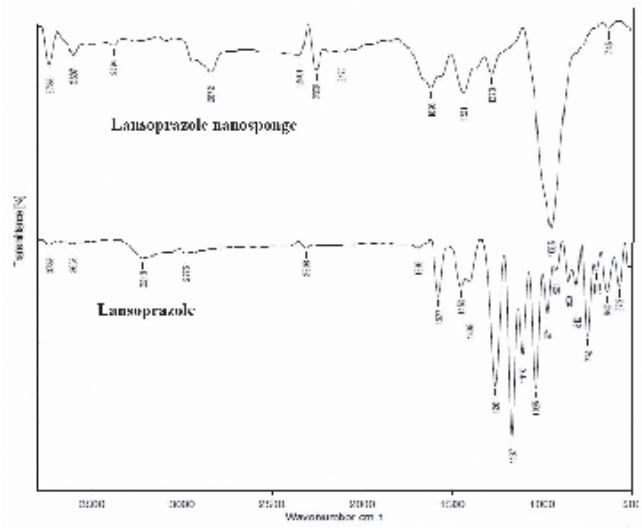

Figure 4. FTIR spectra of lansoprazole and lansoprazole nanosponges

m=0.0089, n=3) and pH 6.8 buffer (r^2=0.9979, m=0.0189, n=3). The dissolution test for optimized lansoprazole nanosponges and coated tablets was carried out according to USP 27 NF 22 by adapting the method B in pH 1.2 and pH 6.8 buffers.

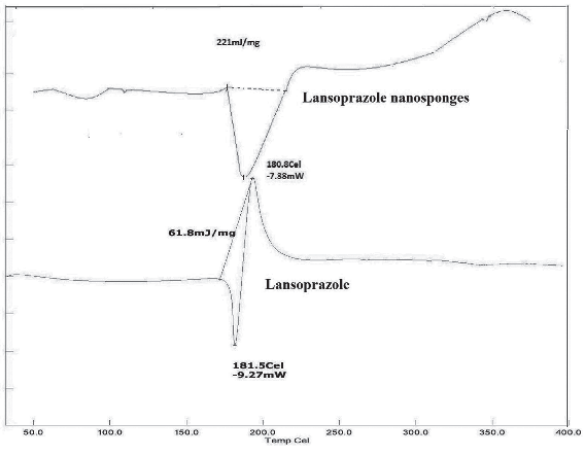

Figure 5. DSC thermograms of lansoprazole and lansoprazole nanosponges

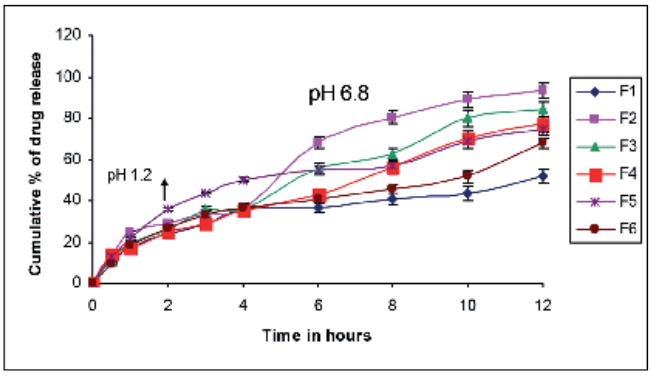

Figure 6. *In vitro* release profiles of lansoprazole nanosponges

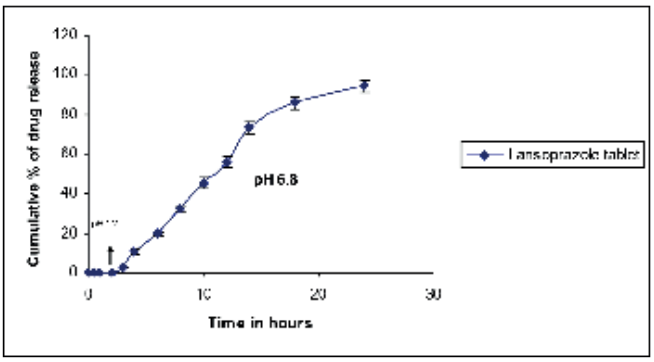

Figure 7. *In vitro* release profile of lansoprazole enteric coated tablet

Dissolution test was carried out using USP apparatus 1 (Model No TDT-08L, Electrolab, Mumbai) at 100 rpm. To reproduce digestive physiological phases, dissolution medium (900 mL) with different pH environments at 37±0.5ºC was used. Six tablets were introduced into the apparatus and the apparatus was run for 2 h in pH 1.2 buffer and 5 mL sample was withdrawn at various time intervals and the same volume of fresh dissolution medium was replaced to maintain sink condition. The samples were filtered, diluted and analyzed UV spectrophotometrically (Shimadzu, Japan) at 306 nm. After 2 h the dissolution medium with the pH of 1.2 was replaced with 6.8 buffer and continued for up to 24 h. Five millilitre samples were withdrawn at regular intervals and the same volume of fresh dissolution medium was replaced to maintain sink condition. The samples were filtered, diluted and analyzed UV spectrophotometrically at 285 nm. Dissolution studies were performed and the mean cumulative percentage of lansoprazole was calculated and plotted against time.

Evaluation of release kinetics (17-20)

To investigate the mechanism of lansoprazole release from nanosponges and enteric coated tablets, the release data was analyzed for zero order, first order, Higuchi model and Korsmeyer-Peppas model. The data was presented in the following graphical representation and regression analysis was performed.

M_t versus t (zero order)

Log cumulative % of drug remained versus t (first order)

M_t versus square root of t (Higuchi)

Log M_t versus log t (Korsmeyer-Peppas)

M_t is the cumulative % of drug released/permeated at time t.

Korsmeyer et al (20) derived a simple relationship which described drug release from a polymeric system.

$M_t/M_\infty = k_t^n$

Where, M_t/M_∞ is the fraction of drug released at time t, k is the rate constant and n is the release exponent. Release curve where $Mt/M\infty < 0.6$ was used to determine the exponent 'n' value. The n value was used to characterize different release mechanisms. For example, n = 0.45 for Case I or Fickian diffusion, $0.45 < n < 0.89$ for anomalous behaviour or non-Fickian transport, n=0.89 for Case II transport, and $n > 0.89$ for Super Case II transport. Fickian diffusional release occurs by the usual molecular diffusion of the drug due to a chemical potential gradient. Case II relaxational release is the drug transport mechanism associated with stresses

Table 5. Comparison of correlation coefficient (r^2) and rate constant of different kinetic models for F2 and enteric coated tablets

	Zero order		First order		Higuchi		Korsmeyer - Peppas		
	r^2	k^0	r^2	k_1	r^2	k_H	r^2	n value	k_{kp}
F2	0.9617	16.84	0.9502	0.227	0.9524	71.47	0.8528	0.581	1.404
Enteric Coated tablet	0.9815	10.83	0.9476	0.121	0.9418	59.81	0.7418	0.071	3.954

and state-transition in hydrophilic glassy polymers, which swell in water or biological fluids. This term also includes polymer disentanglement and erosion. The rate constant 'k', coefficients of correlation (r^2) and 'n' of each model were calculated by linear regression analysis.

RESULTS AND DISCUSSION

Percentage yield value, drug entrapment efficiency, particle size and zeta potential of lansoprazole nanosponges were shown in Table 2.

Percentage yield value of nanosponges was found to be best for F2. Further increasing the concentration of polymer the % yield was found to be decreased due to the sticky nature of the product which can not be filtered. The entrapment efficiency of nanosponges was found to be best for formulation F2. Further increasing the concentration of the polymer, entrapment efficiency was found to be decreased due to low solubility of polymer in aqueous phase (22,23). The size of the nanosponges was found to be in the range 83.4 nm to 190.69 nm (Table 3 and Figure 1). The zeta potential of the nanosponges was found to be in the range -4.9 mV to -5.6 mV (Table 3 and Figure 2). The negative sign indicates the stability of nanosponges.

The SEM images of the lansoprazole nanosponges were shown in Figure 3. SEM analysis revealed that Nanosized spherical particles with numerous pores on surface (lansoprazole nanosponges). The pores are tunneled inwards which may be due to diffusion of dichloromethane from the surface of the nanosponges (5).

The FTIR spectra of pure lansoprazole and lansoprazole nanosponges are shown in Figure 4. FTIR spectra of pure lansoprazole demonstrated the characteristic absorption peaks of 3608 cm for N-H stretching, at 2976 cm for aromatic C-H stretching, 2308 cm for aromatic C-N stretching, 1577 cm for C=C stretching and 1261 for S=O stretching. Lansoprazole nanosponges also showed almost similar absorption peaks indicates good compatibility with polymers (12).

DSC thermogram of pure lansoprazole shows sharp peak at 181.5ºC corresponding to its melting point (Figure 5). Lansoprazole nanosponge showed a similar endothermic peak at 180.8ºC which confirms no polymer drug interaction (12).

Porosity study is performed to check the extent of nanochannels and nanocavities formed. Porosity of the nanosponges can also be assessed by the use of density of nanosponges. Owing to their porous nature, nanosponges exhibit higher porosity compared to the parent polymer used to fabricate the system. Porosity of the nanosponges was found to be 60% and the bulk volume of the nanosponges was found to be 80 mL and true volume was found to be 32 mL.

The concentration of dichloromethane was found to be 298 ppm. According to Guidelines for residual solvents Q3C (ICH), dichloromethane is class II solvent (solvents to be limited) thus the limits of 600 ppm is acceptable without justification.

Lansoprazole tablets were evaluated for weight variation, thickness, hardness, friability and assay. The results of the evaluation are given in Table 4.

In vitro release studies of lansoprazole nanosponges were carried out in triplicate. After 12 h the release was found to be 51.94±3.26, 93.47±3.51, 84.38±3.53, 76.92±3.73, 74.26±2.96 and 67.73±2.49% for the formulations F1, F2, F3, F4, F5 and F6 respectively (Figure 6).

To study the release kinetics of optimized formulation, obtained *in vitro* release data was fitted in various kinetic models such as zero order, first order, Higuchi model and Korsmeyer-Peppas model. The *in vitro* release profile of F2 could be best expressed by zero order kinetic model, as the plot showed highest linearity (r^2=0.961). The release exponent (n) value 0.581 (Table 5) indicates that the release from nanosponges followed non fickian release i.e., by swelling and erosion which is always associated with diffusion and dissolution mechanism.

Based on entrapment efficiency and % drug release profiles F2 was selected as optimized formulation and it was formulated in to tablet by direct compression and coated by dipping the tablets in coating solution (5% w/v cellulose acetate phthalate and 1.5% w/v polyethylene glycol 400 in acetone). After 10 min the tablets were removed and air dried.

The enteric coated tablets were subjected to weight variation, hardness, friability, thickness and *in vitro* dissolution studies. The average weight of all tablets was found to be 101.27±2.78. The deviation of all tablets was found to be within the limit. So, all formulations passed the test for uniformity of weight as per official requirements. Thickness of the tablets was found to be 3.37±0.21 mm. Hardness of tablets was found to be 5.7±0.10 kg/cm^2. Percentage friability of tablets was found to be 0.89 i.e., less than 1%, indicating that the friability was within the prescribed limits. All the tablets showed acceptable properties and complied with the I.P specifications for weight variation, hardness, and friability.

Lansoprazole enteric coated tablet showed no release of drug in acidic medium which is desirable and 94.24±3.02% at the end of 24 h (Figure 7). The *in vitro* release profile of lansoprazole enteric coated tablets could be best expressed by zero order kinetic model, as the plot showed highest linearity (r^2=0.981). The release exponent (n) value 0.071 (Table 5) indicates that the release from coated tablets followed fickian release i.e., release always associated with diffusion mechanism (20).

CONCLUSION

The nanosponges containing lansoprazole exhibited most of the ideal characters required for an oral controlled release dosage forms. The nanosponges of lower particle size 83.4 nm aided with negatively charged surface charge has been achieved. The release profile indicated continuous controlled release up to 12 h. Lansoprazole enteric coated tablet showed no release

of drug in acidic medium which is desirable and controlled release behavior for a period of 24 h. The nanosponge systems have been found to have good potential for prolonged drug release and therefore can be beneficial such as dose reduction, reduced frequency of administration and avoiding related systemic side effects. Hence it can be concluded that the developed oral enteric coated tablet - nanosponges of lansoprazole is considered to be ideal and effective in the management of ulcer and related conditions.

ACKNOWLEDGEMENTS

The authors are thankful to Dr. Reddy's Labs, Hyderabad, India for the gift sample of lansoprazole. We also thank the MNR educational trust and Sri Padmavathi Mahila Visva Vidyalayam for providing necessary facilities to carrying the work.

REFERENCES

1. Vyas SP, Khar RK. Novel Carrier Systems. Molecular Basis of Targeted Drug Delivery. In: Targeted and Controlled Drug Delivery, pp. 38-40, CBS Publishers and Distributors, New Delhi, 2008.
2. Jilsha G, Vidya Viswanad. Nanosponges: A Novel Approach of Drug Delivery System. Int J Pharm Sci Rev Res 19(2), 119-123, 2013.
3. Lala R, Thorat A, Gargote C. Current trends in β- cyclodextrin based drug delivery systems. Int J Res Ayur Pharm 2(5), 1520-1526, 2011.
4. Jenny A, Merima P, Alberto F, Francesco T. Role of β-cyclodextrin nanosponges in propylene photooxidation. Carbohydrate Polymers. 86(1), 127-135, 2011.
5. Renuka Sharma, Roderick BW, Kamla Pathak. Evaluation of kinetics and mechanism of drug release from econazole nitrate nanosponge loaded carbapol hydrogel. Ind J Pham Edu Res 45(1), 25-31, 2011.
6. Matheson AJ and Jarvis B. Lansoprazole: an update of its place in the management of acid-related disorder. Drugs 61(2), 1801-1833, 2001.
7. Nagarajan E, Shanmugasundaram P, Ravichandirana V, Vijayalakshmi A, Senthilnathan B, Masilamani K, Development and evaluation of chitosan based polymeric nanoparticles of an antiulcer drug lansoprazole. J App Pharm Sci 5(4), 20-25, 2015.
8. Shimizu T, Nakano Y, Morimoto S, Tabata T, Hamaguchi N, Igari Y. Formulation study for Lansoprazole fast-disintegrating tablet. I. Effect of compression on dissolution behavior. Chem Pharm Bull 51(8), 942-947, 2003.
9. Venkateswarlu P. Formulation and *In Vitro* Evaluation of Lansoprazole Delayed Release Capsules Int J Innov Pharm Sci Res 4(3), 328-336, 2013.
10. Cavalli R, Trotta F, Tumiatti W. Cyclodextrin-based Nanosponges for Drug Delivery. J Incl Phenom Macrocycl Chem 56(1-2), 209-213, 2006.
11. Swaminathan S, Linda P, Loredana S, Francesco T, Pradeep V, Dino A, Michele T, Gianpaolo Z, Roberta C. Cyclodextrin-based nanosponges encapsulating camptothecin: Physicochemical characterization stability and cytotoxicity. Eur J Pharm Biopharm 74(2), 193-201, 2010.
12. Swaminathan S, Pradeep V, Trotta F, Cavalli R. Nanosponges encapsulating dexamethasone for ocular delivery: formulation design, physicochemical characterization, safety and corneal permeability. J Biomed Nanotechnol 9(6), 998-1007, 2013.
13. Prasanna Reddy Battu, Reddy MS. Residual solvents determination by HS-GC with flame ionization detector in omeprazole pharmaceutical formulations. Int J PharmTech Res 1(2), 230-234, 2009.
14. Bajpai M, Singh DCP, Bhattacharya A, Singh A. Design and *in vitro* evaluation of compression-coated pulsatile release tablets of losartan Potassium. Ind J Pharm Sci 74(2), 101-106, 2012.
15. Kalantzi LE, Karavas E, Koutris EX, Bikiaris DN. Recent advances in oral pulsatile drug delivery. Recent Pat Drug Deliv Formul 3(1), 49-63, 2009.
16. Paulo C, Jose M. Modeling and comparision of dissolution profiles, Eur J Pharm Sci 13(2), 123-133, 2001.
17. Higuchi T. Mechanism of sustained action medication: theoretical analysis of rate of release of solid drugs dispersed in solid matrices. J Pharm Sci 52, 1145-1148, 1963.
18. Brazel CS, Peppas NA. Modeling of drug release from swellable polymers, Eur J Pharm Biopharm 49(1), 47-58, 2000.
19. Lapidus H, Lordi NG. Some factors affecting the release of a water-soluble drug from a compressed hydrophilic matrix. J Pharm Sci 55(8), 840-843, 1966.
20. Korsmeyer RW, Gurny R, Doelker E, Buri P, Peppas NA. Mechanisms of solute release from porous hydrophilic polymers. Int J Pharm 15(1), 25-35, 1983.
21. Peppas NA. Analysis of Fickian and non- Fickian drug release from polymers. Pharm Acta Helv 60(4), 110-111, 1985.
22. Raja CHNV, Kiran Kumar G, Kotapati Anusha. Fabrication and Evaluation of Ciprofloxacin Loaded Nanosponges for Sustained Release. International Journal of Research In Pharmaceutical And Nano Sciences 2(1), 1-9, 2013.
23. Ansari KA, Torne SJ, Pradeep RV, Trotta F, Cavalli R. Paclitaxel loaded nanosponges: *in-vitro* characterization and cytotoxicity study on MCF-7 cell line culture. Curr Drug Deliv 8(2), 194-202, 2011.

Received : 18.01.2016
Accepted : 03.04.2016

Turk J Pharm Sci 13(3), 311-317, 2016
DOI: 10.4274/tjps.2016.05

ORIGINAL ARTICLE

Development and Characterization of Voriconazole Loaded *In Situ* Gel Formulations for Ophthalmic Application

Oküler Uygulama için Vorikonazol Yüklü *In Situ* Jel Formülasyonlarının Geliştirilmesi ve Karakterizasyonu

Neslihan ÜSTÜNDAĞ OKUR[1]*, Ayşegül YOLTAŞ[2], Vildan YOZGATLI[1]

[1]İstanbul Medipol University, Faculty of Pharmacy, Department of Pharmaceutical Technology, Beykoz, 34810, İstanbul, TURKEY
[2]Ege University, Faculty of Science, Department of Biology, Fundamental and Industrial Microbiology Division, Bornova, 35100, İzmir, TURKEY

ABSTRACT

The aim of the this research was to prepare and evaluate the potential use of *in situ* gel formulations for ocular delivery of voriconazole for the treatment of fungal keratitis. An *in situ* gelling system was used to increase the residence time and thus the bioavailability of voriconazole in ocular mucosa. Temperature triggered *in situ* gel formulations were prepared by cold method using polymers like poloxamer 188, poloxamer 407 and sodium alginate. Finally, concentration of voriconazole in formulations was 0.1% (w/w). These formulations were evaluated for clarity, sol-gel transition temperature, gelling capacity, pH, viscosity and drug content. The gelation temperatures of all the formulations were within the range of 32-34˚C. All the formulations exhibited fairly uniform drug content. Furthermore *in vitro* drug release and antifungal activity of these formulations were also evaluated. Drug release study of all the formulations showed sustained release properties. In conclusion, voriconazole loaded *in situ* gels could be offered as a promising strategy for ocular drug delivery for the treatment of fungal keratitis.

Key words: Voriconazole, *In situ* gel, Ocular drug delivery, Characterization, Microbiological study

ÖZ

Bu araştırmanın amacı fungal keratit tedavisi için vorikonazolün göze hedeflendirilmiş potansiyel kullanımı olan *in situ* jel formülasyonlarını hazırlamak ve değerlendirmektir. *In situ* jelleştirici sistemi vorikonazolün oküler mukozada kalış süresini dolayısıyla biyoyararlanımını arttırmak için kullanılmıştır. Sıcaklıktan etkilenen *in situ* jel formülasyonları poloksamer 188, poloksamer 407 ve sodyum alginat gibi polimerler kullanılarak soğuk yöntemle hazırlanmıştır. Son olarak, formülasyonların içindeki vorikonazol konsantrasyonu %0.1 (a/a)dir. Bu formülasyonlar berraklık, sol-jel geçiş sıcaklığı, jelleşme kapasitesi, pH, viskozite ve ilaç içeriği açısından değerlendirilmiştir. Bütün formülasyonların jelleşme sıcaklığı 32-34˚C arasında değişmektedir. Bütün formülasyonlar oldukça uygun ilaç içeriğini göstermiştir. Ayrıca bu formülasyonların *in vitro* ilaç salımı ve antifungal aktivitesi de değerlendirilmiştir. Bütün formülasyonların ilaç salım çalışması sürekli salım özelliği göstermiştir. Sonuç olarak, vorikonazol yüklü *in situ* jeller fungal keratit tedavisinde göze ilaç hedeflendirilmesi için gelecek vadeden bir strateji olarak sunulabilir.

Anahtar kelimeler: Vorikonazol, *In situ* jel, Oküler ilaç dağılımı, Karakterizasyon, Mikrobiyolojik çalışma

INTRODUCTION

The eye is unique in terms of its anatomical and physiological nature and defence mechanisms, which make the targeting of drugs to eye tissues one of the greatest challenges in drug delivery (1,2). One of the major limitations faced in ophthalmic delivery is the attainment and retention of optimum drug concentration at the site of action within the eye (3,4,5). Poor bioavailability of drugs from conventional ocular dosage forms in mainly due to tear production, nasolacrimal drainage and transient residence time, drainage of the instilled solution, tear turnover and limited corneal area (6). Various ophthalmic vehicles such as inserts, ointments, suspensions and aqueous gels, have been developed in order to lengthen the residence time of instilled dose and enhance the ophthalmic bioavailability. These ocular drug delivery systems, however, have not been used extensively because of some drawbacks such as blurred vision from ointments or lack of patient compliance are the main reasons that they have not universally accepted (6,8,9). The effective dose administered may be altered by increasing the retention time of medication into the eye by using *in situ* gel forming systems (10). *In situ* gel forming systems are liquid aqueous solutions

*Correspondence: E-mail: neslihanustundag@yahoo.com Phone: +90216 6815100/5190

before administration but turn to gel under physiological conditions. There are several possible mechanisms that lead to *in situ* gel formation, such as pH change, ionic cross-linkage, and temperature modulation (11,12).

Several *in situ* gel forming systems have been developed to prolong the precorneal residence time of a drug and improve ocular bioavailability. Polymers are employed in such delivery systems to carry various drugs and they may demonstrate a transition from sol(liquid) to gel state once instilled in the cul-de-sac of the eye (13). *In situ* gel forming formulations current a novel idea of deliver drugs to patients as a liquid dosage form, yet achieve sustained release of drug for the desired period. Different delivery systems based on polymers have been developed, which are able to increase the residence time of the formulation at absorption site of drugs. In recent years, there has been an increasing interest in water-soluble polymers are highly advantageous compared with other polymers because, in contrast to very strong gels, they can be easily applied in liquid form to the site of drug absorption. At the site of drug absorption, they swell to form a strong gel that is capable of prolonging the residence time of drug (14).

Keratitis, a disease of the cornea, results from direct infection with viruses, bacteria, fungi, yeast, and amoebae or from immune-related complications (4). Fungal keratitis is a leading cause of serious ocular morbidity and blindness. It is worldwide in distribution, but is more common in the tropics and subtropical regions. In fungal keratitis, early diagnosis and antifungal therapy is necessary in preventing further complications such as hypopyon formation, endophthalmitis, or loss of vision (15).

Table 1. Poloxamers concentrations, gelling temperature and pH of the formulations

Codes	Poloxamer 407 (%)	Poloxamer 188 (%)	Gelling temperature (°C)	pH
F1	15	10	42-43	7.15
F2	15	15	39-40	7.31
F3	15	20	35-36	7.44
F4	15	23	34-35	7.53
F5	15	25	30-32	7.63
F6	18	15	41-42	7.51
F7	18	18	38-39	7.57
F8	18	20	33-34	7.53
F9	18	22	32-33	7.63
F10	18	25	28-29	7.85
F11	20	5	30-32	7.07
F12	20	10	33-34	7.22
F13	20	15	36-37	7.30
F14	20	20	32-33	7.34
F15	20	23	32-33	7.67

Voriconazole (VCZ), $C_{16}H_{14}F_3N_5O$, a second generation antifungal agent possesses phenomenal characteristics like broad-spectrum activity, activity against resistant fungal species, and acceptable tolerability. Almost 100% *in vitro* susceptibility was observed against various fungal isolates associated with keratitis and endophthalmitis. Moreover, studies suggested an excellent efficacy of voriconazole against several ocular mycoses following topical administration (16).

In this study, a new ocular drug delivery system based on the dispersion of voriconazole loaded *in situ* gels coating into sodium alginate was proposed. The characterization properties of the system were investigated, including clarity, gelling capasity, pH, viscosity and drug content. *In vitro* drug release and antifungal activity of these formulations were also evaluated.

EXPERIMENTAL

Materials

VCZ and sodium alginate were purchased from Sigma, Germany. Poloxamer 407 and poloxamer 188 were kind gift from BASF, Turkey. Distilled water was used throughout the study. High pressure liquid chromatography (HPLC) grade acetonitrile (Sigma, Germany) was used for HPLC studies. Roswell Park Memorial Institute (RPMI 1640) medium was puchased from Sigma-Aldrich, Germany (R65504). All the other chemicals and solvents were of analytical or HPLC grade. Dialysis membrane (Spectro/por Dialysis Mebrane, Spectra/por 4, diameter 16 mm, molecular weight of 12-14 kDa) was purchased from Spectrum.

Preparation of in situ gel formulations

Poloxamer analogs were used as the gelling agents, and the *in situ* gels were prepared by using a cold method (17). The polymeric solutions were prepared by dispersing required quantity of Poloxamer 407 and Poloxamer 188 in cold water (5 ºC) using a magnetic stirrer until the poloxamer completely dissolve (approximately 2 hours). The dispersion was kept in a refrigerator for 48 hours to get clear solution.

Determination of sol-gel temperature (Tsol-gel)

20 g of cold sample solution were put into a beaker and placed in a temperature-controlled stirrer. A thermometer was immersed into the sample solution for constant monitoring. The solution was heated at the rate of 2 ºC/min with the continuous with stirring at 200 rpm. The temperature at which the magnetic bar stopped moving due to gelation was reported as the gelation temperature. The maximum limit for gelation was checked up to 60 ºC. Optimum poloxamer ratios were determined and selected with sol-gel temperature as 32-34 ºC which is the eye surface temperature (18). The experiments were repeated four times.

Preparation of voriconazole loaded in situ gel formulations

In situ gels were selected according to pH values and gelling temperatures of formulations. F11 (ratio of P407 and P188 were 20% and 5%, respectively) was selected as optimum formulation for preparation an ocular formulation. After detection of the optimum *in situ* gel compositions sodium alginate of different concentrations (0.1%, 0.3%, and 0.5%) and for each formulations same concentration of VCZ were added in poloxamer solutions with continuous stirring until completely dissolved. Benzalkonium chloride (0.02% w/w) was added as a preservative to the solutions. Sufficient amount of sodium chloride (0.9% w/w) was added to the mixture to maintain the isotonicity. The effect of drug and the other compositions of formulations on gel temperature were also evaluated.

Characterization of in situ gels

The prepared ocular formulations were characterized such as clarity, gelling capacity, pH, viscosity and drug content. In addition gelling temperature of formulations was determined and statistical analysis was performed using t-test. Data were considered statistically significant at $p<0.05$. The experiments were repeated four times.

Clarity of formulations

The clarity of formulations was determined by visual inspection under black and white background, and it was graded as follows: turbid, +; clear, ++; and very clear (glassy), +++.

Gelling capacity

The gelling capacity of the prepared formulation was determined by placing a drop of the formulation in a beaker at 32-34 ºC and it was visually observed for gelling time. It was graded as follows: +; gel after few minutes dissolves rapidly, ++; immediate gelation remains for few mins, +++; immediate gelation remains for nearly an hour.

Determination of pH

The pH of the gel was determined using calibrated pH meter (Mettler Toledo, Switzerland). Determinations were carried out four times and an average of these determinations was taken as the pH of the prepared gels.

Determination of viscosity

The viscosity of the developed formulations was performed with a digital viscometer (Brookfield) equipped with spindle RV2 with 50 rpm at 32±2°C.

Drug content

1 mL of the developed *in situ* gel formulation was dissolved in 100 mL pH 7.4 simulated tear fluid buffer (NaCl: 0.670g, $NaHCO_3$: 0.200g, $CaCl_2.2H_2O$: 0.008 g and distiled water q.s. to 100 g) (19) followed by HPLC estimation of the aliquot to determine drug concentration. The experiments were repeated four times.

HLPC analysis

The HPLC system consisted of a gradient pump and a UV detector supplied by Agilent 1100. C18 column (150x4.6mm,5µm) (GL Sciences, Japan) was used. The samples were analyzed at 256 nm with a 1 mL/min flow rate at 25°C. The mobile phase was a mixture of acetonitrile: ultrapure water (50:50). Retention time of drug was 4.098 min. The method was validated partially linearity, limit of detection (LOD) and limit of quantitation (LOQ), precision, accuracy and specificity, selectivity and stability.

In vitro drug release study

The *in vitro* drug release study was performed using the dialysis bag method (5). *In vitro* release study of *in situ* gel formulations was carried out in simulated tear fluid (pH=7.4) at 50 rpm. The temperature was maintained at 33±1°C to mimic eye surface temperature. 5 g formulation was separated from release media by means of dialysis membrane (Spectra/por, MW of 12-14 kDa) and capped with closures. The membrane was heated 33±1°C for 30 min in bidistilled water before use. 0.5 mL of sample was withdrawn at a predetermined time interval of 1 h to 8 h and the same volume of fresh medium was replaced. The samples were analyzed with HPLC for the drug content. The experiments were repeated three times.

Stability of the in situ gels

In physical stability studies, VCZ loaded *in situ* gels were stored at 5±1ºC in the refrigerator and 25±2ºC and 40±2ºC for 3 months in the stability cabinets (Nüve, Turkey). After storage for 3 months visual appearance, clarity, pH, gelation time of *in situ* gels and VCZ content were investigated. The experiments were repeated three times.

Microbiological studies

Sterility studies

In situ gel formulations in the presence or absence of VCZ were prepared at Laminar air flow Cabinet (Haier HR40-IIA2).

To check the sterility of the prepared ocular formulations sterility control testing were performed. Sterility testing of the *in situ* gel formulations with or without VCZ was carried out under aseptic conditions according to the international pharmacopoeia. For anaerobic bacteria Fluid thioglycollate medium was used. For fungi and aerobic bacteria soya-bean casein digest medium was used. 1 mL of formulation solution was added to each medium and incubated at 35°C for bacteria and 25°C for fungi for 14 days.

To check the suitability of the used mediums for the sterility testing promotion test were performed. For growth promotion test of aerobes, anaerobes and fungi, fluid thioglycollate media (using separate portion of media for each microorganism) were inoculated with 100 CFU of *Staphylococcus aureus* ATCC 6538, *Clostridium sporogenes* ATCC 19404 and *Candida albicans* ATCC 10231. Media were incubated at 35°C for 48 h.

Determination of MIC of VCZ

The broth microdilution test was done in accordance with CLSI guidelines for filamentous fungi (20) and yeasts (21). VCZ was dissolved in dimethyl sulfoxide, final dilutions were made in RPMI 1640 medium buffered to pH 7.0 with 0.165 M MOPS buffer [3-(N-morpholino) propanesulfonic acid] and final concentrations were 500-0.125 µg/mL. Using the spectrophotometric method of inoculum preparation, an inoculum concentration of $1.5(\pm1.0)x10^3$ cells/mL for yeasts and $0.4\text{-}5x10^4$ spores/mL for moulds, and RPMI 1640 medium buffered with MOPS were used. *C. albicans* ATCC 10231, *C. tropicalis* RSKK 2412, *A. fumigatus* ATCC 204305 and *A. flavus* ATCC 204304 which may be possible causes of fungal keratitis were used to evaluate antifungal activity of developed formulations (22,23). A 0.1 mL inoculum was added to each well of the microdilution trays. The MICs were determined after 48 h of incubation. The plates were shaken before the comparison of growth in wells. With an aid of a reading mirror, growth in each well was compared with the VCZ free growth control well. The MIC endpoints were evaluated for the lowest drug concentration that showed a prominent reduction (50%) of the growth in the control well.

Disk diffusion testing

Disk diffusion testing was performed according to CLSI standard M44-A2 for yeasts and M51-A for filamentous fungi. Mueller-Hinton agar (Difco) supplemented with 2% glucose and 0.5 µg/mL methylene blue dye (SSI Diagnostica, Hillerød, Denmark) was used. Blank disks that were 12.1 mm in diameter were impregnated with 20 µL of formulations at final concentration of 1 µg/disk and allowed to dry at room temperature. *C. albicans* ATCC 10231 and *C. tropicalis* RSKK 2412, *A. fumigatus* ATCC 204305 and *A. flavus* ATCC 204304 which may be possible causes of fungal keratitis (22,23) were used to evaluate antifungal activity of developed formulations. The mold inocula were prepared at optical densities ranging from 80 to 82% and a suspension with a 0.5 McFarland standard was utilized for yeasts. The plates were incubated at 35˚C and inhibition zone (IZs, in millimeters) diameters were read by using a digital ruler at 24 and 48 h. Minor trailing growth in the inhibition zones was ignored.

RESULTS AND DISCUSSION

Preparation of in situ gel formulations

Preliminary studies were carried out using different concentrations of polymers evaluated for their gelling temperature in order to identify the compositions suitable for use in the *in situ* gelling system for ocular drug delivery. Temperature sensitive *in situ* gels were successfully prepared by cold method using poloxamer 407, poloxamer 188. Cold method is one of the preferred methods due to providing clear solution for *in situ* gel while hot process causes formation of lumps of polymer as reported and observed in literature (24).

Table 2. Compositions of the *in situ* gels (%)

Components (%)	S	S1	S2	S3	S4
Poloxamer 407	20	20	20	20	20
Poloxamer 188	5	5	5	5	5
Sodium alginate	-	-	0.1	0.3	0.5
Sodium chloride	0.9	0.9	0.9	0.9	0.9
Voriconazole	-	0.1	0.1	0.1	0.1
Benzalkonium chloride	0.02	0.02	0.02	0.02	0.02
Distiled water qs to	100	100	100	100	100

Poloxamer 407 (ethylene oxide and propylene oxide blocks) has excellent thermo-sensitive gelling properties, which is of the most interest in optimising drug formulation. Poloxamer 407 formulations led to enhanced solubilization of poorly water-soluble drugs and prolonged release profile for many applications (e.g., ophthalmic, oral, rectal, topical, nasal and injectable preparations) but did not clearly show any relevant advantages when used alone. Combination with other excipients like Poloxamer 188 or mucoadhesive polymers promotes the action of Poloxamer 407 by optimising sol–gel transition temperature or increasing bioadhesive properties (25). For this purpose poloxamer 188 and poloxamer 407 mixture were used to develop *in situ* gels.

To find out optimum gelling temperature (32±2°C), the poloxamer 407 and poloxamer 188 were mixed various concentrations. Table 1 shows poloxamer concentrations, gelling temperature and pH of the prepared formulations. F11 was selected optimum composition which contains poloxamer 407 (20%) and poloxamer 188 (5%).

After selecting F11 formulation, benzalkonium chloride (0.02%, w/w) was added as a preservative to the solution. Sufficient amount of sodium chloride (0.9% w/w) was added to the mixture to maintain the isotonicity and the formulation was coded as S. 0.1% (w/w) VCZ was loaded and different concentrations of sodium alginate of different concentrations (0.1%, 0.3%, and 0.5%) was added in poloxamer solutions with continuous stirring until completely dissolved. Finally, concentration of VCZ in formulations was 0.1% (w/w). The dispersion was kept in a refrigerator for 48 hours to get clear solution. The components of ocular *in situ* gels in absence or presence of VCZ are shown in Table 2.

Characterization of in situ gels

Characterization of the new drug delivery systems are major issues to be considered in the formulation stage, especially those intended for ocular administration. The physicochemical characterization parameters of *in situ* gels are reported in Table 3.

The clarity of all the formulations was found to be satisfactory, as shown in Table 3. Gelation temperature was changed from 32.5°C to 34.3°C with incorporation of 0.1% w/w VCZ in the poloxamer solution, while the addition of the mucoadhesive polymers played a reverse role on gelation temperature. The results showed that incorporation of sodium alginate into *in situ* gel formulation significantly decreased the gelling temperature ($p<0.05$). When the concentration of

sodium alginate was increased in the *in situ* gels, the gelling temperature was decreased (Table 3). Gelling temperature of the all formulations (S, S1-S4) were found between 32-35°C. This indicates that the formulations can be converting the gel when they installed the eye surface. At 32-34°C, the solutions are converted into gels with high viscosity. The gelling capacity data of prepared formulations presented in Table 3 represent that the formulations all formulations had immediate gelation and exist for an hour.

The pH of an ophthalmic formulation is important for patient compliance. The pH of the prepared formulations ranged between 7.07 and 7.13. The pH of the formulations was appropriate for ocular delivery since they were iso-hydric. This indicated the nonirritancy of the formulation in ocular mucosa. When a formulation is administered to the eye, it stimulates the flow of tears. Tear fluid is capable of quickly diluting and buffering small volumes of added substances, thus eye can tolerate a fairly wide pH range. Ophthalmic solutions may range from 6.5 to 8.5 (26,27).

The formulation should have an optimum viscosity, which will allow its instillation into the eye as a liquid, which will then undergo rapid sol-gel transition due to temperature change. When the *in situ* solutions were installed the 32-34°C surface, the solutions were converted to gel form after few seconds.

All the formulations reflected fairly uniform drug content ensuring adequacy in the method of preparation of the *in situ* gel. Drug content was found to be within the range of 82.68-92.58%. The drug content of the prepared formulations was within acceptable limits and ensured dose uniformity.

In vitro drug release study

The *in situ* gelling formulations of VCZ, S1-S4, were subjected to *in vitro* release studies, which were carried out using simulated tear fluid of pH 7.4 as release medium. Formulations showed sustained drug release for a period of 8 hours (Figure 1). At the end of the 8 h, *in vitro* VCZ release from S1, S2 and S3 formulations was found as 63%, 60% and 60%, respectively ($p>0.05$). S4 formulation was showed slower release than the other formulations. This could be the reason of higher concentration of sodium alginate among the developed formulations. Mandal et al. prepared moxifloxacin hydrochloride loaded *in situ* gel using sodium alginate and hydroxy propyl methyl cellulose as polymers. They were found that when sodium alginate and hydroxy propyl methyl cellulose concentration was increased, release rate was decreased (28).

Stability

The stability studies were carried out at 5±1°C, 25±2°C and 40±2°C for 3 month using stability cabinets. The samples were analyzed periodically on every month, and found that there are no changes in visual appearance, clarity, and gelation time. After 3 month pH values of S1, S2 S3 and S4 formulations were found as 7.12±0.002, 7.18±0.001, 7.20±0.001 and 7.21±0.002, respectively. In addition 92-98% of initial drug content of formulations was kept its stability for in 3 month.

Microbiological studies

The optimized *in situ* gels passed the test for sterility as there was no appearance of turbidity and hence no evidence of microbial growth when incubated for 14 days at 35°C in case of fluid thioglycolate medium and at 20-25°C in the case of soya-bean casein digest medium. Furthermore to control the used

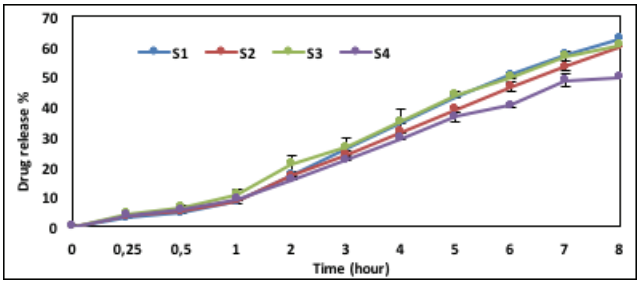

Figure 1. *In vitro* release of voriconazole from *in situ* gels at pH 7.4 simulated tear fluid buffer

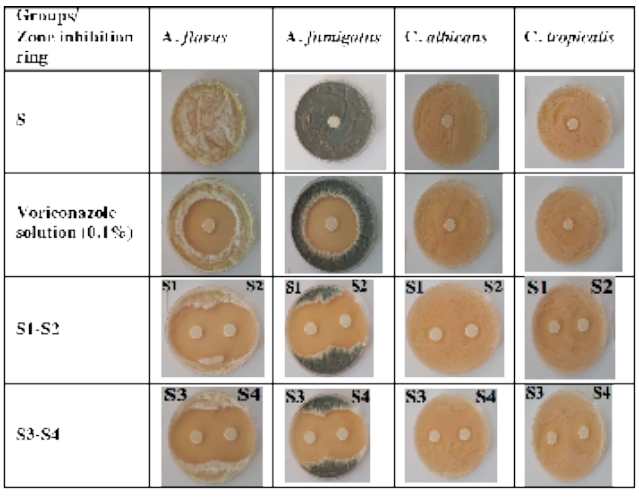

Figure 2. Zone inhibition diameters of formulations against *A. flavus, A. fumigatus, C. albicans and C. tropicalis*

Table 3. Clarity, gelling temperature, pH, drug content, *in vitro* gelation capacity, viscosity, and drug content of *in situ* gels

Formulations	S	S1	S2	S3	S4
Clarity	+++	+++	+++	++	++
Gelling temperature (oC)	32.5±0.03	34.3±0.01	33.1±0.023	32.6±0.012	32.4±0.001
Gelling capacity	+++	+++	+++	+++	+++
pH	7.07±0.002	7.08±0.001	7.1±0.002	7.11±0.001	7.13±0.001
Viscosity (cP)	358±3.1	362±6.21	400±11.32	424±23.15	440±9.17
Drug content (%)	-	83.14±0.36	82.68±1.06	84.11±0.7	92.58±0.35

mediums for suitability of sterility test growth promotion test were performed and it was found that both microorganisms showed visible growth in all media.

The MIC endpoints were evaluated for the lowest drug concentration that showed a prominent reduction (90% and 50%) of the growth in the control well. MIC_{90} values of VCZ against *C. albicans*, *C. tropicalis*, *A. fumigatus* and *A. flavus* were 2, 1, 0.5 and 0.5 µg/mL, respectively and MIC_{50} values were 0.25 µg/mL for all of the microorganisms. In accordance with our study (29) also evaluated the MIC_{90} results in *Aspergillus sp.* as 1 mg/L. (30) determined the MIC values for both clinical and environmental strains of *A. fumigatus* and *A. flavus* and the MIC ranges were 0.25-2 µg/mL for both of the microorganisms and (31) MIC ranges of *A. fumigatus* and *A. flavus* isolates were 0.25-1 and 0.125-1 µg/mL, respectively. For *Candida* species according to CLSI M27-A3 MIC values ≤ 1 µg/mL are accepted as susceptible; 2 µg/mL are dose dependent susceptible and ≥4 µg/mL are accepted as resistant.

The efficacy of groups was investigated using the inhibition zone diameters in disc diffusion test. Disk diffusion testing was performed according to CLSI standard M44-A2 for yeasts and M51-A for filamentous fungi. *C. albicans*, *C. tropicalis*, *A. fumigatus* and *A. flavus* were used as they are the common organisms causing ocular fungal infections (22,23). Figure 2 shows inhibition zone (IZ) diameters of formulations. The developed VCZ loaded *in situ* gels were found to be more effective on more effective on moulds in comparison with yeasts (*A. flavus* than *C. albicans*) (Table 4). In addition to this, sodium alginate is not effective on the *C. albicans*, *C. tropicalis*, *A. fumigatus* and *A. flavus*, because addition of sodium alginate into the *in situ* gel (S1) did not changed the IZ diameter. While absence of voriconazole (S) in the *in situ* gel (blank *in situ* gel) is not effective on *C. albicans*, *A. fumigatus* and *A. flavus*; a minor inhibition zone was seen in *C. tropicalis* which may be caused by benzalkonium chloride (0.02%, w/w) or other components of the gel. Since the interpretive breakpoints of VCZ for susceptible species is ≥17 mm and for resistant is ≤13 mm, we can say that all of organisms are susceptible for all of the formulations (32).

CONCLUSION

In the present study, the potential of VCZ loaded *in situ* gels as drug carriers for ocular delivery was investigated. The present study showed that *in situ* gels of VCZ can successfully be prepared with cold method. The clarity, pH, gellation time and drug content of all formulations was found to be satisfactory. In addition the formulations were found stable for 3 month. Further, all the formulations showed sustained drug release for a period of 8 h, which satisfied to treat ocular disease. The developed *in situ* gels showed anti fungal activiy on *C. albicans*, *C. tropicalis*, *A. fumigatus* and *A. flavus*. In conclusion, this study showed that developed *in situ* gel formulations could be alternatively used as ocular delivery of voriconazole. The present study can open up a window for opthalmic application of *in situ* gels loaded with VCZ, they would be a better alternative to conventional eye drops in the treatment of fungal keratitis of the eye.

Table 4. Zone inhibition diameters of formulations

Groups/ Inhibition Zone (IZ) (cm±SD)	*A. flavus*	*A. fumigatus*	*C. albicans*	*C. tropicalis*
S	0±0	0±0	0±0	2.0±0.1
S1	5.7±0.5	4.8±0.3	2.1±0.2	3.1±0.1
S2	5.2±0.4	5.0±0.3	2.0±0.1	2.8±0.3
S3	5.8±0.1	4.9±0.2	1.9±0.1	3.3±0.1
S4	5.1±0.3	5.0±0.5	2.1±0.1	3.4±0.2

Declaration of Interest

The authors declare no conflict of interest.

REFERENCES

1. Almeida H, Amaral MH, Lobão P, Lobo JM. *In situ* gelling systems: a strategy to improve the bioavailability of ophthalmic pharmaceutical formulations. Drug Discov Today 19, 400-412, 2014.
2. Üstündağ-Okur N, Homan-Gökçe E. Lipid nanoparticles for ocular drug delivery. Int J Ophthalmic Res 1(3), 77-82, 2015.
3. Makwana SB, Patel VA, Parmar SJ. Development and characterization of *in-situ* gel for ophthalmic formulation containing ciprofloxacin hydrochloride. Results Pharma Sci, doi:10.1016/j.rinphs.2015.06.001, 2015.
4. Üstündağ-Okur N, Gökçe EH, Boybıyık DI, Eğrilmez S, Ertan G, Özer Ö. Novel nanostructured lipid carrier based inserts for controlled ocular drug delivery: Evaluation of corneal bioavailability and treatment efficacy on bacterial keratitis. Expert Opin Drug Deliv 12(11), 1-17, 2015.
5. Üstündağ-Okur N, Gökçe EH, Eğrilmez S, Özer Ö, Ertan G. Novel ofloxacin-loaded microemulsion formulations for ocular delivery. J Ocul Pharmacol Ther 30(4), 319-332, 2014.
6. Swapnil D, Sonawane, Lahoti S. Design and evaluation of ion induced *in situ* gel formulation for levofloxacin hemihydrateocular delivery. Int J Pharm Sci Invent 3, 38-43, 2014.
7. Darwhekar G, Jain P, Jain DK, Agrawal G. Development and optimization of dorzolamide hydrochloride and timolol maleate *in situ* gel for glaucoma treatment. Asian J Pharm 1, 93-97, 2011.
8. Jung JH, Abou-Jaoude M, Carbia BE, Plummer C, Chauhan A. Glaucoma therapy by extended release of timolol from nanoparticle loaded silicone hydrogel contact lenses. J Control Release 165, 82–89, 2013.
9. Gallarate M, Chirio D, Bussano R, Peira E, Battaglia L, Baratta F, Trotta M. Development of O/W nanoemulsions for ophthalmic administration of timolol. Int J Pharm 440, 126-134, 2013.
10. Mandal S, Thimmasetty MKMJ, Geetha MS. Formulation and evaluation of an *in situ* gel-forming ophthalmic formulation of moxifloxacin hydrochloride. Int J Pharm Investig 2(2), 78-82, 2012.
11. Hosny KM. Preparation and evaluation of thermosensitive liposomal hydrogel for enhanced transcorneal permeation of ofloxacin. AAPS PharmSciTech 10, 1336-1342, 2009.

12. Hosny KM, Hassan AH. Intranasal *in situ* gel loaded with saquinavir mesylate nanosized microemulsion: Preparation, characterization, and *in vivo* evaluation. Int J Pharm 475(1-2), 191-197, 2014.
13. Varshosaz J, Tabbakhian M, Salmani Z. Designing of a thermosensitive chitosan/poloxamer *in situ* gel for ocular delivery of ciprofloxacin. TODDJ 2, 61-67, 2008.
14. Garala K, Joshi P, Patel J. Formulation and evaluation of periodontal *in situ* gel. Int J Pharm Investig 3, 29-41, 2013.
15. Moemen D, Bedir T, Awad EA, Ellayeh A. Fungal keratitis: Rapid diagnosis using methylene blue stain. EJBAS doi:10.1016/j.ejbas.2015.08.001, 2015.
16. Kumar R, Sinha VR. Preparation and optimization of voriconazole microemulsion for ocular delivery. Colloids Surf B Biointerfaces 117, 82–88, 2014.
17. Qian Y, Wang F, Li R, Zhang Q, Xu Q. Preparation and evaluation of *in situ* gelling ophthalmic drug delivery system for methazolamide. Drug Dev Ind Pharm 36(11), 1340-1347, 2010.
18. Efron N, Young G, Brennan NA. Ocular surface temperature. Curr Eye Res 8, 901-906, 1989.
19. Rathore KS, Nema RK, Sisodia SS. Preparation and characterization of timolol maleate ocular films. J Pharm Tech Res 2(3), 1995-2000, 2010.
20. Clinical and Laboratory Standards Institute. Reference method for broth dilution antifungal susceptibility testing of filamentous fungi; approved standard CLSI document M38-A2. Clinical and Laboratory Standards Institute, Wayne, PA, 2008.
21. Clinical and Laboratory Standards Institute. Reference method for broth dilution antifungal susceptibility testing of yeasts. Approved Standard M27-A3. Clinical Laboratory Standards Institute Wayne, PA. 2009.
22. Ansari Z, Miller D, Galor A. Current thoughts in fungal keratitis: diagnosis and treatment. Curr Fungal Infect Rep 7, 209-218, 2013.
23. Shukla SH, Kumar M, Keshava GBS. Mycotic keratitis: an overview of diagnosis and therapy. Mycoses 51, 183-199, 2008.
24. Borole PM, Chaudhari YS, Dharashivkar SS, Kumavat SD, Shenghani K, Shah PR. Preparation and evaluation of *in situ* gel of levofloxacin hemihydrate for treatment of peridontal disease. IJPRBS 2(3), 185-196, 2013.
25. Dumortier G, Grossiord JL, Agnely F, Chaumeil JC. Review of Poloxamer 407 Pharmaceutical and Pharmacological Characteristics. Pharm Res 23, 2709-2728, 2006.
26. Gonnering R, Edelhauser HF, Van Horn DL, Durant W. The pH tolerance of rabbit and human corneal endothelium. Invest Ophthalmol 18, 37-390, 1979.
27. Üstündağ-Okur N, Gökçe EH, Boybıyık DI, Eğrilmez S, Özer Ö, Ertan G. Preparation and *in vitro–in vivo* evaluation of ofloxacin loaded ophthalmic nano structured lipid carriers modified with chitosan oligosaccharide lactate for the treatment of bacterial keratitis, Eur J Pharm Sci 2014; 63: 204-215.
28. Mandal S, Thimmasetty MKMJ, Prabhushankar GL, Geetha MS. Formulation and evaluation of an *in situ* gel-forming ophthalmic formulation of moxifloxacin hydrochloride. Int J Pharm Investig 2(2), 78-82, 2012.
29. Espinel-Ingroff A, Johnson E, Hockey H, Troke P. Activities of voriconazole, itraconazole and amphotericin B *in vitro* against 590 moulds from 323 patients in the voriconazole Phase III clinical studies. J Antimicrob Chemother 61, 616-620, 2008.
30. Araujo R, Pina-Vaz C, Rodrigues AG. Susceptibility of environmental versus clinical strains of pathogenic Aspergillus. Int J Antimicrob Agents 29, 108-111, 2007.
31. Arikan S, Sancak B, Alp S, Hascelik G, Mcnicholas P. Comparative *in vitro* activities of posaconazole, voriconazole, itraconazole, and amphotericin B against Aspergillus and Rhizopus, and synergy testing for Rhizopus. Med Mycol 46, 567-573, 2008.
32. Pfaller MA, Diekema DJ, Rinaldi MG, Barnes R, Hu B, Veselov AV, Tiraboschi N, Nagy E, Gibbs DL. Results from the ARTEMIS DISK global antifungal surveillance study: a 6.5-year analysis of susceptibilities of candida and other yeast species to fluconazole and voriconazole by standardized disk diffusion testing. J Clin Microbiol 43(12), 5848-5859, 2005.

Received : 31.01.2016
Accepted : 24.03.2016

Turk J Pharm Sci 13(3), 318-322, 2016
DOI: 10.4274/tjps.2016.06

ORIGINAL ARTICLE

Determination of Cytotoxic and Anticandidal Activities of Three *Verbascum L.* Species from Turkey: *V. cheiranthifolium* Boiss. var. *asperulum* (Boiss.) Murb. Monorg., *V. pycnostachyum* Boiss. & Heldr and *V. orgyale* Boiss. & Heldr

Türkiye'den Üç *Verbascum L.* Türünün Sitotoksik ve Antikandidal Aktivitelerinin Belirlenmesi; *Verbascum cheiranthifolium* Boiss. var. *Asperulum* (Boiss.) Murb. Monorg., *Verbascum pynostachyum* Boiss. & Heldr ve *Verbascum orgyale* Boiss. & Heldr

Sevim KÜÇÜK[1]*, Filiz ÖZDEMİR[2], Gökalp İŞCAN[3], Zerrin İNCESU[2]

[1]Anadolu University, Faculty of Pharmacy, Department of Pharmaceutical Botany, Eskişehir, TURKEY
[2]Anadolu University, Faculty of Pharmacy, Department of Biochemistry, Eskişehir, TURKEY
[3]Anadolu University, Faculty of Pharmacy, Department of Pharmacognosy, Eskişehir, TURKEY

ABSTRACT

Purpose of this study is to determine of cytotoxic and *anticandidal* activities of *Verbascum cheiranthifolium* Boiss. var. *asperulum* (Boiss.) Murb. Monorg., *Verbascum pynostachyum* Boiss. & Heldr and *Verbascum orgyale* Boiss. & Heldr belonging to *Verbascum* genus growing in Turkey. The cytotoxic effects of methanolic extract of Verbascum *cheiranthifolium* var. *asperulum*, *V. pycnostachyum* and *V. orgyale* species on the cervical (HeLa) and ovarian cancer (Skov-3) cells were investigated using colorimetric assay. The results indicated that methanolic-extract of *V. pycnostachyum* had a promising toxic effect on both cell lines as compared to the other species. Furthermore, this effect was more significant on Skov-3 cells rather than HeLa cells. Anticandidal effects of the methanolic extracts were evaluated in comparison with standard antifungal agents according to Clinical Laboratory Standards Institute (CLSI) reference methods, for the first time here. *V. pynostactum* and *V. orygale* extracts were demonstrated stronger inhibitory effects than the *V. cheriantifolium* var. *asperulum*. Remarkably, *Candida krusei* was inhibited by *V. pycnostachyum* extract at the concentration of the 62.5 µg/mL.

Key words: Scrophulariaceae, *Verbascum*, Cytotoxicity, Anticandidal activities

ÖZ

Bu çalışmada Türkiye'de yetişen *Verbascum L.* cinsine ait üç türün; *Verbascum cheiranthifolium* Boiss. var. *asperulum* (Boiss.) Murb. Monorg., V. *pycnostachyum* Boiss. & Heldr, ve *V. orgyale* Boiss. & Heldr. türlerinin sitotoksik ve antikandidal aktivitelerinin belirlenmesi amaçlanmıştır. *Verbascum cheiranthifolium* var. *asperulum*, *V. pycnostachyum* and *V. orgyale* türlerinin metanol ekstrelerinin sitotoksik etkileri servikal (HeLa) ve ovaryum kanser (Skov-3) hücrelerinde kolorimetrik metod kullanılarak araştırılmıştır. Elde edilen sonuçlar; *V. pycnostachyum* türünün metanol ekstresinin diğer türlere oranla her iki hücre hattında da umut verici toksik etkiye sahip olduğu gösterilmiştir. Buna ek olarak; bu etki Skov-3 hücrelerinde HeLa hücrelerine kıyasla daha anlamlıdır. Üç türe ait metanol ekstresinin antikandidal etkileri "Klinik Laboratuvar Standartları Enstitüsü" (CLSI)'nün mikrodilüsyon standart protokolleri kullanılarak standart antifungal ajanlarla karlılaştırmalı şekilde ilk kez bu çalışma ile ortaya konmuştur. *V. pycnostachyum* ve *V. orygale ekstreleri V. cheriantifolium*'a göre daha kuvvetli inhibitör etkiler göstermiştir. *Verbascum pycnostachyum* ekstresi dikkat çekici olarak *Candida krusei*'yi, 62.5 g/mL konsantrasyonda inhibe etmiştir.

Anahtar kelimeler: Scrophulariaceae, *Verbascum*, Sitotoksisite, Antikandidal aktivite

*Correspondence: E-mail: salan@anadolu.edu.tr Phone: +90 05452997214

INTRODUCTION

Verbascum L. (1753: 177) (Scrophulariaceae) includes about 360 species throughout world (1). In Turkey, with the additional 130 hybrids, the genus is represented by 246 species, 6 imperfectly known or doubtful records (2-5). The endemism ratio (80%) of the genus is very high with 196 endemic species (4,5).

In Turkey, the species *V. cheiranthifolium* var. *asperulum*, *V. pycnostachyum* and *V. orgyale* known as "Bozkulak", "Eğirdir sığır kuyruğu" and "Söke sığır kuyruğu" respectively (2,4).

Many plant species among the flora of Turkey play an important role in traditional medicine. There are approximately 9000 plant species, some of them are widely used in folkloric medicine due to their antimicrobial and anticarcinogenic properties, in Turkish flora (6,7). One of the well-known *Verbascum* species is *V. thapsus* L., which has been used for the treatment of several diseases including asthma, spasmodic cough, migraine and earache. Moreover, *V. thapsus, V. fruticulosum V. undulatum* and *V. georgicum* had anti-malarial and anti-viral effects that were investigated by both *in vitro* and *in vivo* studies (6).

It is reported that leaves and flowers of *Verbascum* species have expectorant, mucolytic and demulcent properties, and they are used to treat respiratory disorders such as bronchitis, dry coughs, tuberculosis, asthma in Anatolia (8,9). *Verbascum* species are also used to treat hemorrhoids, rheumatic pain, superficial fungal infections, wounds and diarrhea. Furthermore these species demonstrate several inhibitory activities against the murine lymphocytic leukemia and influenza viruses A2 and B. Macerated oil prepared from the flowers is used for reducing earache, applied externally for eczema and other types of inflammatory skin disorders (10).

Verbascum species have some folkloric usages such as sedative and treatment of dysmenorrhoea and rheumatalgia. It was also notified the usage for healing wounds in animal care.

Iridoid and neolignan type glycosides, oleanan type terpenes, flavonoids, polysaccharides, saponins, steroids and alkaloids were major compounds isolated from *Verbascum* species (11). In several bioactivity studies on *Verbascum sp.* reported that crude extracts of roots, leaves, flowers and aerial parts have been shown anti-proliferative (12), anti-inflammatory (13), antioxidant (14,15), anti-histaminic, anti-fungal, anti-bacterial, (16), wound healing (17), anti-microbial (18) and anti-cancer effects (19).

In the present study, three species belonging to *Verbascum* genus, were evaluated for their cytotoxic (on cervical and ovarian cancer cell lines) and anticandidal effects for the first time.

EXPERIMENTAL

Plant materials

The plant materials were collected from following localities; *Verbascum cheiranthifolium* var. *asperulum* B3 Eskişehir, Bozdağ region, 18.6.2014, 39° 53' 24'' K - 030° 33'' 16'' D, 1267 m, (ESSE:14686); *Verbascum pycnostachyum* C3: Antalya, Korkuteli-Fethiye region, 37º 02' 53'' N, 30º 06' 26'', 1370 m, 20.06.2007, ESSE 14730 (AKDU 6093) and *Verbascum orgyale* C3:Antalya: Antalya-Geyikbayırı region, 36° 52' 41'' N - 30° 26' 37'' E, 1008 m, 15.07.2007, (ESSE 14622, AKDU 6064) in Turkey. Voucher specimens are deposited in the Herbarium of the Faculty of Pharmacy (ESSE), Anadolu University in Eskişehir and Herbarium of the Biology Department, Akdeniz University in Antalya, Turkey (AKDU).

Extraction

Air dried plant materials were macerated with 70% MeOH (MERCK) at 25°C for 24h on orbital shaker. After evaporation and lyophilization steps the dry extract was kept at +4°C until bioactivity studies.

Cell culture

The human cervical adenocarcinoma cells (HeLa) were maintained in Eagle's Minimum Essential Medium (EMEM) (Sigma-Aldrich, UK) supplemented with 20% Fetal Bovine Serum (FBS) (Gibco, UK), 1% penicillin-streptomycin and 4% sodium bicarbonate as adherent monolayers. The human ovarian adenocarcinoma cells (Skov-3) were cultured in Dulbecco's Modified Eagle Medium (DMEM) (Sigma-Aldrich, UK) supplemented with 10% FBS and 1% penicillin-streptomycin. The cell lines were routinely subcultured using 0.25% tripsin-EDTA solution (Sigma-Aldrich, UK).

Stock solution of extract of *Verbascum sp*. were prepared in sterile ddH_2O and that was diluted in culture medium to prepare final concentrations of extracts. The cells were incubated with each *Verbascum sp*. (0,1-3 mg/mL) for 24 hours at 37°C (20).

Cell viability assay

MTT[3-(4,5-dimethylthiazol-2-yl)-2,5-diphenyl-2H-tetrazolium bromide] is a non-radioactive assay and measures the reduction of yellow MTT by mitochondrial succinate dehydrogenase. The reduction of MTT can only occur in metabolically active cells. The assay was performed as mentioned in Mossman. HeLa and Skov-3 cells (2×10^4) were seeded in 96-well plates in the presence and absence of different concentrations of *Verbascum sp*. for 24 hours at at 37°C in a 5% CO_2/95% air atmosphere. After incubation time, 20 ml of MTT (5 mg/mL) was added to each well and the cells were incubated for a further 2 hours. The reduction of MTT was measured by ELISA (ELX 808 IU) reader at a wavelength of 540 nm.

Viability (%)=(Absorbance of the treated cells) / (Absorbance of the control wells) ×100. Each concentrations was tested in two different experiments run in triplicate.

Anticandidal activity

Anticandidal activities of the methanolic extracts were evaluated by partly modified reference method of Clinical and Laboratory Standards Institute (*CLSI*) M27-A2 (21).

Candida albicans ATCC 90028, *C. utilis* NRRL Y-900, *C. glabrata* ATCC 66032, *C. tropicalis* ATCC 750, *C. parapsilosis* ATCC 22019 and *C. krusei* ATCC 6258 were used as pathogenic test microorganisms. Stock cultures stored in 50% glycerol at -85˚C, were inoculated in Mueller Hinton Agar (Acumedia) plates and incubated at 37˚C for 24 h for checking purity and viability. After incubation, selected colonies were suspended in 0.85% NaCl solution and adjusted to McFarland No: 0.5. Serial dilutions of the extracts were prepared in range of 4000 to 7 µg/mL. After incubation at 37˚C for 24h, MIC values was determined by visual reading of wells without growing. Amphotericin B (Sigma) and Ketoconazole (Sigma) were used as standard antifungal agents.

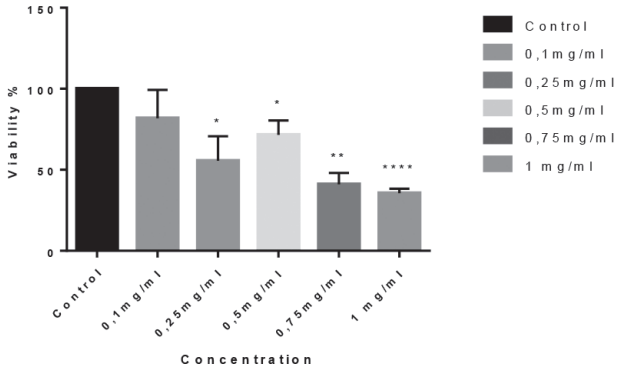

Verbascum pycnostochyum (A)

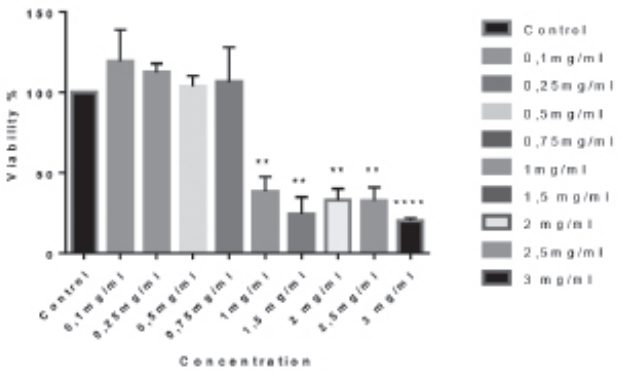

Verbascum cheiranthifolium var. *asperulum* (B)

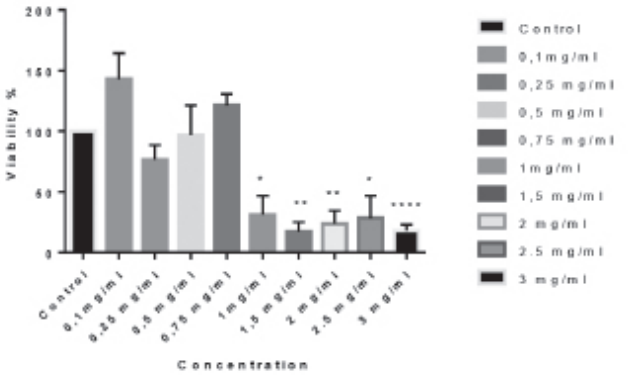

Verbascum orgyale (C)

Figure 1. Treatment of either *V. pycnostachyum*, *V. cheiranthifolium* var. *asperulum* or *V. orgyale* extracts with HeLa cells decreased the cell viability in a dose-dependent manner. *Bars* indicate mean ± standard deviation. All comparisons were made relative to untreated control cells. The significant differences were indicated as p< 0.05 using one-way ANOVA. The graphic was created by using GraphPad Prism 6 software. [*p<0.1; **p<0.01; ****p<0.001].

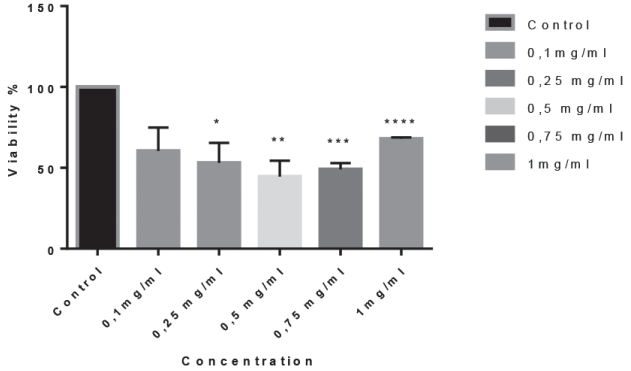

Verbascum pycnostochyum (A)

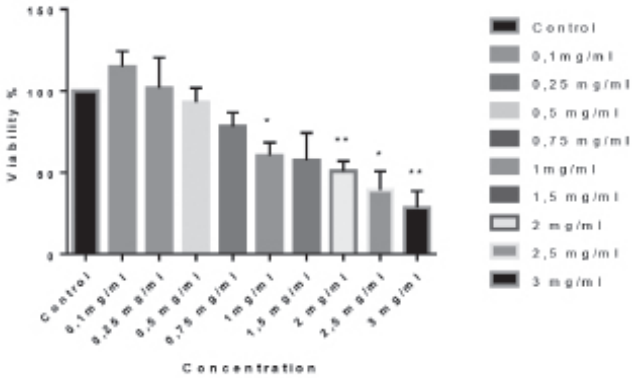

Verbascum cheiranthifolium var. *asperulum* (B)

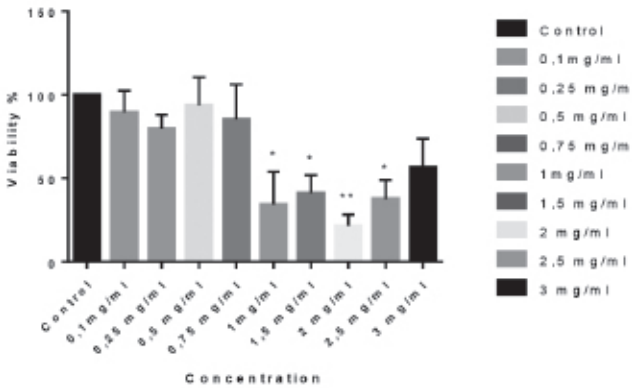

Verbascum orgyale (C)

Figure 2. The percentage of cell viability after treating Skov-3 cells with either *V. pycnostachyum*, *V. cheiranthifolium* var. *asperulum* or *V. orgyale* methanolic-extract. *Bars* indicate mean ± standard deviation. All comparisons were made relative to untreated control cells. The significant differences were indicated as p<0.05 using one-way ANOVA. The graphic was created by using GraphPad Prism 6 software. [*p<0.1; **p<0.01; ****p<0.001].

Table 1. Anticandidal Activity (µg/mL, MIC)

	C. albicans	*C. tropicalis*	*C. parapsilosis*	*C. utilis*	*C. glabrata*	*C. krusei*
V. cherianthifolium var. asperulum	1000	250	>4000	2000	>4000	250
V. orygale	125	250	125	250	>4000	125
V. pycnostachyum	1000	250	125	250	>4000	**62.5**
Amphotericin B	0.031	1.0	0.25	0.5	2.0	1.0
Ketoconazole	0.008	0.031	0.031	0.25	0.25	0.25

RESULTS AND DISCUSSION

Cytotoxicity results

The effects of V. pynostachyum, V. cheiranthifolium var. asperulum and V. orgyale methanol-extracts were assessed on HeLa (Figure 1) and Skov-3 (Figure 2) cells after 24 hours incubation with each extract using the MTT assay. The results obtained here indicated that all Verbascum *sp.* reduced the cell viability of both HeLa and Skov-3 cells in a dose-dependent manner. Particularly, the cell viability of both cell lines was significantly declined after treatment of V. pycnostachyum extract as compared to other Verbascum *sp.* that cytotoxic effect was observed at lower concentration (0.5 mg/mL - 44.62% cell viability) on Skov-3 cells rather than HeLa cells (0.5 mg/mL - 71.54% cell viability).

V. orgyale methanolic-extract was shown a similar effect on both cell lines; HeLa (1 mg/mL - 30.96% cell viability) (Figure 1C) and Skov-3 (1 mg/mL - 34.22% cell viability) (Figure 2C). On the other hand, a dramatic decrease in cell viability for HeLa was observed after incubation of 0.93 mg/mL V. cheiranthifolium var. asperulum methanol-extract (Figure 1B) as compared to the cell viability rate of Skov-3 cells treated with 2.01 mg/mL extract (Figure 2B).

The studies about the isolation of bioactive compounds have been reported that flavonoids, saponins, phenylpropanoid (12) and the phenylethanoid glycosides (22) were isolated although the type of bioactive compounds varies depending on the various *Verbascum sp.* Specifically, the isolation works on methanolic-extract and structure elucidation studies of *V. pynostachyum* were shown that it contained iridoids-glycosides, aukubin, ajugol, ajugosid, harpagoside, phenylethanoid glycoside and verbascoside (10). It has been reported that verbascoside has a hydrophilic character (19) and saponins (23) to possess anti-cancer and antimicrobial activity.

In this study, particularly *V. pynostachyum* species having a significant cytotoxic effect on Skov-3 cells that might be caused by the compounds such as verbascoside. However, in order to explain the relationship between activity-structure, it is necessary to determine the content of bioactive compounds of *V. pynostachyum* methanolic-extract.

Anticandidal activity results

Anticandidal activities of the methanolic extracts of *V. cherianthifolium* var. *asperulum, V. orygale* and *V. pynostachyum* were evaluated by using CLSI M27-A2 reference method. Tested *Candida* species were moderately inhibited by the extracts between the concentrations of the 62,5-4000 µg/mL (minimal inhibitory concentration). Remarkably, *V. pynostachyum* showed strong effects on *Candida krusei* having a MIC value of 62,5 µg/mL. *V. orygale* and *V. pynostachyum* demonstrated better effects than *Verbascum cherianthifolium* var. *asperulum* against all tested *Candida* strains. All extracts were assumed to have the MIC values outside of the tested range against *Candida glabrata* ATCC 66032 (Table 1). In the previous study on *Verbascum* species, extract of the *V. sinuatum* L. showed anticandidal effect at the concentration of 32 µg/mL against *C. albicans* (25). In another study methanolic extract of the *V. georgicum* which have antimicrobial constituents reported as a novel antimicrobial raw material (6). According to a scientific review on bioactivities of *Verbascum* species, methanol and ethanol extracts showed strong inhibitory effects on *Candida albicans* and Gram (+) bacteria strains due to the their saponin content (26).

Today, especially in immunocompromised people, *Candida* infections causes major health problems. There are few available systemic antifungal drugs, additionally the rate of drug resistance is increasing dramatically to available drugs. The search for new natural antifungal agents against pathogenic *Candida* species is extremely important (24).

ACKNOWLEDGMENTS

The authors would like to thank Bio. Nur İpek Önder and BİBAM for invaluable help in cytotoxic assay and lyophilisation. This study was supported by the Anadolu University, Commission of the Scientific Research Projects (No: 1304S069).

REFERENCES

1. Mabberley, DJ. Mabberley's plant-book (3th ed.). Cambridge University Press, Cambridge: XVIII , 1021, 2008.
2. Huber-Morath A. *Verbascum* L., In: Davis, P.H. (Ed.). Flora of Turkey and The East Aegean Islands, University Press, Edinburgh, Vol.6, pp 453-603, 1978.
3. Davis PH, Mill RR, Tan K. (Eds). Flora of Turkey and The East Aegean Islands (Suplement), Vol.10, University Press, Edinburgh, pp 190-2, 1988.
4. Karavelioğulları FA, *Verbascum* L. *In*: Güner A, Aslan S, Ekim T, Vural M, Babaç MT. (eds.). Türkiye Bitkileri Listesi (Damarlı Bitkiler).

Nezahat Gökyiğit Botanik Bahçesi ve Flora Araştırmaları Derneği Yayını, İstanbul, pp 850-70, 2012.

5. Karavelioğulları FA, Yüce E, Başer B. *Verbascum duzgunbabadagensis* (Scrophulariaceae), a new species from eastern Anatolia, Turkey, Phytotaxa 181 (1), 047-053, 2014.
6. Sengül M, Ögütçü H, Adigüzel A, Sahin A, Kara A, Karaman I, Güllüce M. Antimicrobial Effects of *Verbascum georgicum* Bentham Extract, Turk J Bot 29, 105, 2005.
7. Baytop T. Türkiye'de Bitkiler ile Tedavi, 2. Baskı, Nobel Tıp Kitabevleri, Istanbul, pp 334-5, 1999.
8. Tuzlacı E. Şifa Niyetine, Türkiye'nin Bitkisel Halk İlaçları, Alfa Yayınları 1702, İstanbul, pp 379-383, 2006.
9. Senatore F, Rigano D, Formisano C, Grassia A, Basile A, Sorbo S. Phytogrowth-inhibitory and antibacterial activity of *Verbascum sinuatum*. Fitoterapia 78, 244, 2007.
10. Tatlı I, Schuhly W, Akdemir ZS. Secondary metabolites from bioactive methanolic extract of *Verbascum pycnostachyum* Bioss. Helder flowers. HU J Fac Pharm 27, 23-32, 2007.
11. Turker AU, Camper ND. Biological Activity of Common Mullein, A Medicinal Plant, J Ethnopharmacol 82, 117-125, 2002;
12. Klimek B, Stepien H. Effect of some constituents of mullein (*Verbascum sp.*) on proliferation of rat splenocytes *in vitro*, Eur J Pharm Sci 2, 123, 1994.
13. Lee JH, Lee JY, Kang HS, Jeong CH, Moon JH, Whang WK. The effect of acteoside on histamine release and arachidonic acid release in RBL-2H3 mast cells. Arch Pharm Res 29, 508–13, 2006.
14. Alan S, Saltan FZ, Göktürk RS, Sökmen M, Taxonomical Properties of Three *Verbascum* L. Species Growing In Tukey and Their Antioxidant Activities, Asian J Chem 21, 5438-5452, 2009.
15. Quirantes-Piné R, Herranz-Lopez M, Funes L, Borrás-Linares I, Micol V, Segura-Carretero A. Phenylpropanoids and their metabolites are the major compounds responsible for blood-cell protection against oxidative stress after administration of *Lippia citriodora* in rats, Phytomedicine 20, 1112–8, 2013.
16. Abougazar H, Bedir E, Khan, IA, Çalış I, Wiedemannioside A-E: New Phenylethanoid Glycosides from the Roots of *Verbascum wiedemannianum*, Planta Medica 69(9) 814-9, 2003.
17. Mehdinezhad B, Rezaei A, Mohajeri D, Ashrafi A, Asmarian S, Sohrabi-Haghdost I, Hokmabad RV, Safarmashaei S. Comparison of *in vivo* wound healing activity of *Verbascum thapsus* flower extract with zinc oxide on experimental wound model in rabbits. Adv Environ Biol 5, 1501-9, 2011.
18. Dulger B, Kirmizi S, Arslan H, Güleryüz G. Antimicrobial activity of three endemic *Verbascum* species. Pharm Biol, 40, 587-9, 2002.
19. K orkina LG, Pastore S, Dellambra E, De Luca C. New molecular and cellular targets for chemoprevention and treatment of skin tumors by plant polyphenols: a critical review. Curr Med Chem, 20, 852–68, 2013.
20. Tatlı I, Akdemir Z.S. Cytotoxic Activity on Some Verbascum Species Growing in Turkey. Hacettepe University Journal of the Faculty of Pharmacy, 26:2, 77-85, 2006.
21. CLSI (NCCLS) M27-A2 Reference Method for Broth Dilution Antifungal Susceptibility Testing of Yeasts; Approved Standard—Second Edition, 2002.
22. Dembitsky VM. Astonishing diversity of natural surfactants: 5. Biologically active glycosides of aromatic metabolites. Lipids 40, 869–900, 2005.
23. Riaz M, Zia-Ul-Haq M, Jaafar HZE. Common mullein, pharmacological and chemical aspects. Rev Bras Farmacog 23, 948-59, 2013.
24. Moran GP, Sullivan DJ, Henman MC, McCreary CE, Harrington BJ, Shanley DB, Coleman DC, Antifungal drug susceptibilities of oral *Candida dubliniensis* isolates from human immunodeficiency virus (HIV)-infected and non-HIV-infected subjects and generation of stable fluconazole-resistant derivatives *in vitro*. Antimicrob Agents Ch 41, 617, 1997.
25. Amin JN, Batool M, Abu-hadid Mahmoud M, Screening antibacterial and antifungal activities and evaluation of the exhaustive extractions yields for *Verbascum sinuatum* L., Int J Res Ayurveda Pharm 6(1), 2015.
26. Tatlı II, Akdemir ZŞ, Traditional Uses and Biological Activities of *Verbascum* species, FABAD J Pharm Sci 31, 85-96, 2006.

Received : 04.02.2016
Accepted : 05.05.2016

Turk J Pharm Sci 13(3), 323-327, 2016
DOI: 10.4274/tjps.2016.07

ORIGINAL ARTICLE

The Importance of *Asphodeline* Species on Enzyme Inhibition: Anti-Elastase, Anti-Hyaluronidase and Anti-Collagenase Potential

Asphodeline Türlerinin Enzim İnhibisyonundaki Önemi: Anti-Elastaz, Anti-Hyalüronidaz ve Anti-Kollajenaz Potansiyeli

Mert İLHAN[1], Gökhan ZENGİN[2], Esra KÜPELİ AKKOL[1], Abdurrahman AKTÜMSEK[2], İpek SÜNTAR[1]*

[1]Gazi University, Faculty of Pharmacy, Department of Pharmacognosy, 06330 Ankara, TURKEY
[2]Selçuk University, Faculty of Science, Department of Biology, 42250 Konya, TURKEY

ABSTRACT

Asphodeline species are widespread in the inner Anatolia region in Turkey and used for the treatment of skin disorders, earaches and haemorrhoids. The aim of the present study is to investigate *in vitro* inhibitory effects of the extracts prepared from the stems, seeds, leaves and roots of *Asphodeline brevicaulis* subsp. *brevicaulis* var. *brevicaulis*, *A. baytopae* and *A. cilicica* on hyaluronidase, collagenase and elastase enzymes. Hyaluronidase, collagenase and elastase inhibitory effects of the extracts were performed by using *in vitro* enzyme inhibitory assays based on spectrophotometric evaluation. The methanol extract of the roots of *A. cilicica* displayed the highest hyaluronidase, collagenase and elastase inhibitory activities. On the other hand, the acetone extract of the roots of *A. cilicica*, the acetone extract of the leaves of *A. brevicaulis* subsp. *brevicaulis* var. *brevicaulis*, the acetone and the methanol extracts of seeds of *A. baytopae*, acetone and the methanol extract of the roots of *A. baytopae*, the aqueous extract of the stems of *A. cilicica*, the acetone and the methanol extracts of the leaves of *A. cilicica*, the aqueous extract of the roots of *A. cilicica* possessed significant collagenase, hyaluronidase and elastase inhibitory activities. In the present study, extracts of *Asphodeline* species significantly inhibited collagenase, elastase and hyaluronidase enzymes, suggesting their utilization for the treatment of wounds, cancer, cardiovascular diseases, inflammation, bone destruction and fibrosis, as well as skin aging.

Key words: *Asphodeline*, Xanthorrhoeaceae, Collagenase, Elastase, Hyaluronidase

ÖZ

Asphodeline türleri Türkiye'de İç Anadolu Bölgesi'nde geniş bir yayılış göstermektedir ve halk arasında deri hastalıkları, kulak ağrıları ve hemoroit gibi rahatsızlıklara karşı kullanılmaktadır. Bu çalışmanın amacı, *Asphodeline brevicaulis* subsp. *brevicaulis* var. *brevicaulis*, *A. baytopae* ve *A. cilicica* bitkilerinin gövde, tohum, yaprak ve köklerinden hazırlanan ekstrelerin hyalüronidaz, kollajenaz ve elastaz enzimleri üzerindeki *in vitro* inhibitor etkinliklerini araştırmaktır. Bu ekstrelerin inhibitor etkileri spektrofotometrik yöntemlerle değerlendirilmiştir. *A. cilicica* köklerinden hazırlanan metanol ekstresinin en yüksek hyalüronidaz, kollajenaz ve elastaz inhibitor aktivitelere sahip olduğu belirlenmiştir. Diğer yandan, *A. cilicica* köklerinden hazırlanan aseton ekstresinin, *A. brevicaulis* subsp. *brevicaulis* var. *brevicaulis* yapraklarından hazırlanan aseton ekstresinin, *A. baytopae* köklerinden ve tohumlarından hazırlanan aseton ve metanol ekstrelerinin, *A. cilicica* gövdesinden hazırlanan sulu ekstrenin, *A. cilicica* yapraklarından hazırlanan aseton ve metanol ekstrelerinin, *A. cilicica* köklerinden hazırlanan sulu ekstrenin önemli ölçüde kollajenaz, elastaz ve hyalüronidaz etki gösterdiği belirlenmiştir. Sonuç olarak bu çalışmada *Asphodeline* türlerinden hazırlanan ekstrelerin kollajenaz, elastaz ve hyalüronidaz enzimlerini önemli ölçüde inhibe ettiği ortaya koyulmuştur. Bu nedenle bu sonuçlar bitkinin yara, kanser, kardiyovasküler rahatsızlıklar, enflamasyon, kemik yıkımı ve fibrozis gibi hastalıkların tedavisinde kullanılabileceğini destekler niteliktedir.

Anahtar kelimeler: *Asphodeline*, Xanthorrhoeaceae, Kollajenaz, Elastaz, Hyalüronidaz

INTRODUCTION

Asphodeline Rchb. genus (Xanthorrhoeaceae), represented by 14 species in the world, is growing wild in south-west Asia and Middle-Eastern countries as well as in Mediterranean region. In Turkey, *Asphodeline* genus comprises of 20 taxa, 12 of which are endemic to Turkey showing that Turkey is one of the gene centres of this genus (1-3). In rural areas in Turkey, several *Asphodeline* species are known in the name of "çiriş" and are widespread in inner Anatolia region. Especially *Asphodeline cilicica* E. Tuzlacı, *A. damascena* (Boiss.) Baker, *A. globifera* J. Gay Ex Baker, *A. lutea* (L.) Rchb. and *A. taurica* (Pallas) Kunth are consumed as food in salads (4). This genus

*Correspondence: E-mail: ipesin@gazi.edu.tr Phone: +90 312 202 31 76

was recorded to have economical and nutritional importance with high levels of essential amino acids and polyphenols (3-7). Besides their nutritional properties, *Asphodeline* species also possess medicinal features and are employed in medical practices in traditional medicine. For instance, *A. globifera* has been used for alleviating the symptoms of haemorrhoids; *A. damascena* and *A. cilicica* were recorded to be utilized for the treatment of earaches (8); and *A. lutea* has been used for the treatment of skin diseases (9). Due to their mentioned use above, many phytochemical researches have been conducted on *Asphodeline* species revealing the presence of secondary metabolites such as antraquinones, sesquiterpenes, flavonoids and naphthalene type compounds (6,10-13). Enzymes have very important roles in the pathogenesis of several diseases including cancer, inflammation, Alzheimer's and Parkinson's diseases, familial hypercholesterolemia, myasthenia gravis etc. (14-17). Due to the important roles of these enzymes on several diseases, novel drugs that display inductive or inhibitory effects should be developed.

In the present research, *in vitro* inhibitory effects of the extracts obtained from the stems, seeds, leaves and roots of *A. brevicaulis* (Bertol.) J. Gay ex Baker subsp. *brevicaulis* (Bertol.) J. Gay ex Baker var. *brevicaulis* (Bertol.) J. Gay ex Baker, *A. baytopae* E. Tuzlacı and *A. cilicica* on hyaluronidase, collagenase and elastase enzymes, which are the major enzymes responsible for dehydration of the skin, were investigated.

EXPERIMENTAL

Plant materials

Asphodeline species were collected at the end of flowering stage (May-July) and information regarding the collection sites of the plants and herbarium numbers were presented in Table 1. Taxonomic identification of the plant materials were confirmed by the senior taxonomist Dr. Murad Aydın Sanda, from the Department of Biology, Selçuk University. The voucher specimens were deposited at the KNYA Herbarium of Department of Biology, Selçuk University, Konya, Turkey.

Preparation of the plant extracts

The plant materials (stem, root, seed and leaf) were dried at the room temperature. The dried parts were ground to a fine powder using a laboratory mill. For each of the powdered parts (10 g) were separately extracted with 250 mL acetone and methanol in a Soxhlet apparatus for 6-8 h. The residue was extracted with 250 mL hot distilled water for 30 min and the extracts were filtered concentrated under vacuum at 40°C by using a rotary evaporator. The aqueous extracts were lyophilized (-80°C, 48 h). Yields of the extracts were given in Table 1.

In vitro enzyme inhibitory assays

Hyaluronidase inhibiton assay

Hyaluronidase inhibiton assay was performed according to the methods described by Lee & Choi (1999) and Sahasrabudhe & Deodhar (2010) with some modifications (18-20).

An amount of 50 µL an aliquot of bovine hyaluronidase (7900 units/mL) was dissolved in 0.1 M acetate buffer (pH 3.6). This mixture then was mixed with 50 µL of different concentrations of the extracts prepared in 5% DMSO. An aliquot of 50 µL of 5% DMSO was added instead of the extracts in the control group. After incubation at 37°C for 20 min, 50 µL of calcium chloride (12.5 mM) was added to the mixture and reincubated for another 20 minutes at 37°C. 250 µL sodium hyaluronate (1.2 mg/mL) was added and incubated for 40 minutes at 37°C.

Table 1. The collection cites and herbarium numbers of Asphodeline species; parts used for the extraction, extract types and percentage yields of the extracts

Plant name	Collection site	Herbarium no	Extract type	Parts used	Yield (w/w, %)
A. brevicaulis subsp. *brevicaulis* var. *brevicaulis*	Mersin, Arslanköy, between Arslanköy and Yeniköy, 37° 00' 20.9"N, 34° 29' 24.6 E, alt. 1077 m	KNYA-GZ1004	Acetone	Sm/ R/ Lf / Sd	1.73/ 1.28/ 2.71/ 3.91
			Methanol		12.64/ 16.04/ 11.21/ 10.27
			Aqueous		18.05/ 14.1/ 20.35/ 20.41
A. baytopae	Mersin, Gulnar, between Gulnar and Aydincik, 36° 16' 07" N, 33° 22' 11" E, alt. 751 m	KNYA-GZ1003	Acetone	Sm/ R/ Lf / Sd	0.88/ 4.68/ 2.66/ 2.71
			Methanol		4,16/ 39.06/ 22.38/ 6.42
			Aqueous		4.32/ 27.56/ 25.91/ 10.00
A. cilicica	Adana, between Catalan and Aladag, 37° 27'37'' N, 35° 20' 12'' E, alt. 1080 m	KNYA-GZ1005	Acetone	Sm/ R/ Lf / Sd	2.88/ 2.42/ 4.07/ 3.52
			Methanol		8.85/ 7.39/ 13.32/ 14.47
			Aqueous		10.78/ 9.35/ 13.04/ 24.49

Abbreviations: alt.: altitude; Sm: Stem, R: Root, L: Leaf, Sd: Seed

Table 2. Collagenase and elastase inhibitory activity of the extracts of *Asphodeline* species

Material	Parts used	Extract type	Concentration (µg/mL)	Collagnease inhibition (%) ± S.E.M.	Elastase inhibition (%) ± S.E.M.
A. brevicaulis subsp. *brevicaulis* var. *brevicaulis*	Stem	Acetone	100	15.79±1.83	19.43±1.95
		Methanol	100	14.66±1.48	12.63±1.59
		Aqueous	100	15.99±1.64	19.47±1.93
	Seed	Acetone	100	13.44±2.14	8.12±1.66
		Methanol	100	17.06±1.64	16.42±1.82
		Aqueous	100	14.73±2.14	10.17±2.34
	Leaf	Acetone	100	**31.38±1.14****	**39.39±1.61****
		Methanol	100	10.93±2.26	8.37±2.11
		Aqueous	100	8.66±1.22	6.30±1.82
	Root	Acetone	100	20.34±2.42	22.49±2.22
		Methanol	100	23.64±2.31	28.78±1.98
		Aqueous	100	14.38±1.91	15.85±1.80
A. baytopae	Stem	Acetone	100	19.31±2.64	25.46±1.64
		Methanol	100	13.43±2.54	20.10±1.76
		Aqueous	100	7.56±1.48	9.29±1.84
	Seed	Acetone	100	**30.55±1.28****	**40.22±1.46****
		Methanol	100	**37.22±1.40*****	**42.32±1.76****
		Aqueous	100	9.53±1.82	11.83±1.80
	Leaf	Acetone	100	16.33±1.77	18.29±1.85
		Methanol	100	18.89±1.82	21.16±2.34
		Aqueous	100	8.46±2.54	9.68±1.49
	Root	Acetone	100	**31.70±1.56****	**41.51±1.40****
		Methanol	100	**29.85±2.49***	**31.88±1.92***
		Aqueous	100	10.36±1.99	14.87±1.55
A. cilicica	Stem	Acetone	100	12.26±2.83	14.64±1.72
		Methanol	100	9.41±1.34	7.84±1.90
		Aqueous	100	**35.38±1.43*****	**45.97±1.44****
	Seed	Acetone	100	16.66±2.04	20.66±1.89
		Methanol	100	15.36±1.92	18.54±2.34
		Aqueous	100	8.52±1.78	9.44±1.62
	Leaf	Acetone	100	**36.71±1.21****	**43.32±1.58****
		Methanol	100	**34.22±1.49****	**47.42±1.41****
		Aqueous	100	8.33±1.63	13.83±1.63
	Root	Acetone	100	**37.61±1.73*****	**48.44±1.53****
		Methanol	100	**39.90±1.15*****	**53.78±1.33****
		Aqueous	100	**28.77±1.70***	**30.15±1.70***
Epigallocathecin gallate			100	**48.62±1.14*****	**84.31±1.24*****

*: p<0.05; **: p<0.01; ***: p<0.001; S.E.M.: Standard error of the mean

The mixture was treated with 50 µL of 0.4 M NaOH and 100 µL of 0.2 M sodium borate and then incubated for 3 min in the boiling water. *p*-Dimethylaminobenzaldehyde solution (1.5 mL) was added to the reaction mixture after cooling to room temperature and was further incubated at 37°C for 20 minutes to develop a color. The absorbance of this colored solution was measured at 585 nm by using Beckmann Dual Spectrometer (Beckman, Fullerton, CA, USA).

Collagenase inhibiton assay

The method for the collagenase inhibition was performed according to the method of Barrantes & Guinea (2003) with some modifications (20,21).

The samples were dissolved in DMSO. *Clostridium histolyticum* (ChC) was dissolved in 50 mM Tricine buffer (with 0.4M NaCl and 0.01M $CaCl_2$, pH 7.5). Then, 2 mM N-[3-(2-Furyl)acryloyl]-Leu-Gly-Pro-Ala (FALGPA) solution was prepared in the same buffer. 25 µL buffer, 25 µL test sample and 25 µL enzyme were added to each well and incubated for 15 minutes. 50 µL substrate was added into the mixture. The decrease of the optical density (OD) was immediately measured at 340 nm using a spectrophotometer.

The ChC inhibitory activity of each sample was calculated according to the following formula:

ChC inhibition activity (%)= $OD_{Control} - OD_{Sample} \times 100 / OD_{Control}$ where $OD_{control}$ and OD_{sample} represent the optical densities in the absence and presence of sample, respectively.

Elastase inhibiton assay

According to the method described by Melzig et al. (2001), the sample solution and human neutrophil elastase enzyme (HNE) (17 mU/mL) were mixed in 0.1 M Tris-HCl buffer (pH 7.5). The mixture was incubated at 25°C for 5 min. N-Methoxysuccinyl-Ala-Ala-Pro-Val *p*-nitroanilide (MAAPVN) was added into the mixture and incubated at 37°C for 1 h. By the addition of 1 mg/mL soybean trypsin inhibitor, the reaction was stopped and the optical density was immediately measured at 405 nm. The HNE inhibitory activities were calculated according to the equation given in the ChC inhibitory assay (20,22).

Statistical analysis of the data

The data was statistically analyzed using one-way analysis of variance (ANOVA). The values of $p \leq 0.05$ were considered statistically significant.

RESULTS

Turkey is considered as one of the gene centers of *Asphodeline* genus with 20 taxa, as it is represented in Europe by only three species. Plants of the genus *Asphodeline* have traditionally been used as either food or therapeutical agent in various parts of the world as well as in Turkey (1,2). In the previous study, *Asphodeline* species were found to possess acetylcholinesterase, butyrylcholinesterase, amylase, glucosidase and tyrosinase inhibitory activities (3). Indeed, enzymes are known to be involved in the pathogenesis of several diseases, for instance hyaluronidase, collagenase and elastase enzymes involves in the pathogenesis of wound, cancer, cardiovascular diseases, inflammation, bone destruction and fibrosis (20,23-26). Collagen and elastin are the major components of the connective tissue and hyaluronic acid keeps the moist.

Table 3. Hyaluronidase inhibitory activity of the extracts of *Asphodeline* species

Material	Parts used	Extract type	Concentration (µg/mL)	Hyaluronidase inhibition (%) ± S.E.M.
A. brevicaulis subsp. *brevicaulis* var. *brevicaulis*	Stem	Acetone	100	20.16±1.42
		Methanol	100	15.72±1.93
		Aqueous	100	14.78±2.16
	Seed	Acetone	100	20.16±1.42
		Methanol	100	15.72±1.93
		Aqueous	100	14.78±1.46
	Leaf	Acetone	100	21.49±1.32
		Methanol	100	15.72±1.93
		Aqueous	100	14.78±2.16
	Root	Acetone	100	27.55±1.82
		Methanol	100	28.12±1.74
		Aqueous	100	14.39±1.44
A. baytopae	Stem	Acetone	100	27.48±2.69
		Methanol	100	12.64±1.81
		Aqueous	100	7.74±1.21
	Seed	Acetone	100	29.95±1.86
		Methanol	100	28.67±1.72
		Aqueous	100	10.46±2.18
	Leaf	Acetone	100	22.83±1.39
		Methanol	100	28.37±2.66
		Aqueous	100	18.53±2.28
	Root	Acetone	100	**35.14±1.44***
		Methanol	100	18.22±1.93
		Aqueous	100	13.82±2.94
A. cilicica	Stem	Acetone	100	17.26±1.95
		Methanol	100	9.50±1.38
		Aqueous	100	**45.51±1.25****
	Seed	Acetone	100	32.29±2.12
		Methanol	100	16.23±2.19
		Aqueous	100	12.21±1.63
	Leaf	Acetone	100	**39.26±1.11****
		Methanol	100	*42.30±1.14***
		Aqueous	100	16.48±1.86
	Root	Acetone	100	**47.20±1.01****
		Methanol	100	**49.49±1.17****
		Aqueous	100	25.14±1.81
Tannic acid			100	**87.33±0.94*****

*: p<0.05; **: p<0.01; ***: p<0.001; S.E.M.: Standard error of the mean

Inhibition of hyaluronidase, collagenase and elastase enzymes could therefore improve skin aging (20,27-29). In the present study we aimed to investigate *in vitro* inhibitory effects of the extracts prepared from the different parts of *A. baytopae, A. brevicaulis* subsp. *brevicaulis* var. *brevicaulis*, *A. cilicica* on hyaluronidase, collagenase and elastase enzymes.

The results revealed that the methanol extract prepared from the roots of *A. cilicica* (ACRM) displayed the highest hyaluronidase, collagenase and elastase inhibitory activity with the inhibition value of 49.49%, 39.90% and 53.78%, respectively. It was also found that acetone extract of the roots of *A. cilicica* (ACRAc) demonstrated 37.61% and 48.44% inhibitiory effect on collagenase and elastase enzymes, respectively. In addition, acetone extract of the leaves of *A. brevicaulis* subsp. *brevicaulis* var. *brevicaulis* (ABrLAc) demonstrated inhibitiory effect with the values of 31.38% and 39.39% on collagenase and elastase enzymes, respectively. Acetone and methanol extracts of the seeds of *A. baytopae* (ABaSdAc and ABaSdM), acetone and methanol extracts of the roots of *A. baytopae* (ABaRAc and ABaRM), aqueous extract of the stems of *A. cilicica* (ACSmAq), acetone and methanol extracts of the leaves of *A. cilicica* (ACLAc and ACLM), aqueous extract of the roots of *A. cilicica* (ACRAq) possessed significant collagenase and elastase inhibitory activities. On the other hand, ABaRAc, ACSmAq, ACLAc, ACLM and ACRAc were detected to possess significant hyaluronidase inhibitory effect (Table 2 and 3).

DISCUSSION

According to the ethnobotanical studies, *Asphodeline* species such as *A. cilicica*, *A. damascena*, *A. globifera*, *A. lutea*, and *A. taurica* are consumed as food in salads (4). Due to the information regarding its consumption as food, the nutritional features of these species were investigated in our previous research revealing their high amount amino acid composition (4). *Asphodeline* species are used not only as food, but also as therapeutic agents for earaches, skin disorders and haemorrhoids in folk medicine (8,9,13). Due to their several medicinal utilization by people living in rural areas, *Asphodeline* species recently have attracted the researchers' attention to either verify the therapeutical usage in scientific platform or to investigate the phytochemical ingredients.

There have been several studies indicating the enzyme inhibitory activities of phenolic compounds and anthraquinones. Sawabe et al. (1998) investigated the inhibitory effects of water extracts obtained from sixty-six natural medicines on hyaluronidase, elastase and tyrosinase enzymes. The study pointed out that the enzyme inhibitory effect is positively correlated with high amount of phenolic content (30). Moreover, Lee et al. (2001) isolated a new phenolic compound, encoded CC-517, from *Areca catechu* L. and revealed its significant anti-hyaluronidase and anti-elastase activities. The compound inhibited human neutrophil elastase with the IC_{50} value of 60.8 µg/mL; hyaluronidase with the IC_{50} value of 210 µg/mL. It also exhibited more potent elastase inhibitory effect than oleanolic acid and ursolic acid (31).

Tanaka et al. (1990) conducted a study on collagenase inhibitory effect of 44 anthraquinone type compounds. Results of the

study demonstrated the inhibitory activity of anthraquinones, amongst emodin being the most potent active inhibitor with the IC_{50} value of $4x10^{-5}$ M (32). Furthermore, Zembower et al. (1992) synthesized several anthraquinone analogues and evaluated their elastase inhibitory activity on human leukocyte. Consequently, it was reported that 1,8 dihydroxyanthraquinone analogues possess elastase inhibitory effect (33).

Previous researches reported that *Asphodeline* species have high antioxidant capacity and phenolic content (7,13,34). Similarly, Zengin et al. (2015) recently investigated the antioxidant and enzyme inhibitory effects as well as anthraquinone profile of the methanol extracts obtained from the roots of eight *Asphodeline* species. According to the results, *A. cilicica* was found to possess the highest total phenolic content, while *A. brevicaulis* subsp. *brevicaulis* var. *brevicaulis* and *A. baytopae* had the highest total anthraquinone content. Therefore, the inhibitory effects of *A. cilicica, A. brevicaulis* subsp. *brevicaulis* var. *brevicaulis* and *A. baytopae* could be attributed to its phenolic and anthraquinone contents (3).

CONCLUSION

In the present study, ACRM, ACRAc, ABrLAc, ABaSdAc, ABaSdM, ABaRAc, ABaRM, ACSmAq, ACRAq significantly inhibited collagenase, elastase and hyaluronidase enzymes, suggesting that these extracts could be used for the treatment of several diseases including wound, cancer, cardiovascular diseases, inflammation, bone destruction and fibrosis as well as potential ingredients for the cosmetic formulations to avoid skin aging.

REFERENCES

1. Mathews VA, Tuzlaci E, *Asphodeline* Reichb. In: Flora of Turkey and East Aegean Islands, Ed(s): P.H. Davis, pp. 88-97, University Press, Edinburgh, 1984.
2. Tuzlaci E, Revision of the genus *Asphodeline* (Liliaceae). A new infrageneric classification, Candollea 42, 559-576, 1987.
3. Zengin G, Locatelli M, Ceylan R, Aktumsek A, Anthraquinone profile, antioxidant and enzyme inhibitory effect of root extracts of eight *Asphodeline* taxa from Turkey: Can *Asphodeline* roots be considered as a new source of natural compounds?, J Enzyme Inhib Med Chem 1-6, 2015.
4. Zengin G, Aktumsek A, Guler GO, Cakmak YS, Giron-Calle J, Alaiz M, Vioque J, Nutritional quality of protein in the leaves of eleven *Asphodeline* species (Liliaceae) from Turkey., Food Chem 135, 1360-1364, 2012.
5. Lazarova I, Marinova E, Todorova-Nikolova G, Kostova I, Antioxidant properties of *Asphodeline lutea* of Bulgarian origin, Riv Ital Sostanze Gr 86, 181-188, 2009.
6. Todorova G, Lazarova I, Mikhova B, Kostova I, Anthraquinone, naphtalene, and napthoquinone components of *Asphodeline lutea*, Chem Nat Compd 46, 322-323, 2010.
7. Lazarova I, Zengin G, Aktumsek A, Gevrenova R, Ceylan R, Uysal S, HPLC–DAD analysis of phenolic compounds and antioxidant properties of *Asphodeline lutea* roots from Bulgaria and Turkey, Ind Crops Prod 61, 438-441, 2014.
8. Tuzlaci E, Çiriş plants of Turkey, J Pharm Marmara 1, 69-89, 1985.
9. Ali-Shtayeh MS, Yaniv Z, Mahajna J, Ethnobotanical survey in the Palestinian area: A classification of the healing potential of medicinal plants, J Ethnopharmacol 73, 221-232, 2000.
10. Ulubelen A, Tuzlaci E, Sesquiterpene lactones, flavonoids and anthraquinones from *Asphodeline globifera* and *Asphodeline damascena*, Phytochemistry 24, 2923-2924, 1985.
11. Ulubelen A, Terem B, Tuzlaci E, Antraquinones and sesquiterpene lactones from *Asphodeline anatolica*, Fitoterapia 2, 159, 1988.
12. Ulubelen A, Tuzlaci E, Atılan N, Antraquinones and sesquiterpene lactones from Asphodeline anatolica, Fitoterapia 2, 159, 1989.
13. Zengin G, Aktumsek A, Investigation of antioxidant potentials of solvent extracts from different anatomical parts of *Asphodeline anatolica* E. Tuzlaci: An endemic plant to Turkey, Afr J Tradit Complement Altern Med 11, 481-488, 2014.
14. Kolins J, Gilroy J, Serum enzyme levels in patients with myasthenia gravis afte aerobic and ischaemic exercise, J Neurol Neurosurg Psychiatry 35, 34-40, 1972.
15. Goldstein JL, Brown MS, Familial hypercholesterolemia: identification of a defect in the regulation of 3-hydroxy-3-methylglutaryl coenzyme A reductase activity associated with overproduction of cholesterol, Proc Natl Acad Sci U S A 70, 2804-2808, 1973.
16. Goldstein M, Lieberman A, The role of the regulatory enzymes of catecholamine synthesis in Parkinson's disease, Neurology 42, 8-12, 1992.
17. Cole SL, Vassar R, The Alzheimer's disease beta-secretase enzyme, BACE1, Mol Neurodegener 2, 22, 2007.
18. Lee KK, Choi JD, The effects of *Areca catechu* L extract on anti-aging, Int J Cosmet Sci 21, 285-295, 1999.
19. Sahasrabudhe A, Deodhar M, Anti-hyaluronidase, anti-elastase activity of *Garcinia indica*, Int J Bot 6, 299-303, 2010.
20. Suntar I, Kupeli Akkol E, Keles H, Yesilada E, Sarker SD, Arroo R, Baykal T, Efficacy of *Daphne oleoides* subsp. *kurdica* used for wound healing: identification of active compounds through bioassay guided isolation technique, J Ethnopharmacol 141, 1058-1070, 2012.
21. Barrantes E, Guinea M, Inhibition of collagenase and metalloproteinases by aloins and aloe gel, Life Sci 72, 843-850, 2003.
22. Melzig MF, Loser B, Ciesielski S, Inhibition of neutrophil elastase activity by phenolic compounds from plants, Pharmazie 56, 967-970, 2001.
23. Girish KS, Kemparaju K, Nagaraju S, Vishwanath BS, Hyaluronidase inhibitors: A biological and therapeutic perspective, Curr Med Chem 16, 2261-2288, 2009.
24. Alam SR, Newby DE, Henriksen PA, Role of the endogenous elastase inhibitor, elafin, in cardiovascular injury: from epithelium to endothelium, Biochem Pharmacol 83, 695-704, 2012.
25. Moroy G, Alix AJ, Sapi J, Hornebeck W, Bourguet E, Neutrophil elastase as a target in lung cancer, Anticancer Agents Med Chem 12, 565-579, 2012.
26. Kumar V, Abbas AK, Aster JC, Robbins SL, Robbins basic pathology. 9th ed. Philadelphia, Elsevier, 2013.
27. Demina NS, Lysenko SV, Collagenolytic enzymes synthesized by microorganisms, Mikrobiologiia 65, 293-304, 1996.
28. Thring TS, Hili P, Naughton DP, Anti-collagenase, anti-elastase and anti-oxidant activities of extracts from 21 plants, BMC Complement Altern Med 9, 27, 2009.
29. Abdul Wahab N, Abdul Rahman R, Ismail A, Mustafa S, Hashim P, Assessment of antioxidant capacity, anti-collagenase and anti-elastase assays of Malaysian unfermented cocoa bean for cosmetic application, Nat Prod Chem Res 2, 2014.
30. Sawabe Y, Yamasaki K, Iwagami S, Kajimura K, Nakagomi K, Inhibitory effects of natural medicines on the enzymes related to the skin, Yakugaku Zasshi 118, 423-429, 1998.
31. Lee KK, Cho JJ, Park EJ, Choi JD, Anti-elastase and anti-hyaluronidase of phenolic substance from *Areca catechu* as a new anti-ageing agent, Int J Cosmet Sci 23, 341-346, 2001.
32. Tanaka T, Metori K, Mineo S, Matsumoto H, Satoh T, Studies on collagenase inhibitors. II. Inhibitory effects of anthraquinones on bacterial collagenase., Yakugaku Zasshi 110, 688-692, 1990.
33. Zembower DE, Kam CM, Powers JC, Zalkow LH, Novel anthraquinone inhibitors of human leukocyte elastase and cathepsin G, J Med Chem 35, 1597-1605, 1992.
34. Atasü E, Flavonoids of *Asphodeline lutea* Reichb. flowers, J Fac Pharm Ankara 10, 102-111, 1980.

Received : 17.03.2016
Accepted : 18.03.2016

Turk J Pharm Sci 13(3), 328-334, 2016
DOI: 10.4274/tjps.2016.08

ORIGINAL ARTICLE

Gastroprotective Effects of Various *Scrophularia striata* Extracts on Ethanol-Induced Gastric Ulcer in Rats

Scrophularia striata Ekstrelerinin Ratlarda oluşturulan Etanol-Nedenli Gastrik Ülser Modeli Üzerindeki Gastroprotektif Etkileri

Maryam RAFIEI[1], Fatemeh NAMAZI[2,*], Hamid RAJAIAN[1], Saeed NAZIFI[3]

[1]Shiraz University, School of Veterinary Medicine, Department of Basic Sciences, Shiraz, IRAN
[2]Shiraz University, School of Veterinary Medicine, Department of Pathobiology, Shiraz, IRAN
[3]Shiraz University, School of Veterinary Medicine, Department of Clinical Studies, Shiraz, IRAN

ABSTRACT

This study was conducted to investigate the influence of various extracts of *S. striata* in ethanol-induced gastric ulcer model in rats. 100 male rats were divided into 10 groups and received the following medications: Normal control group without treatment; comparative standard control group received 20 mg/kg omeprazole; Groups 4-9 were given aqueous, hydroalcoholic and etheric extracts at 100 and 400 mg/kg, respectively; vehicle control group given DMSO as solvent solution. After one hour all the rats (except normal control group) and also ulcer control group were given 4 mL/kg 75% EtOH solution to induce ulceration. The rats were sacrificed after one hour; the gastric mucosal injuries were estimated through assessment of the gross appearance of ulcer areas, histopathology and parameters including MDA, TAC, PGE_2 and HSP70 in the gastric tissue homogenate. The ulcer control group showed severe mucosal injury compared with aqueous and etheric extracts which grossly showed significant reduction of ulcer areas and histopathologically showed marked reduction of mucosal necrosis, edema and leukocytes infiltration. A significant increase in the levels of HSP70, PGE_2 and TAC with a reduction in the level of MDA was observed in the rats treated with etheric and especially aqueous extracts. The results of the present study revealed significant protection of *S. striata* towards ethanol-induced gastric mucosal injury.

Key words: Ethanol, Gastric ulcer, Gastroprotective, *Scrophularia striata*, Antioxidant, Histopathology

ÖZ

Bu çalışma, *Scrophularia striata'nın* farklı polaritedeki ekstrelerinin ratlarda etanol-nedenli gastrik ülser modelindeki etkisini araştırmak amacıyla yürütüldü. Yüz erkek sıçan 10 gruba ayrıldı: Normal kontrol grubu hayvanlarına hiçbir tedavi uygulanmadı; karşılaştırmalı standart kontrol grubuna 20 mg/kg omeprazol; grup 4-9'a sırasıyla 100 ve 400 mg/kg dozlarda sulu, sulu alkollü ve eterli ekstreler; taşıyıcı kontrol grubuna ise çözücü olarak DMSO uygulandı. Bir saat sonra ülser oluşturmak için tüm ratlara (normal kontrol grubu dışında) ve ülser kontrol grubuna 4 mL/kg %75 ETOH verildi. Ratlar bir saat sonra sakrifiye edildi; gastrik mukozal hasarlar, gözle görünür ülser bölgelerinin tespit edilmesiyle, histopatolojik analizlerle ve mide dokusu homojenatında MDA, TAC, PGE_2 ve HSP70 belirlenmesiyle değerlendirildi. Ülser kontrol grubunda şiddetli mukozal hasar tespit edilirken, sulu ve eterli ekstre grubunda ülser alanlarında anlamlı küçülme, histopatolojik analizlerde mukozal nekrozda, ödem ve lökosit infiltrasyonunda azalma tespit edildi. Sulu ve eterli ekstre ile tedavi edilen ratlarda HSP70, PGE_2 ve TAC seviyelerinin anlamlı bir şekilde arttığı, MDA seviyesinin ise azaldığı görüldü. Çalışma sonuçları, etanol-nedenli gastrik mukozal hasara karşı *Scrophularia striata'nın* anlamlı derecede koruyucu etki sağladığını gösterdi.

Anahtar kelimeler: Etanol, Gastrik ülser, Gastroprotektif, *Scrophularia striata*, Antioksidan, Histopatoloji

INTRODUCTION

Peptic ulcer disease is one of the most common disruptions of the mucosal integrity of the stomach (a gastric ulcer) and small intestine (a duodenal ulcer) (1). It has generally been accepted that gastric ulcers are multifactorial and appear to be due to an imbalance among the aggressive factors (such as acid/pepsin, bile, alcohol, tobacco and caffeine, *H. pylori* infection, NSAIDs, stresses) and mucosal defensive mechanisms (including mucus secretion, bicarbonate production, mucosal blood flow, cellular repair mechanisms, prostaglandin E, growth factors) (2).

Peptic ulcer treatment using synthetic drugs (such as H2 blockers, proton pump inhibitors and NSAIDs) results in adverse effects, relapses and drug interactions (3). Therefore, herbal medicines containing active chemical components are considered as the main source of new drugs and appropriate alternatives for treatment of the various diseases including peptic ulcer.

*Correspondence: E-mail: fnamazi@shirazu.ac.ir Phone: +98 7132286950

Scrophularia striata, commonly known as figwort, belongs to a family of flowering plants called Scrophulariaceae. It is native to Iran and grows wild in meadows, hillsides and impassable areas of Ilam Province (4). The Scrophulariaceae family consists of about 3000 species and 220 genera. Species of *Scrophularia* share square stems, opposite leaves and open two-lipped flowers forming clusters at the end of their stems (5).

Several chemical components including cinnamic acid, three flavonoids (quercetine, isorhamnetin-3-O-rutinoside and nepitrin) and one phenylpropanoid glycoside (acteoside 1) have been identified in the aerial parts of *S. striata* (6). It appears that some compounds isolated from this species have the inhibitory effects on a variety of malignant and inflammatory disorders (7). Hence, the present study was carried out to determine the gastroprotective effects of *Scrophularia striata* on ethanol-induced gastric ulcer.

EXPERIMENTAL

Omeprazole

In the present study, omeprazole was used as a comparative standard control drug for antiulcer study. The drug was dissolved in distilled water and administered orally to the rats at 20 mg/kg (5 mL/kg) according to previous study (8).

Plant specimen and preparation of extraction

The aerial parts of S. striata were collected from the Zagros mountain range, Kermanshah Province, in May 2014. The plant sample was authenticated and voucher specimen was deposited at the Herbarium of Faculty of Sciences, Kharazmi University, Tehran, Iran (No: 5379). The plant aerial parts were air dried at room temperature and made into powder using a blender. The aqueous, hydroalcoholic and etheric extracts were obtained by maceration of the 200 g plant powder with 1L distilled water, ethanol/water (70/30) and petroleum ether for 2 days at room temperature, respectively. Extracts were filtered through a Whatman#1 paper and the solvents were evaporated under reduced pressure at temperature below 45 ºC with a rotary evaporator. Then the filtrates were lyophilized in a lyophilizator and stored under light protection and low temperature (-4 ºC) prior to use.

The aqueous and hydroalcoholic extracts were then dissolved in distilled water and etheric extract was dissolved in dimethyl sulfoxide (DMSO). The extracts were administered orally (4 mL/kg) to rats at dosages of 100 and 400 mg/kg.

Experimental animals for gastric ulcer

100 adult healthy male rats of *Sprague Dawley* strain weighing 200-250 g were housed in stainless steel cages and allowed to adapt to the conditions of the animal house for 14 days before the experiments. Animals were divided randomly into 10 equal groups of 10. 24 hours before the experiment, the rats were fasted and allowed access to water. Their access to water was inhibited for 2 hours before the start of experiment.

Gastric ulcer induction by ethanol

The experimental protocol is detailed below: Normal control group (NC) was left without treatment. Standard control group (SC) received omeprazole (20 mg/kg) orally. Experimental groups were orally administered with aqueous extract at 100 mg/kg (AE100) and 400 mg/kg (AE400), hydroalcoholic extract at 100 mg/kg (HA100) and 400 mg/kg (HA400) and etheric extract at 100 mg/kg (EE100) and 400 mg/kg (EE400). Vehicle control group (VC) received DMSO (4 mL/kg) orally. After one hour all the rats (except normal control group) and also ulcer control group (UC) were orally administered with 75% ethanol (4 mL/kg).

After one hour, rats were sacrificed by an overdose of ether and stomachs were isolated and cut open along the greater curvature. Stomachs were gently rinsed with 0.9% normal saline solution to remove gastric contents and blood.

Gross evaluation of gastric lesions

The ulcer area (mm^2) of each individual hemorrhagic lesion was measured and analyzed using computer software (Axiovision, Carl Zeiss Microimaging GmbH, Germany). According to the method of Andrade et al. (9), a score for the ulcer was noted and the ulcers were classified as: Level I ulcer area<1 mm^2; Level II ulcer area=1-3 mm^2; Level III ulcer area >3 mm^2.

The following parameters were determined:

Ulcerative lesion index (ULI)=1×(number of ulcers level I)+2×(number of ulcers level II)+3×(number of ulcers level III).

Percentage protective ratio=100-[ULI pretreated]/ [ULI control]×100.

Histopathological evaluation

A portion of gastric tissue was collected from animals and fixed in 10% neutral buffered formalin, embedded in paraffin, sectioned at 5 µm and stained with haematoxylin and eosin (H&E) for light microscopic examination.

Preparation of homogenate

Tissue homogenates were prepared for the PGE_2, MDA, TAC and HSP70 assays in gastric tissue of experimental groups. All the processes were handled at 4˚C throughout according to previous study (10). The gastric mucosa was weighed, minced with scissors, and homogenized using 0.1 M phosphate buffer (pH 7.4) (5 cc for each g of tissue) in homogenizer. After centrifugation at 2000-3000 rpm for 20 min, the supernatant was extracted and frizzed in -80 ºC for later use.

Measurement of PGE_2

The supernatants were subjected to a PGE_2 assay using a rat PGE_2 Eliza kit (Shanghai Crystal Day Biotech Co., LTD).

Measurement of membrane lipids peroxidation (MDA)

Tissue malondialdehyde (MDA) (mmol/L) was determined according to the method of Lykkesfeldt. A reaction mixture containing 8.1% sodium dodecyl sulfate, 20% acetate buffer (pH 3.5) and 0.8% thiobarbituric acid (TBA) was mixed well

with 0.2 mL of stomach tissue homogenate for 3 min and then incubated at 95°C for 60 min. After cooling with running water, the TBA-reactive substance (MDA) was extracted with 1 mL of H_2O and 2.5 mL of n-butanol: Pyridine mixture (15:1, v/v). The upper organic layer containing the MDA, which was produced by lipid peroxidation, was measured at 532 nm (11,12).

Measurement of total antioxidant capacity (TAC)

Determination of total antioxidant capacity (TAC) in tissue homogenate by commercial kit (Labor Diagnostika Nord (LDN) Com, Nordhorn, Germany) was based on the reaction of peroxides with peroxidase followed by a color reaction of the chromogenic substrate tetramethylbenzidine. The change in color was measured colorimetrically at 450 nm and expressed as millimoles per liter.

Measurement of heat shock protein 70 (HSP70)

The supernatants were subjected to a HSP70 assay using a rat HSP Eliza kit (Shanghai Crystal Day Biotech Co., LTD).

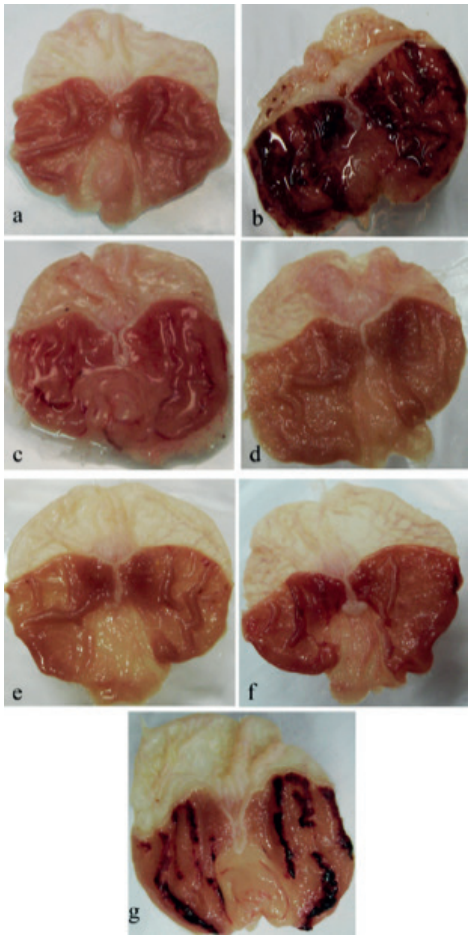

Figure 1. The effects of *S. striata* extracts on ethanol-induced gastric ulcer. a) Normal control group; b) Ulcer control group; c) Rats treated with omeprazole; d) Rats treated with aqueous extract at 400 mg/kg; e) Rats treated with 100 mg/kg aqueous extract; f) Rats treated with 400 mg/kg etheric extract; g) Rats treated with 400 mg/kg hydroalcoholic extract

Statistical analysis

The results were expressed as mean ± standard deviation (SD). The data were analyzed statistically by one-way ANOVA with Tukey's post-hoc test, using SPSS software, version 20. $P<0.05$ was considered as significant.

Animal ethics

This experiment was accomplished under the approval of the state committee on animal ethics, Shiraz University, Shiraz, Iran. Also, the recommendations of European Council Directive (86/609/EC) of November 24, 1986, regarding the standards in the protection of animals were used for experimental purposes.

RESULTS

Gross evaluation of gastric lesions

Gastroprotective effects of *S. striata* extracts on ethanol-induced gastric ulcer are shown in Figure 1 and Table 1. The ulcer control rats showed severe mucosal injury with ulcer area 20.75±11.09 mm^2. In the rats treated with aqueous and

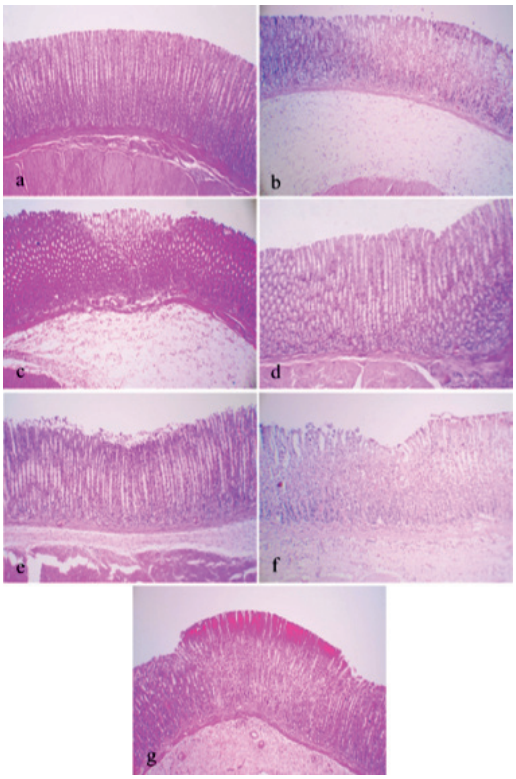

Figure 2. Histopathological evaluation of gastric tissue sections of rats. a) Normal control group: No lesion was seen; b) Ulcer control group: Mucosal necrosis, severe edema with leukocytes infiltration in submucosal layer; c) Rats treated with omeprazole: Mild mucosal damage with moderate edema and infiltration of leukocytes in the submucosal layer; d) Rats treated with aqueous extract at 400 mg/kg: No edema and leukocyte infiltration was seen; e) Rats treated with 100 mg/kg aqueous extract: Mild edema and little leukocyte infiltration in the submucosal layer; f) Rats treated with 400 mg/kg etheric extract: Mild mucosal damage with mild edema and infiltration of leukocytes; g) Rats treated with 400 mg/kg hydroalcoholic extract: Moderate edema and infiltration of leukocytes in the submucosal layer with mucosal necrosis. H&E, ×80

etheric extracts, the ulcer area was significantly reduced in a dose-dependent manner ($p<0.05$). The ulcer area was significantly decreased from 20.75±11.09 mm^2 in ulcer control group to 1.00±0.86 mm^2 in the rats treated with 400 mg/kg of aqueous extract. Also, in the rats treated with omeprazole, a decrease was observed in ulcer area (5.70±4.47 mm^2). Although the ulcer area in all groups had statistically significant difference with the rats treated with hydroalcoholic extract and ulcer control group, the significant inhibition of gastric ulcer in rats treated with aqueous and etheric extracts of *S. striata* was comparable to omeprazole (a standard drug used for gastric ulcer).

Histopathological evaluation of gastric lesions

No lesions were observed in the tissue sections from the rats of normal control group (Figure 2a), while the rats of ulcer control group showed extensive damage to the gastric tissue, including mucosal hemorrhage and necrosis, severe edema and leukocyte infiltration in the submucosal layer (Figure 2b).

In the rats treated with omeprazole, mild mucosal damage with moderate edema and infiltration of leukocytes in the submucosal layer was observed (Figure 2c).

The tissue sections of the group treated with aqueous extract at 400 mg/kg was near-normal architecture and no edema and leukocyte infiltration were seen. The rats treated with 100 mg/kg aqueous extract showed the normal glandular pattern with mild edema and little leukocyte infiltration in the submucosal layer (Figure 2d and 2e).

The tissue sections of groups treated with 100 and 400 mg/kg etheric extract revealed mild mucosal damage with mild edema and infiltration of leukocytes Figure 2f.

In the rats treated with 100 and 400 mg/kg hydroalcoholic extract, moderate edema and infiltration of leukocytes in the gastric submucosal layer with mucosal necrosis was observed in which mucosal damage was more severe at 400 mg/kg (Figure 2g).

Table 1. The effect of *S. striata* extracts in ethanol-induced gastric ulcer

Group	Ulcerative lesion index	Percentage of protective ratio (%)
PC	20.75±11.09^a	-
SC	5.70±4.47^b	72.53
AE100	1.00±0.92^b	95.18
AE400	1.00±.086^b	95.18
HA100	18.14±7.96^a	12.58
HA400	21.50±5.48^a	3.61
EE100	4.00±3.78^b	80.72
EE400	1.14±1.06^b	94.5
VC	5.29±3.30^b	74.5

Different letters indicate statistically significant differences ($p<0.05$)

In the tissue sections of vehicle group, lesions were similar to the rats treated with omeprazole.

Evaluation of parameters in the gastric tissue homogenate

The mean ± SD of parameters values, including MDA, TAC, PGE_2 and HSP70 in the gastric tissue homogenate of rats are presented in Table 2.

MDA increased in all groups in comparison with ulcer control group and the highest amount of MDA was observed in the rats of ulcer control group which showed a significant difference with all groups ($p<0.05$). There was no significant difference between normal control group and rats treated with aqueous extract of *S. striata.* The MDA level in the groups treated with other extracts and omeprazole had statistically significant difference with the normal control group and the rats treated with aqueous extract (Figure 3).

The most significant reduction in TAC was observed in rats of ulcer control group. Although the TAC level of normal control group showed a significant difference with all groups ($p<0.05$), this parameter increased in the rats treated with various extracts and was statistically significant in groups treated with aqueous and etheric extracts in comparison with the ulcer control group. In addition, the TAC level in rats treated with aqueous extract was higher as compared with the rats treated with omeprazole and showed significant difference (Figure 4).

Although the PGE_2 level presented significant difference between normal control group and other groups, this parameter increased in the rats treated with aqueous and etheric extracts in comparison with ulcer control group and showed significant difference. There was no significant difference between the rats treated with hydroalcoholic extract and ulcer control group (Figure 5).

Table 2. The mean ± SD of parameters value in the gastric tissue homogenate of rats

Group	PGE_2 (ng/mL)	HSP70 (ng/mL)	MDA (nmol/mL)	TAC (mmol/L)
NC	0.26±0.01^a	0.53±0.06^a	2.96±0.11^b	2.96±0.11^a
UC	0.13±0.01^b	0.39±0.05^b	3.66±0.18^a	1.73±0.25^b
SC	0.22±0.01^c	0.46±0.04^{ab}	3.27±0.05^c	2.01±0.03^{ce}
AE100	0.23±0.01^c	0.50±0.04^a	3.08±0.05^b	2.28±0.05^d
AE400	0.23±0.01^c	0.51±0.04^a	3.01±0.04^b	2.28±0.03^d
HA100	0.14±0.01^b	0.40±0.06^b	3.43±0.10^d	1.82±0.11^b
HA400	0.13±0.01^b	0.40±0.10^b	3.46±0.08^d	1.84±0.09^{bc}
EE100	0.22±0.01^c	0.48±0.04^{ab}	3.28±0.05^c	2.01±0.03^{ce}
EE400	0.21±0.00^c	0.47±0.03^{ab}	3.28±0.05^c	2.03±0.04^e
VC	0.21±0.01^c	0.45±0.03^{ab}	3.07±0.03^b	2.24±0.03^d

Different letters indicate statistically significant differences ($p<0.05$)

No statistically significant difference was observed in the HSP70 level between the rats treated with aqueous extract and the normal control group, but there was a significant difference between these groups with ulcer control group (p<0.05). Although this parameter increased in the rats treated with etheric extract and omeprazole, no significant difference was seen with other groups (Figure 6).

In general, the most curative effect of *S. striata* was related to aqueous extract. Although the hydroalcoholic extract resulted in improvement of some parameters, it did not have curative effects.

DISCUSSION

A key experimental model for evaluation of agents with potential anti-ulcer effect is ethanol-induced gastric injury as ethanol has been considered as a cause of gastric ulcer in humans (13). Oral administration of ethanol results in gastric mucosal damage and alterations in vascular (14). In fact, ethanol causes gastric mucosal injury via direct effects including dehydration, disruption of cellular membranes and cytotoxic effects and also indirect effects via the recruitment of leukocytes (15). In addition, ethanol leads to stasis of blood flow and disruption of gastric microvessels, which in turn inflict hemorrhage and necrosis (15,16). Ethanol-induced necrotic lesions decrease defensive factors such as the mucus production and secretion of bicarbonate (17).

The mentioned effects are probably because of biological actions like lipid peroxidation, intracellular oxidative stress, formation of free radicals, changes in permeability and depolarization of the mitochondrial membrane (18). The defensive mechanism against free radicals is weakened by ethanol (19). Ethanol consumption results in hemorrhagic damage, severe submucosal edema and epithelial cell injury. In the present study, similar lesions were also observed in gastric tissue sections of ulcer control group. The results of this study revealed aqueous extract of *S. striata,* especially at 400 mg/kg have therapeutic effects on ethanol-induced gastric ulcer as tissue structure was near-normal architecture and no edema and leukocyte infiltration were seen in tissue sections.

With both short and long-term use, omeprazole is effective in the treatment of gastroesophageal reflux and peptic ulcer disease (20). Omeprazole functions as an acid inhibitor and offers a protective role such as gastric mucosa (21). Also, this agent, as mucosal protection, is effective in the treatment of nonacid dependent models like ethanol-induced ulcer (22). In the rats treated with omeprazole, mild mucosal damage

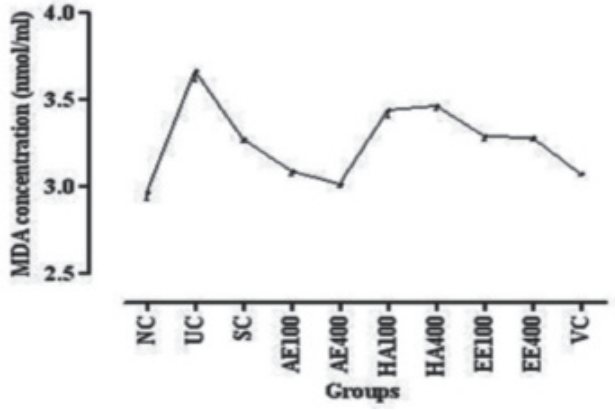

Figure 3. The effect of *S. striata* extracts on MDA levels in the gastric tissue homogenate of rats

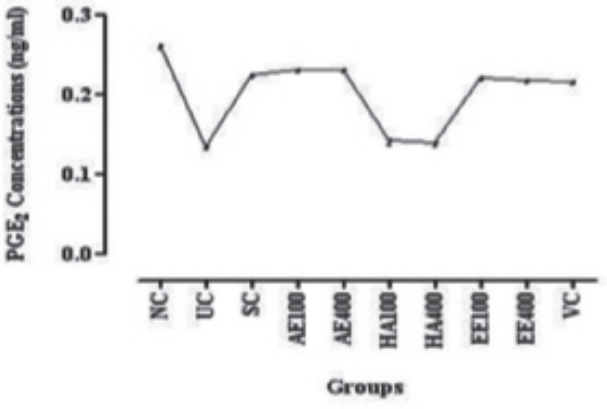

Figure 5. The effect of *S. striata* extracts on PGE2 levels in the gastric tissue homogenate of rats

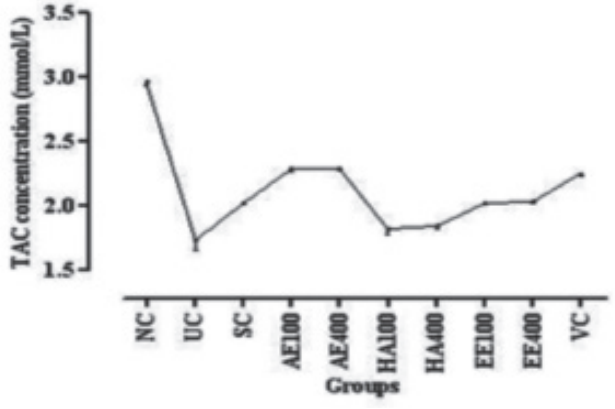

Figure 4. The effect of *S. striata* extracts on TAC levels in the gastric tissue homogenate of rats

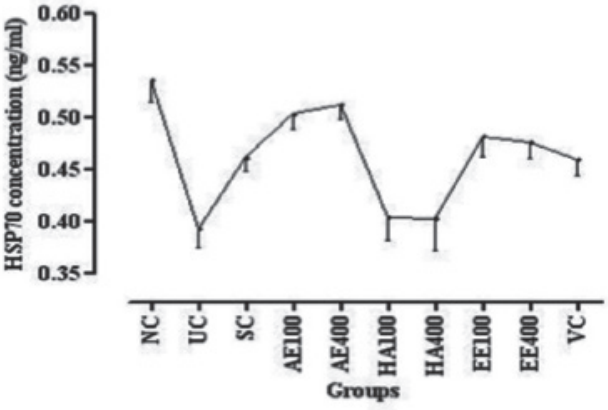

Figure 6. The effect of S. *striata* extracts on HSP70 levels in the gastric tissue homogenate of rats

with moderate edema and infiltration of leukocytes in the submucosal layer were seen which were similar to those observed in the rats treated etheric extract.

Treatment of the rats with *S. striata* extract showed significant antioxidant activity by reduction of MDA and increase of the TAC level in response to ethanol-induced oxidative stress. Oxidative stress plays a key role in the pathogenesis of different diseases including gastric ulcer, and antioxidants perform a significant role in protection of gastric mucosa against necrotic injury (23). Several studies have reported the involvement of oxidative stress in the pathogenesis of ethanol-induced gastric injury (13,15). Ethanol causes damage to the gastric mucosal microcirculation, resulting in hypoxia, formation of free radicals and lipid peroxidation (24). It seems free radicals formation plays an important role in the production of lipid peroxides together with interference in antioxidant activity (25). Free radicals can reduce enzyme activity such as antioxidant enzymes (26).

MDA is the final product of lipid peroxidation (27). An important pathophysiologic event in various diseases containing gastric ulcer is lipid peroxidation (28) which leads to impaired membrane integrity and ion transport, and finally, loss of cellular function. Oxygen free radicals produced in the gastric tissue might damage cell membranes and increase MDA level (29).

One mechanism involved in the healing of ulcer is removal of oxygen free radicals (Mei 30). Antioxidants like catalase and SOD are the first defensive barrier against free radicals by removing them and preventing their harmful effects (15). Various studies have reported the cytoprotective effect of some antioxidants in the healing of gastric lesions. For instance, melatonin prevented ethanol-induced gastric damage, probably because of its antioxidant effect (31).

Previous studies have shown prostaglandins affect various components of the mucosal defense, including maintaining blood flow, stimulating bicarbonate and mucus secretion, increasing the resistance of epithelial cells to injury and preventing leukocyte recruitment (32). In the present study, ethanol consumption led to decreasing PGE_2 that was consistent with previous studies (13,22). PGE_2 is the most abundant prostaglandin of alimentary system which performs an important role in the regulation of gastric mucus secretion (33) and its mucosal content can be reduced by ethanol (34). PGE_2 improves blood flow, actively maintaining the cellular integrity in the mucosa (34). In addition, this prostaglandin increases mucus secretion and bicarbonate to reinforce the resistance of mucosal cells to the necrotizing effect of irritants (33). The findings of the present study revealed that the gastroprotective effect of *S. striata* is related to PGE_2 because its mucosal level was elevated by compound.

HSPs play an important role in both normal and pathologic situations (35). HSP70 is a 70 kDa protein and a member of heat shock proteins family (36) which is expressed by mammalian cells. These proteins act as a molecular chaperone and protect the cellular homeostatic processes from various injurious agents through preservation of the structure of normal proteins and repair or removal of damaged proteins (37,38). HSP70 protects mitochondria and interferes with the stress-induced apoptosis, resulting in cytoprotection (38). Ethanol-induced oxygen reactive species inhibit the expression of HSP70 and increase the expression of BAX, while HSP70 protects cells from oxidative stress or heat shock (39).

Jin et al. (40) reported that when the PGE_2 level is decreased by NSAID, HSP70 can play an important role in gastric mucosal adaptation. In the present study, the HSP70 levels increased in various groups, which was observed as a significant difference between the rats treated with aqueous extract and ulcer control group. Oyake et al. (41) showed the overexpression of Hsp70 protects gastric mucosal against monochloramine-induced damage. Also, HSP70 induction protected rats from ethanol-induced gastric mucosal injury (15).

In conclusion, the findings of the present study indicated the efficiency of *S. striata* extract in improving free radicals-induced injury and exerting the protective effects in ethanol-induced gastric ulcer model. These effects were related to increased PGE_2 secretion, prevention of consumption of antioxidant sources and maintaining MDA at normal level.

ACKNOWLEDGMENTS

The authors would like to thank the Research Council of Shiraz University and School of Veterinary Medicine, Shiraz University for financial and technical support of this study.

REFERENCES

1. Dhasan PB, Jegadeesan M, Kavimani S, Antiulcer activity of aqueous extract of fruits of *Momordica cymbalaria* Hoof F. in Wistar rats, Pharmacognosy Res 2(1), 58-61, 2010.
2. Tulassay Z, Herszényi L, Gastric mucosal defense and cytoprotection, Best Pract Res Clin Gastroenterol 24(2), 99-108, 2010.
3. Srinivas LT, Lakshmi SM, Shama SN, Reddy GK, Prasanna KR, Medicinal plants as anti-ulcer agents, J Pharmacogn Phytochem 2(4), 91-97, 2013.
4. Azadbakht M, Classification of Medical Plants, Tehran, Teimorzadeh Pub, p. 276-277, 2000 [In Persian].
5. Zamanian Azodi M, Ardashiri Lajimi A, Ahmadi N, Gilanchi S, Abbasi N, Hematian A, The Study of Antibiotic Properties of *Scrophularia Striata* Aqueous Extract on *Staphylococcus aureus*, J Ilam Univ Med Sci 20, 51-58, 2013.
6. Monsef-Esfahani HR, Hajiaghaee R, Shahverdi AR, Khorramizadeh MR, Amini M, Flavonoids, cinnamic acid and phenyl propanoid from aerial parts of *Scrophularia striata*, Pharm Biol 48(3), 333-336, 2010.
7. Azadmehr A, Afshari A, Baradaran B, Hajiaghaee R, Rezazadeh S, Monsef-Esfahani H, Suppression of nitric oxide production in activated murine peritoneal macrophages in vitro and ex vivo by *Scrophularia striata* ethanolic extract, J Ethnopharmacol 124, 166-169, 2009.

8. Mahmood AA, Mariod AA, Al-Bayaty F, Abdel- Wahab SI, Anti-ulcerogenic activity of *Gynura procumbens* leaf extract against experimentally-induced gastric lesions in rats, J Med Plant Res 4(8), 685-69, 2010.
9. Andrade SF, Antoniolli D, Comunello E, Cardoso LGV, Carvalho JCT, Bastos JK, Antiulcerogenic activity of crude extract, fractions and populnoic acid isolated from Austroplenckia populnea (Celastraceae), Z Naturforsch C 61, 329-333, 2006.
10. Yildirim A, Sahin YN, Suleyman H, Yilmaz A, Yildirim S, The role of prednisolone and epinephrine on gastric tissue and erythrocyte antioxidant status in adrenalectomized rats, J Physiol Pharmacol 58(1), 105-116, 2007.
11. Hagar HH, El-Etter E, Arafa M, Taurine attenuates hypertension and renal function induced by cyclosporine in rats, Clin Exp Pharmacol Physiol 33, 189-196, 2006.
12. Zal F, Mostafavi-Pour Z, Vessal M, Comparison of the effects of vitamin E and/or quercetin in attenuating chronic cyclosporine A-included nephrotoxicity in male rats, Clin Exp Pharmacol Physiol 34, 720-724, 2007.
13. Liu Y, Tian X, Gou L, Fu X, Li S, Lan N, Protective effect of l-citrulline against ethanol-induced gastric ulcer in rats, Environ Toxicol Pharmacol 34(2), 280-287, 2012.
14. Mofleh IA, Mofleh IA, Alhaider AA, Mossa J, Al-Sohaibani M, Al-Yahya M, Gastroprotective effect of an aqueous suspension of black cumin Nigella sativa on necrotizing agents-induced gastric injury in experimental animals, Saudi J Gastroenterol 14, 128, 2010.
15. Park SW, Oh TY, Kim YS, Sim H, Park SJ, Jang EJ, Artemisia asiatica extracts protect against ethanol-induced injury in gastric mucosa of rats, J Gastroenterol Hepatol 23(6), 976-984, 2008.
16. Li W, Huang H, Niu X, Fan T, Mu Q, Li H, Protective effect of tetrahydrocoptisine against ethanolinduced gastric ulcer in mice, Toxicol Appl Pharm 272(1), 21-29, 2013.
17. Ferreira MDP, Nishijima CM, Seitoetal LN, Gastroprotective effect of Cissus sicyoides (Vitaceae): involvement of microcirculation, endogenous sulfhydryls and nitric oxide, J Ethnopharmacol 117(1), 170-174, 2008.
18. Sannomiya M, Fonseca VBM, DaSilvaetal A, Flavonoids and antiulcerogenic activity from Byrsonima crassa leaves extracts, J Ethnopharmacol 97(1), 1–6, 2005.
19. Kurban S, Mehmetoğlu İ, The effect of alcohol on total antioxidant activity and nitric oxide levels in the sera and brains of rats, Turk J Med *Sci* 38, 199-204, 2008.
20. Ode OJ, Asuzu OV, Investigation of cassia singueana leaf extract for antiulcer effects using ethanol-induced gastric ulcer model in rats, Int J Pl. An and Env Sci 1, 1-7, 2011.
21. Li XQ, Andersson TB, Ahlstrom M, Weidolf L, Comparison of inhibitory effects of the proton pump-inhibiting drugs omeprazole, esomeprazole, lansoprazole, pantoprazole, and rabeprazole on human cytochrome P450 activities, Drug Metab Dispos 32, 821–827, 2004.
22. Golbabapour S, Hajrezaie M, Hassandarvish P, Abdul N, Hadi H, Nordin N. Acute toxicity and gastroprotective role of M. Pruriens in ethanol-induced gastric mucosal injuries in rats. Biomed Res Int doi:10.1155/2013/974185, 2013.
23. Bardi DAA, Sarah Khan MA, Sabri SZ, Kadir FA, Mahmood AA, Zahra AA, Antiulcerogenic activity of typhonium flagelliforme aqueous leaf extract against ethanol-induced gastric mucosal injury in rats, Sci Res Essays 6(15), 3232-3239, 2011.
24. Huh K, Kwon TH, Shin US, Kim WB, Ahn BO, Oh TY, Inhibitory effects of DA9601 on ethanol-induced gastrohemorrhagic lesions and gastric xanthine oxidase activity in rats, J Ethnopharmacol 88(2-3), 269-273, 2003.
25. Konturek SJ, Konturek PC, Brzozowski T, Prostaglandins and ulcer healing, J Physiol Pharmacol 56(5), 5-31, 2005.
26. Pratibha R, Sameer R, Rataboli PV, Bhiwgade DA, Dhume CY, Enzymatic studies of cisplatin induced oxidative stress in hepatic tissue of rats, Eur J Pharmacol 532(3), 290-293, 2006.
27. Dursun H, Bilici M, Albayrak F, Ozturk C, Saglam MB, ALP HH, Antiulcer activity of fluvoxamine in rats and its effect on oxidant and antioxidant parameters in stomach tissue, BMC Gastroenterol 9, 36, 2009.
28. Bandyopadhyay D, Biswas K, Reiter RJ, Banerjee RK, Gastric toxicity and mucosal ulceration induced by oxygen derived reactive species: protection by melatonin, Cur Mol Med 1(4), 501-513, 2001.
29. Cadirci E, Suleyman H, Aksoyetal H, Effects of *Onosma armeniacum* root extract on ethanol-induced oxidative stress in stomach tissue of rats, Chem Biol Interact 170(1), 40-48, 2007.
30. Mei X, Xu D, Xu S, Zheng Y, Novel role of Zn(II)-curcumin in enhancing cell proliferation and adjusting proinflammatory cytokine-mediated oxidative damage of ethanol-induced acute gastric ulcers, Chem Biol Interact 197(1), 31-39.
31. Bilici D, Süleyman H, Banoğlu ZN, Kiziltunc A, Avci B, Ciftçioğlu A, Melatonin prevents ethanol-induced gastric mucosal damage possibly due to its antioxidant effect, Digest Dis Sci 47, 856-61, 2002.
32. Miller TA, Protective effects of prostaglandins against gastric mucosal damage: current knowledge and proposed mechanisms, Am J Physiol 245(5), G601-G623, 1983.
33. Brzozowski T, Konturek PC, Konturek SJ, Brzozowska I, Pawlik T, Role of prostaglandins in gastroprotection and gastric adaptation, J Physiol Pharmacol 56, 33-55, 2005.
34. Zhao W, Zhu F, Shen W, Fu A, Zheng L, Yan Z, Protectiveeffects of DIDS against ethanol-induced gastric mucosal injury in rats, ABBS 41(4), 301-308, 2009.
35. Arya R, Mallik M, Lakhotia SC, Heat shock genes-integrating cell survival and death, J Biosci 32(3), 595-610, 2007.
36. Ngosuwan J, Wang NM, Fung KL, Chirico WJ, Roles of cytosolic Hsp70 and Hsp40 molecular chaperones in post-translational translocation of presecretory proteins into the endoplasmic reticulum, J Biol Chem 278(9), 7034-7042, 2003.
37. Kim HP, Morse D, Choi AM, Heat-shock proteins: new keys to the development of cytoprotective therapies, Expert Opin Ther Targets 5, 267-287, 2006.
38. Rokutan K, Role of heat shock proteins in gastric mucosal protection, J Gastroenterol Hepatol 15, D12–D19, 2000.
39. Suemasu S, Tanaka K, Namba T, Ishihara T, Katsu T, Fujimoto M, A role for HSP70 in protecting against indomethacin-induced gastric lesions, J Biol Chem 284(29), 19705-19715, 2009.
40. Jin M, Otaka M, Okuyama A, Itoh S, Otani S, Odashima M, Association of 72-kDa heat shock protein expression with adaptation to aspirin in rat gastric mucosa, Digest Dis Sci 44(7), 1401-1407, 1999.
41. Oyake J, Otaka M, Matsuhashi T, Jin M, Odashima M, Komatsu K, Over-expression of 70-kDa heat shock protein confers protection against monochloramine-induced gastric mucosal cell injury, Life Sci 79(3), 300-305, 2006.

Received : 03.03.2016
Accepted : 20.05.2016

Turk J Pharm Sci 13(3), 335-341, 2016
DOI: 10.4274/tjps.2016.09

ORIGINAL ARTICLE

Voltammetric Determination of Nimesulide Using Multiwalled Carbon Nanotubes Modified Carbon Paste Electrode

Çok Duvarlı Karbon Nanotüp ile Modifiye Edilmiş Karbon Pasta Elektrot Kullanılarak Nimesulidin Voltametrik Miktar Tayini

Fatma AĞIN*, Vildan SERDAROĞLU

Karadeniz Technical University, Faculty of Pharmacy, Department of Analytical Chemistry, Trabzon, TURKEY

ABSTRACT

A multiwalled carbon nanotubes (MWCNTs) modified carbon paste electrode (CPE) was prepared for voltammetric determination of anti-inflammatory drug nimesulide (NIM). The electro-oxidation of NIM was exhibited irreversible and diffusion controlled process with MWCNTs modified CPE. The linear response between peak current and concentration in the quantitative determination of NIM by differential pulse voltammetry in 0.1 M phosphate buffer solution (PBS) at pH 5.0 obtained in the range of the concentration from 6×10^{-8} -1×10^{-5} M with limit of detection (LOD) 1.07×10^{-9} M and limit of quantification (LOQ) 3.24×10^{-9} M. Differential pulse voltammetry was developed according to linear response of NIM with high selectivity, precision, accuracy using modified electrode was successfully applied to the determination of NIM in pharmaceuticals and human serum samples.

Key words: Carbon paste electrode, Determination, Multiwalled carbon nanotubes, Nimesulide, Voltammetry

ÖZ

Antienflamatuvar ilaç etken maddesi nimesulidin (NIM) voltametrik miktar tayini için çok duvarlı karbon nanotüp ile modifiye edilmiş karbon pasta elektrot hazırlanmıştır. NIM'in çok duvarlı karbon nanotüp ile modifiye edilmiş karbon pasta elektrot ile elektro-oksidasyonu tersinmez ve difüzyon kontrollü bir özellik göstermiştir. NIM'in diferansiyel puls voltametrisi ile 0.1 M fosfat tampon çözeltisinde pH 5.0 de miktar tayininde derişim ve pik akımı arasındaki doğrusallık 6×10^{-8} 1×10^{-5} M derişim aralığında, saptama sınırı 1.07×10^{-9} M ve tayin alt limiti 3.24×10^{-9} M olarak bulunmuştur. Çok duvarlı karbon nanotüp ile modifiye edilmiş karbon pasta elektrodu kullanarak NIM'nin doğrusal cevabına göre yüksek seçicilik, kesinlik, ve doğrulukla geliştirilen diferansiyal puls voltametrisi, NIM'nin farmasötik preparatlardan ve insan serum numunelerinden miktar tayinine başarılı bir şekilde uygulanmnıştır.

Anahtar kelimeler: Karbon pasta elektrot, Tayin, Çok duvarlı karbon nanotüp, Nimesulid, Voltametri

INTRODUCTION

Nimesulide, N-(4-nitro-2 methanosulfonanilid) (Figure 1), is a new non-steroidal anti-inflammatory drug that is selective for cyclooxygenase-2 and effective in reducing the pain which is associated with rheumatoid arthritis and osteoarthirits (1). pK_a value of NIM is 6.46 that is very important for gastric tolerability, and this avoids the back diffusion of the hydrogen ions that are liable for tissue damage. NIM is nearly completely biotransformed to 4-hydoxynimesulide in free and conjugated forms and it provides to promote to the anti-inflammatory activity of NIM (2,3).

There are several reports on the determination of NIM in the literature for example HPLC (high performance liquid chromatography) (4), with spectrophotometry UV (ultraviolet) (5,6), capillary electrophoresis (7). Most of this methods appear as time-consuming, expensive, complicated and lengthy procedures. Electrooxidation of NIM at gold electrode (8), electroreduction of NIM using glassy carbon electrode modified with SiC (silicon carbide) (9) and MWCNTs (multiwalled carbon nanotubes) modified glassy carbon electrode (10) have been reported in the literature. Electrochemical methods have certain advantages for example fast response, low cost and high sensitivity compare to other analytical methods (11,12).

Carbon nanotubes (CNTs) can be used as electrode material for electrochemical and bioelectrochemical applications

*Correspondence: E-mail: fagin@ktu.edu.tr Phone: +90 462 377 88 22

because of their unique characteristics and useful properties for example high chemical stability, conductivity, aspect ratio, and extremely high mechanical strength and modules (13-16). CNTs are largely used as working electrode modification material for drug analysis due to they have the capability for promoting electron transfer reactions and developing sensitivity in electrochemistry (17).

In this study, a sensitive MWCNTs modified CPE was prepared for electroanalytical determination and it used to investigate electro-oxidative behavior of NIM with cyclic and differential pulse voltammetry. The prepared MWCNTs modified CPE was exhibited rapid response, high selectivity, sensitivity, low detection limit, and good reproducibility and successfully used electroanalytical determination of NIM.

EXPERIMENTAL

Instrumentation

Voltammetric measurements were carried out with a computer-controlled Autolab Pgstat128n potentiostat/galvanostat with Nova 10.0 software (Metrohm-Autolab, The Netherlands). A three-electrode electrochemical cell analyzer contains a carbon paste electrode with modification

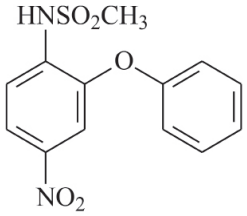

Figure 1. Molecular structure of nimesulide

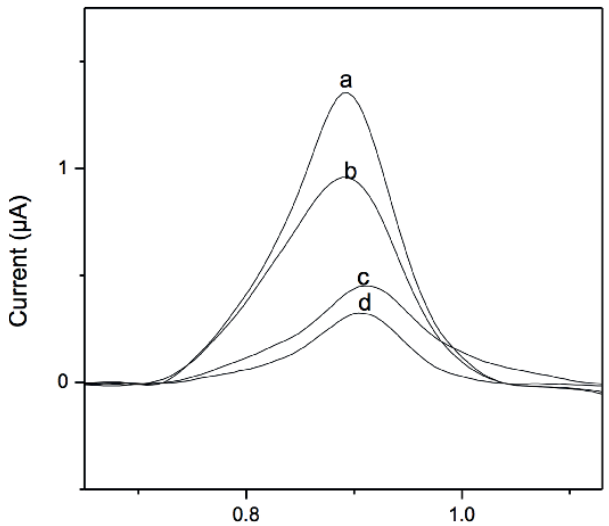

Figure 2. Differential pulse voltammograms 10 µM of NIM in 0.04 M Britton-Robinson buffer at pH 7.0, (a) 0.2%, 2.5 µL; (b) 0.5%, 1 µL; (c) 0.5%, 3 µL, (d) 0.2%, 5 µL of MWCNTs

MWCNTs as working electrode, a platinum wire as the counter electrode and Ag/AgCl electrode as the reference electrode. The pH measurements were carried out using model Hanna HI2211 pH meter (Romania) with an accuracy of ±0.05 pH at room temperature.

Reagents

Nimesulide and its pharmaceutical dosage form tablet (100 mg per tablet) were supplied by Sanovel-Turkey. They were used without further purification. Stock solutions of NIM (1×10^{-3} M) were prepared in methanol and stored at +4°C away from light. NIM working solutions for voltammetric investigation were prepared by the direct dilution of the stock solution with selected supporting electrolyte containing a constant amount of methanol (20% (v/v)). Graphite powder (d=2.2 g/mL, Merck, Germany) and paraffin oil (d=0.84 g/mL, Aldrich, U.S.A) as the binding agent were used for preparing the pastes. MWCNTs was purchased from NanoLab. U.S.A, with purity 95%, 30±10 nm diameter, and 1-5 µm lengths.

Phosphate buffer solutions (PBS) (0.1 M) were prepared from phosphoric acid (Merck, Germany) for pH 4.0 and disodium hydrogen phosphate (Aldrich, U.S.A.), sodium dihydrogen phosphate (Merck, Germany) for pH 5.0-8.0. Britton-Robinson (BR) buffer solutions (0.04 M) were prepared at pH 3.0-9.0 from 0.04 M phosphoric acid (Merck, Germany), 0.04 M boric acid (Aldrich, U.S.A.) and 0.04 M acetic acid (Merck, Germany). Acetate (AT) buffer solutions (1 M) at pH 3.5, 4.5 were prepared from 1 M acetic acid (Merck, Germany). pH was adjusted with 5 M sodium hydroxide (Aldrich, U.S.A.) solution.

Sartorius Arium proUV nanopure water (resistivity ≥18 MΩ cm), and analytical reagents were used for the preparation

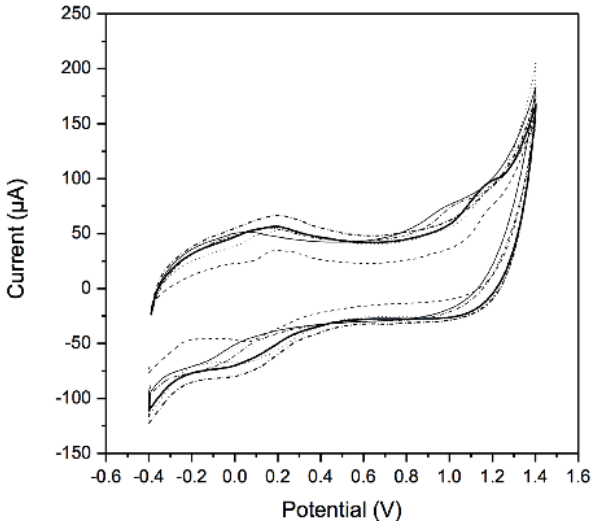

Figure 3. Cyclic voltammograms of NIM in 1 M acetate buffer at pH 3.5 (-----), 0.1 M phosphate buffer at pH 4.0 (·····), pH 5.0 (▬), 0.04 M Britton-Robinson buffer pH 7.0 (–·–·–), pH 9.0 (—) with MWCNTs modified CPE. Short dash dot line 0.1 M phosphate buffer at pH 5.0; NIM concentration: 100 µM; scan rate 100 mV/s

of solutions. All of the experiments were performed at room temperature (25±1°C).

Preparation of bare and MWCNTs modified carbon paste electrodes

The ratio of graphite powder and paraffin oil to binder were optimized for NIM, and then the carbon paste electrode was prepared homogeneous paste by thoroughly hand-mixing the from optimized graphite powder and paraffin oil in the ratio of 75:25 (w/w). A portion of the homogeneous paste was packed into the cave of the teflon tube. A copper wire inserted into the carbon paste provided the electrical contact. When necessary, a new surface was obtained by pushing an excess of the paste out of the tube and polishing with a weighing paper.

The MWCNTs were dispersed in DMF with loading 0.2% (w/v) and sonicated for 4h to obtain a homogeneous mixture. A selected 2.5 µL of the dispersion was dropped directly on the surface of CPE. The resulting modified electrode was named as MWCNTs modified CPE. The MWCNTs modified CPE electrode dried for overnight at room temperature.

Pharmaceutical assay

Ten tablets (each tablet contains 100 mg NIM) were first weighed and then finely powdered. The required amount of powder equivalent to 10^{-3} M of NIM was diluted to 100 mL with methanol and sonicated for 15 min. The analyzed solutions were prepared by taking suitable aliquots of the clear supernatant liquor and diluting with the selected supporting electrolyte NIM working solutions for voltammetric investigation were prepared by the direct dilution of the stock solution with selected supporting electrolyte containing a constant amount of methanol (20% v/v).

Analysis of serum

Drug-free human serum samples were obtained from healthy people and stored frozen in the dark until assay. An aliquot volume of serum sample was fortified with NIM dissolved in methanol to achieve final concentration of 1×10^{-3} M and treated with acetonitrile to removing serum proteins effectively. Blank and stock solution of NIM were transported to ultrasonic bath and agitated for 15 min and subsequently centrifuged for 15 min at 5000 rpm to separate serum protein residues and supernatant. Appropriate volumes of this supernatant were taken carefully and transferred into the volumetric flask and diluted up to the required volume with the selected supporting electrolyte containing a constant amount of methanol (20% v/v).

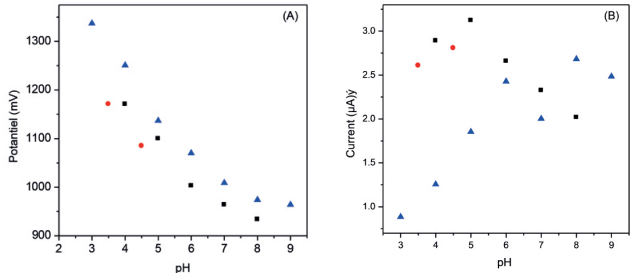

Figure 4. Plots of peak potential, (E_p), versus pH (A) and peak current (I_p), versus pH (B) from cyclic voltammetry voltammograms of 100 µM of NIM with MWCNTs modified CPE. Squares indicate 0.1 M phosphate buffer solution, tringle 0.04 M Britton-Robinson buffer solution and circles 1 M acetate buffer solution

Validation of the analytical methods

The ruggedness, precision, and accuracy of the studied methods, were checked by assaying five replicate samples on the same day and on different days over a week. Relative standard deviations (%) were also calculated to check the ruggedness and precision of the method. The accuracy of the methods was expressed as bias (%) (18,19). Each of the solutions was freshly prepared just before the experiments and protected from the light. All of the measurements were carried out at room temperature (25±1°C). The calibration equation for differential pulse voltammetry method was constructed by plotting the peak current against NIM concentration.

RESULTS AND DISCUSSION

Effect of volume variations on the peak current was investigated at two different concentrations of MWCNTs suspension (0.2% and 0.5% in DMF) to optimize MWCNTs volume for determination of NIM (Figure 2). The suspension amounts of 2.5 µL and 5 µL for 0.2% of MWCNTs, 1 µL and 3 µL for 0.5% of MWCNTs suspension were studied for 10 µM NIM with CV and DPV. As shown in Figure 1, the peak current reaches its maximum value when the suspension amount is 2.5 µL for 0.2% MWCNTs. So, 2.5 µL was chosen as the optimized amount for 0.2% MWCNTs suspension.

The electro-oxidation behavior of NIM on MWCNTs modified CPE was studied by CV at a scan rate of 100 mV/s between

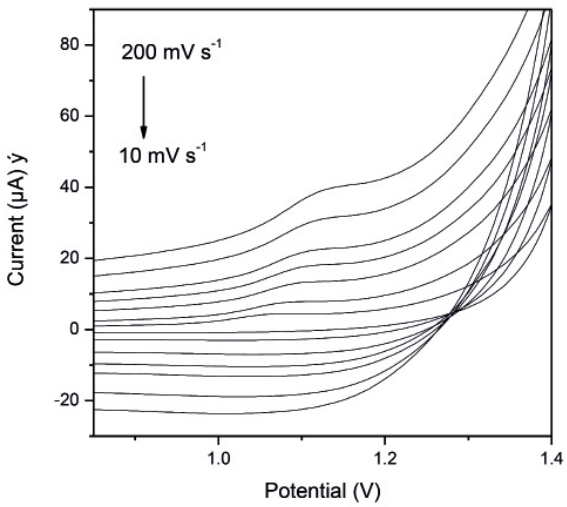

Figure 5. Cyclic voltammograms of 100 µM of NIM in 0.1 M phosphate buffer solution at pH 5.0 at scan rates of 10, 25, 50, 75, 100, 150 and 200 mV/s with MWCNTs modified carbon paste electrode

pH 3.0 and 9.0 in different buffer solutions. The cyclic voltammetric measurements (Figure 3) performed for 100 µM NIM solution exhibit that NIM has irreversible electrochemical oxidation behavior on MWCNTs modified CPE.

Effect of pH on the anodic peak current and peak potential of 100 µM NIM were analyzed with cyclic and differential pulse voltammetry in different buffer solutions between pH 3.0 and 9.0 using MWCNTs modified CPE electrode. Due to detection responses for CV and DPV are similar, only cyclic voltammetry responses of NIM were exhibited in Figure 4. As shown in Figure 4, NIM show irreversible anodic peak in the studied all pH values. The peak potential in the oxidation process of NIM shifted to less positive potentials (Figure 4A) with increasing pH. Anodic peak of NIM exhibited a pH dependent behavior between pH 3.0 and 7.0 with linear relationship (equation 1).

E_p (mV)= 1298-64.1pH; r=0.992 (between pH 3.0 and 7.0) (equation 1)

The observed pH dependence in the electro-oxidation behavior of NIM indicated that the methylsulfonamide group (electroactive group) corresponding to the NIM main oxidation peak was in acid-base equilibrium with pK_a of about 7.0. The breaking point of the curve was close to the pK_a value of NIM, at about 6.56 (20). The obtained slope value for plot of peak potential versus pH was close to theoretical value of 59 mV/pH in the Nerst equation. This corresponds to the oxidation process of NIM involves equal number of electrons and protons (21,22). The peak potential of NIM nearly was pH independent (Figures 4A), above pH 7.0. This attributed because of a change in the protonation-deprotonation process of the methylsulfonamide and the oxidation potential of NIM remains pH independent and before the electron transfer rate-determining step there are no proton transfer steps. The conjugate base must be formed by rapid dissociation of the protonated form at pH<pK_a. The plot of peak current versus pH is shown in Figure 4B. The maximum peak current and well peak shape of oxidation NIM were obtained in 0.1 M PBS at pH 5.0. Thus, electroanalytical determination of NIM and further studies were studied in 0.1 M PBS at pH 5.0.

The effect of scan rate over the range of 10.0-200.0 mV/s on the peak potential and peak current was studied by CV in PBS at pH 5.0. The peak potential of 100 µM NIM in 0.1 M PBS at pH 5.0 is moved to the anodic direction with the scan rate increasing (Figure 5). The plot of logarithm of peak

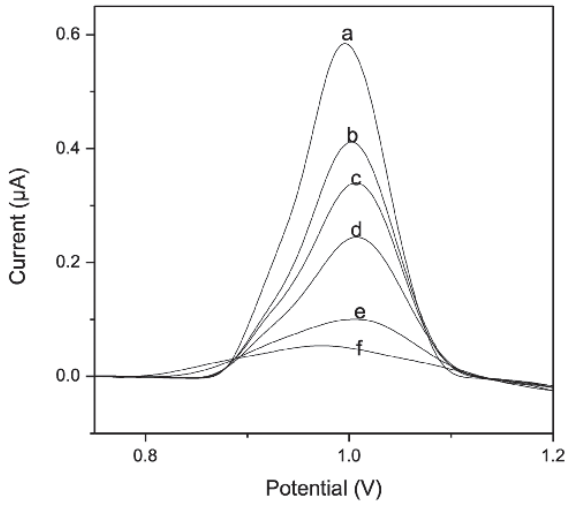

Figure 6. Differential pulse voltammograms (a) 10, (b) 8, (c) 6, (d) 4, (e) 1, (f) 0.4 µM of NIM solution in 0.1 M phosphate buffer solution at pH 5.0 with MWCNTs modified carbon paste electrode

Table 1. Validation data of calibration lines for the quantitative determination of NIM by DPV for MWCNTs modified carbon paste electrode in 0.1 M PBS at pH 5.0 and serum samples

	MWCNTs modified carbon paste electrode	
	Supporting electrolyte	Spiked serum
	DPV	DPV
Peak potential (V)	1.006	1.012
Linearity range (µM)	0.06-10	0.4-40
Slope (µA/µM-1)	89055	29531
Intercept (µA)	+0.1008	+0.0672
Correlation coefficient	0.9922	0.9977
Limit of detection (µM)	0.00107	0.0363
Limit of quantification (µM)	0.00324	0.1101
Repeatability of peak current (R.S.D.%)	0.581	0.424
Repeatability of peak potential (Relative standard deviation %)	0.418	0.255
Reproducibility of peak current (Relative standard deviation %)	0.808	0.669
Reproducibility of peak potential (Relative standard deviation %)	0.961	0.566

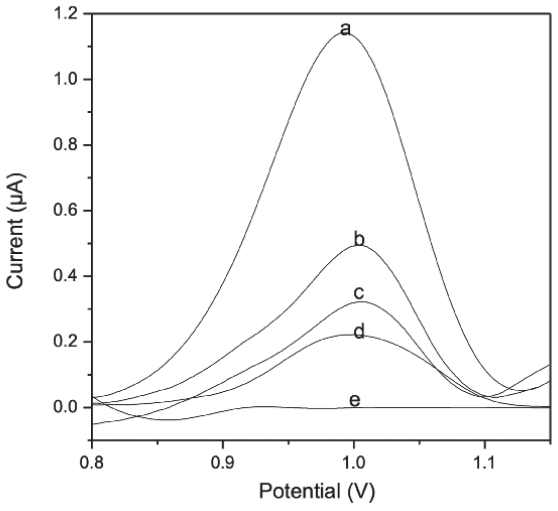

Figure 7. Differential pulse voltammograms (a) 40, (b) 20, (c) 8, (d) 6 µM of NIM solution (f) blank solution in spiked serum 0.1 M phosphate buffer solution at pH 5.0 with MWCNTs modified carbon paste electrode

current versus the logarithm of scan rate showed a linearity with a slope value of 0.341 (equation 2) and the plot of peak current versus square root scan rate exhibited a straight line with a slope value of 0.166 (equation 3). These values of the slopes were found to be close to the theoretical value of 0.5. This contributes that the electro-oxidation process of NIM is diffusion controlled process on the MWCNTs modified CPE (23). Related equations are noted below:

$\log I_p = 0.341 \log v - 0.339$ r=0.991 n=8 (equation 2)

$I_p = 0.166\ v^{1/2} + 0.519$ r=0.991 n=8 (equation 3)

Validation of the analytical procedure

Voltammetric studies for determination of the NIM were carried out by DPV. DPV was selected due to the peaks are sharper and better determined at lower concentration of NIM than the peaks derived by CV. The anodic peak current increased linearly with increasing concentration of NIM in the DP voltammograms, as shown in Figure 6. The MWCNTs modified CPE showed linearity in the range from 0.06 and 10 µM of NIM for DPV.

The related validation parameters for DPV and characteristics of the calibration equation are reported in Table 1. The developed DPV was validated according to standard validation procedures (24,25). Limit of detection and limit of quantification were calculated according to 3 s/m and 10 s/m, respectively, by using the standard deviation of the anodic peak response (s) and the slope value of the calibration curve (m) (26). The limit of detection value that was obtained in this study was the lowest value than the reported value in the literature for the electroanalytical determination of NIM.

We have investigated repeatability, reproducibility, precision, recovery, bias%, and selectivity for validation NIM with MWCNTs modified CPE. All validation results for NIM with MWCNTs modified CPE were repetitive, selective, reproducibility measurements, as shown in Table 1. The validation results demonstrate good precision, accuracy, repeatability and reproducibility (Table 1).

Table 2. The results for the determination of NIM from tablet dosage forms and recovery experiments in 0.1 M PBS buffer at pH 5.0 by DPV for MWCNTs modified carbon paste electrode

	Tablet (mg)
	DPV
Labeled claim (mg)	100
Amount found (mg)*	100.41
Relative standard deviation %	0.278
Bias %	+0.406
Added (mg)	33.3
Found (mg)*	34.16
Average recovered (%)	100.64
Relative standard deviation % of recovery	0.817
Bias %	+0.627

Determination of NIM in pharmaceutical dosage forms

The MWCNTs modified CPE was applied for the determination of NIM in Nimes® tablet dosage form. Each NIM tablet in pharmaceutical dosage form contains 100 mg NIM and inactive ingredients. The developed DPV was carried out to direct determination of NIM in pharmaceutical dosage form, using the related calibration straight line. Pretreatment such as evaporation, extraction was not required for tablet dosage form. The results obtained from the tablet dosage form are listed in Table 2. The proposed method could be successfully applied for NIM assay in tablet dosage form without any interference.

Determination of NIM in spiked human serum samples

The differential pulse voltammetry optimized was successfully carried out to the voltammetric determination of NIM in protein-free spiked human serum samples. Acetonitrile was used as a serum precipitating agent. No evaporation or extraction other than centrifugal protein separation at 5000 rpm was required before analyse for the drug. The calibration equation parameters and validation parameters were shown in Table 1. Obtained recovery results of human serum samples were given in Table 3.

Differential pulse voltammograms of 40 and 6 µM of NIM obtained serum spiked were exhibited in Figure 7. As shown in Figure 7, no oxidation or noise peaks were present in

Table 3. Results of obtained for NIM determination from spiked serum

	DPV
Added concentration (µM)	8.00
Obtained concentration (µM)	8.02
Number of experiments	5
Average recovered (%)	99.83
Relative standard deviation % of recovery	0.692
Bias %	+0.25

Table 4. Electrochemical detection of NIM at different modified electrodes

Electrode	Method	Linear range (µM)	Limit of detection (µM)	Reference
Glassy carbon electrode modified by cysteic acid/CNTs	DPV	0.1-10	0.05	27
Barium doped zinc oxide nanoparticles modified glassy carbon electrode	DPV	0.1-10	0.0018	28
Gold electrode	DPV	0.2-1.2	0.0011	8
Multiwalled carbon nanotubes modified carbon paste electrode	DPV	0.06-10	0.00107	This work

the potential range where the analytical peak was formed analytical peak and determination of NIM was successfully applied in human serum samples.

Serum samples was kept in +4˚C in darkness and the stability of serum samples was studied by five consecutive analyses of the serum samples over a period of, approximately, five hours. The peak currents and peak potentials of NIM was not shown significant changes between the first and last measurements.

As it is shown in Table 4, the MWCNTs modified CPE was compared to other modified electrode in the literature according to their linear range and limit of detection. The linear range for determination of NIM with MWCNTs modified CPE at this method are better than other electrochemical methods reported in literature (27, 28, 8). When compared to limit of detection values for NIM with gold electrode (10), barium doped zinc oxide nanoparticles modified electrode glassy carbon electrode (28) and MWCNTs modified CPE (this study), this study has lowest limit of detection value.

CONCLUSION

Carbon paste electrode was modified with multiwalled carbon nanotubes and optimized for NIM. The prepared MWCNTs modified CPE was used electroanalytical determination of NIM CV and DPV. The MWCNTs modified CPE for electroanalytical determination of NIM using DPV was carried out highly selectively, simply and stably from pharmaceutical dosage forms and human serum samples. Additionally, simplicity of the electrode preparation is very practical. Thus, multiwall carbon nanotubes modified carbon paste electrode is a practical sensor and very useful for the voltammetric determination of NIM.

REFERENCES

1. Quattrini M, Paladin SA. A Double-Blind Study Comparing Nimesulide with Naproxen in the Treatment of Osteoarthritis of the Hip. Clin Drug Invest 10(3), 139-146, 1995.
2. Fallavena PRB, Schapoval EES. pKa determination of nimesulide in methanol-water mixtures by potentiometric titrations. Int J Pharm 158(1), 109-112, 1997.
3. Furlanetto S, Orlandini S, Aldini G, Gotti R, Dreassi E, Pinzauti S. Designing experiments to optimise and validate the adsorptive stripping voltammetric determination of nimesulide. Anal Chim 413(1-2), 229-239, 2000.
4. Patravale VB, Souza S, Narkar Y. HPTLC determination of nimesulide from pharmaceutical dosage forms. J Pharm Biomed Anal 25(3-4), 685-688, 2001.
5. Lakshimi CSR, Reddy MN. Spectrophotometric Estimation of Nimesulide and its Formulations. Microchim Acta 132(1), 1-6, 1999.
6. Chandran S, Saggar S, Priya KP, Saha RN. New Ultraviolet Spectrophotometric Method for the Estimation of Nimesulide Drug Dev Ind Pharm 26(2), 229-234, 2000.
7. Doğrukol-Ak D, Tuncel M, Aboul HY. A capillary zone electrophoretic method for the determination of nimesulide in pharmaceutical preparation and serum. J Sep Sci 24(9), 743-748, 2001.
8. Malode SJ, Nandibewoor ST. Electro-oxidation of nimesulide at gold electrode and its determination in pharmaceutical dosage form and human biological fluid. Asian Journal of Pharmaceutical and Clinical Research 6(3), 71-76, 2013.
9. Ghavami R, Navae A. Determination of nimesulide in human serum using a glassy carbon electrode modified with SiC nanoparticles. Microhimica Acta 176(3), 493-499.
10. Zhang J, Tan X, Zhao D, Tan S, Huang Z, Mi Y, Huang Z. Study of nimesulide and its determination using multiwalled carbon nanotubes modified glassy carbon electrodes. Electrochim Acta 55(3-4), 2522-2526, 2010.
11. Yardım Y, Şentürk Z. Electrochemical Behavior of Folic Acid at A Boron-Doped Diamond Electrode: Its Adsorptive Stripping Voltammetric Determination in Tablets. Turkish Journal of Pharmaceutical Sciences 11(1), 87-100,2014.
12. Ağın F, Karadaş N, Uslu B, Özkan SA. Voltammetric and RP-LC assay for the antidepressant drug mirtazapine: A validated method for the pharmaceutical dosage form. Maced J Chem Chem En 32(1), 41-55, 2013.
13. Du D, Huang X, Cai J, Zhang A, Ding J, Chen S. An amperometric acetylthiocholine sensor based on immobilization of acetylcholinesterase on a multiwall carbon nanotube–cross-linked chitosan composite. Anal Bioanal Chem 387(3), 1059-1065, 2007.
14. Gooding JJ. Nanostructuring electrodes with carbon nanotubes: A review on electrochemistry and applications for sensing. Electrochim Acta 50(15), 3049-3060, 2005.
15. Male KB, Hrapovic S, Luong JHT. Electrochemically-assisted deposition of oxidases on platinum nanoparticle/multi-walled carbon nanotube-modified electrodes. Analyst 132(12), 1254-1261, 2007.
16. Du D, Huang X, Cai J, Zhang A. Comparison of pesticide sensitivity by electrochemical test based on acetylcholinesterase biosensor. Biosens Bioelectron 23(2), 285-289, 2007.
17. Dirk M, Guldi NM, Carbon nanotubes and related structures, Wiley, New York, 2010.
18. Bievre P, Günzler H, Validation in chemical measurements, Springer, New York, 2005.
19. Ermer J, Miller H, Method validation in pharmaceutical analysis, Wiley-VCH, Veinheim, 2005.
20. Singh S, Sharda N.; Mahajan, L. Spectrophotometric determination of pKa of nimesulide. International Journal of Pharmaceutics 176(2), 261-264, 1999.
21. Álvarez-Lueje A, Vásquez P, Núñez-Vergara LJ, Squella JA. Voltammetric study of nimesulide and its differential pulse polarographic determination in pharmaceuticals. Electroanal 9(15), 1209-1213, 1997.
22. Wang J. Electroanalytical techniques in clinical chemistry and laboratory medicine, VCH Publishers, New York, 1988.
23. Laviron E, Roullier L, Degrand CA. Multilayer model for the study of space distributed redox modified electrodes: Part II. Theory and application of linear potential sweep voltammetry for a simple reaction. J Electroanal Chem 112(1), 11-23, 1980.
24. Riley CM, Rosanske TW, Development and validation of analytical methods, Elsevier Science Ltd., New York, 1996.
25. Hart JP, Electroanalysis of biologically important compounds, Ellis Horwood Ltd., England, 1990.

26. Berry IR and Harpaz D, Validation of active pharmaceutical ingredients 2nd ed., CRC Press, Washington, 2001.

27. Wang C, Shao X, Liu Q, Qu Q, Yang G, Hu X. Differential pulse voltammetric determination of nimesulide in pharmaceutical formulation and human serum at glassy carbon electrode modified by cysteic acid/CNTs based on electrochemical oxidation of L-cysteine. J Pharmaceut Biomed 42(2), 237–244, 2006.

28. Bukkitgar SD, Shetti NP, Kulkarni MR, Doddamani RM. Electro-oxidation of nimesulide at 5% barium-doped zinc oxid nanoparticle modi ed glassy carbon electrode. J Electroanal Chem 762, 37–42, 2016.

Received : 07.04.2016

Accepted : 12.05.2016

Turk J Pharm Sci 13(3), 342-346, 2016
DOI: 10.4274/tjps.2016.10

ORIGINAL ARTICLE

Cytotoxic Effect of *Conyza canadensis* (L.) Cronquist on Human Lung Cancer Cell Lines

Conyza canadensis (L.) Cronquist'in İnsan Akciğer Kanser Hücre Hatları Üzerine Sitotoksik Aktivitesi

Fatma AYAZ[1], Mehmet SARIMAHMUT[2], Nurgün KÜÇÜKBOYACI[1,*], Engin ULUKAYA[3]

[1]Gazi University, Faculty of Pharmacy, Department of Pharmacognosy, 06330 Ankara, TURKEY,
[2]Uludag University, Faculty of Science and Arts, Department of Biology, 16059 Bursa, TURKEY,
[3]İstinye University, Medical School, Department of Medical Biochemistry, 34010 İstanbul, TURKEY

ABSTRACT

Asteraceae family plants are receiving great attention because they have potential anticancer activity. Therefore, in this study, the cytotoxic effect of *Conyza canadensis* (L.) Cronquist (Asteraceae) were tested against human lung adenocarcinoma cell lines (A549 and H1299) for the first time. Cytotoxic effect of the *n*-hexane, chloroform, *n*-butanol and remaining water (R-H_2O) extracts fractioned from the methanol extracts of the aerial parts and roots of *C. canadensis* was investigated using Sulforhodamine B (SRB) assay and percent (%) viability was measured. The results indicate that the extracts of *C. canadensis* have cytotoxic activities on these cells in a dose-dependent manner. The root extracts exhibited relatively higher cytotoxic effects than the aerial parts of the plant. The most active extract was found to be *n*-hexane extract of the roots with IC_{50} values 94.73 and 84.85 µg/mL on A549 and H1299 cell lines, respectively. These results suggest that *C. canadensis* exhibits moderate cytotoxic effect in lung cancer cells. This might be taken into account in its use for therapeutic purposes.

Key words: Asteraceae, *Conyza canadensis*, Cytotoxic activity, Lung cancer, Sulforhodamine B assay

ÖZ

Asteraceae familyası bitkileri antikanser aktivite potansiyaline sahip olmalarından dolayı büyük ilgi görmektedir. Bundan dolayı, bu çalışmada, *Conyza canadensis* (L.) Cronquist'in (Asteraceae) insan akciğer kanser hücre hatlarına karşı (A549 ve H1299) sitotoksik etkisi ilk kez test edilmiştir. *C. canadensis*'in kökleri ve toprak üstü kısımlarının metanol ekstresinden fraksiyonlanan *n*-hekzan, kloroform, *n*-butanol ve kalan sulu (R-H_2O) ekstrelerinin sitotoksik etkisi Sülforodamin B (SRB) yöntemiyle incelenmiş ve % canlılık oranı hesaplanmıştır. Sonuçlar *C. canadensis* ekstrelerinin kanser hücreleri üzerinde doza bağlı olarak sitotoksik aktiviteye sahip olduğunu göstermiştir. Kök ekstreleri relatif olarak toprak üstü kısımlarından daha yüksek aktivitede bulunmuştur. En aktif ekstre A549 ve H1299 hücre hatları üzerine IC_{50} değerleri sırasıyla 94.73 ve 84.85 µg/mL olan köklerin *n*-hekzan ekstresi olarak tespit edilmiştir. Bu sonuçlar *C. canadensis*'in akciğer kanseri hücrelerinde orta derecede sitotoksisite gösterdiğini belirtmektedir. Bu durum bitkinin terapötik amaçlar için değerlendirilebileceğini göstermektedir.

Anahtar kelimeler: Asteraceae, *Conyza canadensis*, Sitotoksik aktivite, Akciğer kanseri, Sülforodamin B testi

INTRODUCTION

Cancer is a major group of diseaes and is still among the leading of death in the world (1). Natural products are important sources of anticancer lead molecules. Many success plant-derived anticancer drugs such as paclitaxel, docetaxel, vincristin, etoposide, camptothecin, irinotecan are clinically available; however due to the rapid development of resistance to chemotherapeutic drugs and their side effetcs, novel anticancer drugs of natural sources are under an extensive search for cancer therapy (2,3).

The family Asteraceae which contains over 1600 genera and more than 23000 species is the largest family with rich chemical constituents (4). It has a broad medicinal utilization worldwide in which over 300 species of the family are known to have ethnomedicinal uses for cancer related diseases (5). The number of studies related to the cytotoxicity of Asteraceae plants and their secondary metabolites have

*Correspondence: E-mail: nurgun@gazi.edu.tr Phone: +90 312 202 31 77

intensively investigated in recent years. In these studies, sesquiterpene lactones and flavonoids have been principally stated to be responsible compounds for the cytotoxic effects (6-10). These compounds induce apoptosis after disrupting cell cycle of cancer cells *in vitro* and *in vivo* and also inhibit angiogenesis and metastasis (11,12).

The genus *Conyza* Less. belongs to the family Asteraceae and consists of about fifty species all over the world. In Turkey, the genus *Conyza* is represented by three species in the flora of Turkey, namely *C. canadensis* (L.) Cronquist, *C. bonariensis* (L.) Cronquist, and *C. albida* Willd. ex. Sprengel (13,14). *C. canadensis* (syn. *Erigeron canadensis* L.), known as "Canadian fleabane" or "horseweed", is native throughout of North America and is also widespread in Europe. It is an annual plant erecting 10 to 180 cm high, with sparsely hairy stems (15). *C. canadensis* was reported to be used for its diuretic, antibacterial, anti-inflammatory, tonic, astringent, antihaemorrhagic properties as well as for the treatment of diarrhea and dysentery in folk medicines (16-18). In addition, a decoction of the plant is used anticancer purposes in North America (19).

The phytochemical studies on *C. canadensis* have so far pointed out to presence of terpenes, acetylene derivatives, flavonoids, benzoic acid derivatives, alkaloids, essential oils, sphingolipids, fatty acids and sterols (20-26). Among them, C_{10} acetylenes such as diyn-ene (e.g. *E*-lachnophyllum methyl ester) and ene-diyn-ene (e.g. matricaria methyl ester isomers), and C_{10} lactones (e.g. 8*Z*-matricaria-γ-lactone) are typical constituents of the genus (20,26).

C. canadensis have been demonstrated to exert several biological activities such as cytotoxic, antifungal, antibacterial, antiviral, anti-inflammatory, antioxidant, and antiagregant (26-33). In previous studies, the extracts from *C. canadensis* were reported to have prominent cytotoxic effects on various cancer cell lines (26,34-37). To the best of our knowledge, there is no scientific report available in support of the cytotoxic effect of *C. canadensis* on A549 and H1299 human lung cancer cells. The aim of the present study was to investigate the possible *in vitro* cytotoxic effect of the extracts from the aerial parts and roots of *C. canadensis* in human lung adenocarcinoma cell lines (A549 and H1299).

EXPERIMENTAL

Chemicals

In the extraction procedure, methanol, *n*-hexane, chloroform and *n*-butanol were of analytical grade and were purchased from Merck Co. (Darmstadt, Germany). Analytical thin layer chromatography (TLC) was performed on precoated Kieselgel 60 F_{254} plates (Art. 5554, Merck). The plates sprayed with anisaldehyde reagent [76% methanol (Merck) and 19% ortho-phosphoric acid (Riedel-De Haën, Buchs, SG Switzerland), 5% *p*-anisaldehyde (Merck)], 30% H_2SO_4 (Merck) solution in MeOH (Merck) and 1% vanillin-H_2SO_4 solution [vanillin (Boehringer Mannheim, Mannheim, Germany) and H_2SO_4 (Merck)].

Plant material

Conyza canadensis (L.) Cronquist was collected from Balcova, Izmir, Turkey, in the flowering-fruit stage, in November 2013. The plant was identified by Prof. Dr. Mecit Vural from the Department of Botany, Faculty of Science, Gazi University. A voucher specimen (F. Ayaz 29) has been deposited at Herbarium of Gazi University (GAZI), Ankara, Turkey.

Preparation of extracts

39.52 g powdered aerial parts (CCH) and 40.25 g roots (CCR) of the plant were extracted with 80% methanol by stirring at 40°C for 6 h three times (3×300 mL). Following filtration, the combined methanol extracts were evaporated *in vacuo* at 40°C to dryness. The concentrated MeOH extracts (100 mL) were further fractionated by successive solvent extractions with *n*-hexane (3×100 mL), chloroform (3×100 mL) and *n*-butanol saturated with H_2O (3×100 mL) in a separatory funnel. Each extract as well as remaining aqueous phase (R-H_2O) after solvent extractions was evaporated to dryness under reduced pressure to yield "*n*-Hexane extract" (0.04 g for CCH, 0.29 g for CCR), "$CHCl_3$ extract" (0.14 g for CCH, 0.30 g for CCR), "*n*-BuOH extract" (2.63 g for CCH, 1.86 g for CCR) and "R-H_2O extract" (1.03 g for CCH, 2.83 for CCR), respectively.

Phytochemical analysis

1 mg/mL of *C. canadensis* extracts were applied to silica gel plates. The *n*-hexane and $CHCl_3$ extracts were developed with the mixture of *n*-hexane:acetone (7:3) as a mobile phase. TLC plates were evaluated under UV light at 254 and 366 nm for the determination of fluorescent compounds. Anisaldehyde reagent and 30% H_2SO_4 were sprayed to the plates to visualize the separated compounds and then plates were heated for 5 min at 100°C. Terpenes were appeared in pink, purple and green coloration with anisaldehyde reagent. In addition, terpenes also showed red coloration under UV 254 nm sprayed with 30% H_2SO_4 after heating for 5 min at 100°C. The *n*-butanol and R-H_2O extracts were developed in a mixture of solvent system $CHCl_3$:MeOH:H_2O (61:32:7) and then sprayed with 1% vanillin-H_2SO_4 solution. The plates were heated for 5 min at 100°C before examined under UV light. Flavonoids detected as yellow and orange zones on the plates (38).

Cell culture

A549 and H1299 human lung adenocarcinoma cells were kindly provided by Prof. Hakan Akça (Pamukkale University, Faculty of Medicine, Denizli, Turkey). A549 and H1299 cells were cultured in RPMI 1640 medium supplemented with penicillin G (100 U/mL), streptomycin (100 mg/mL), L-glutamine, and 10% fetal bovine serum at 37°C in a humidified atmosphere containing 5% CO_2.

Cytotoxicity assay

For the Sulforhodamine B (SRB) assay, which is routinely performed by National Cancer Institute (NCI) for *in vitro* drug screening, *n*-hexane, chloroform, *n*-butanol and remaining

water extracts were added to 96-well plates to make up a final concentration range of 1.56 µg/mL to 100 µg/mL by serial dilutions (six two-fold dilutions). Then, A549 and H1299 cells were seeded at a density of $5x10^3$ cells per well of 96-well plates. Subsequently, cells were incubated with various concentrations of the aerial parts and roots extracts for 48 h. The assay was terminated by the addition of ice-cold 50% (w/v) trichloroacetic acid. SRB 0.4% (w/v) in 1% (v/v) acetic acid staining was then performed. The bound dye was extracted using 10 mM unbuffered Tris and optical density was measured at 564 nm with an ELISA plate reader (FLASH Scan S12, Analytik Jena, Germany). Viability of treated cells was calculated in reference to the untreated control cells by using the following formula:

Cell viability (%)= [100×(Sample Abs)/(Control Abs)].

RESULTS AND DISCUSSION

The cytotoxic effect of the extracts from the aerial parts and roots of *C. canadensis* on lung cancer cell lines (A549 and H1299) were first investigated by the SRB assay after treating cells with increasing doses of extracts (1.56 µg/mL-100 µg/mL) for 48 h. It was found that the extracts inhibited growth of cells in a dose-dependent manner and prominently reduced the cell viability at the 100 µg/mL. The cytotoxic effects after the treatment with the extracts against human lung adenocarcinoma cell lines were shown in Figures 1a, 1b, 2a and 2b.

In order to compare antigrowth effects of various concentrations of the aerial parts and roots extracts of *C. canadensis*, the root extracts exhibited relatively higher antigrowth effects than the aerial parts extracts. The strongest cytotoxic activity was detected for the *n*-hexane extract of the roots with IC_{50} values 94.73 and 84.85 µg/mL on A549 and H1299 cell lines, respectively. Overall, the antigrowth effects of the extracts were not dependent on the cell line. Considering the fact that A549 expresses wild type p53 and H1299 is p53 null, it can be stated that the resulting antigrowth effects of the extracts are p53 independent (39). This may actually be favorable because majority of cancers have mutated p53, thereby these extracts would still be active against even p53-mutated ones.

To the best of our knowledge, this is the first attempt rationalizing the cytotoxic effect of *C. canadensis* on A549 and H1299 human lung cancer cells. Neverthless, a few

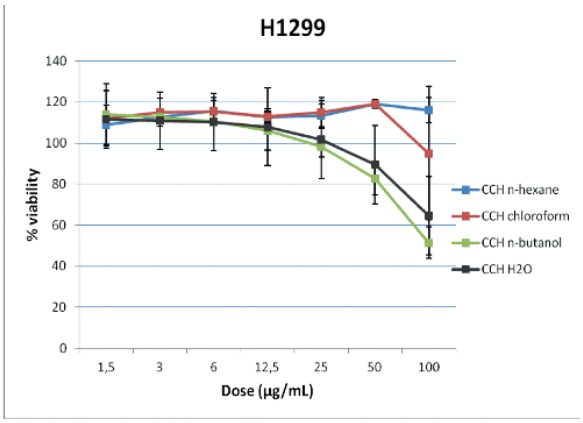

Figure 1a. The cytotoxic effects with different concentrations of the aerial parts extracts of *C. canadensis* on H1299 cell lines

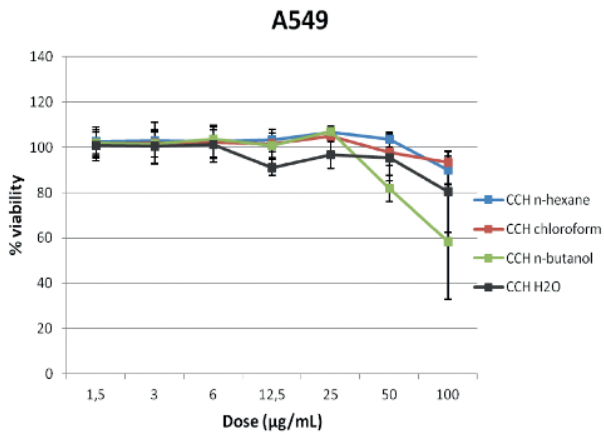

Figure 1b. The cytotoxic effects with different concentrations of the aerial parts extracts of *C. canadensis* on A549 cell lines

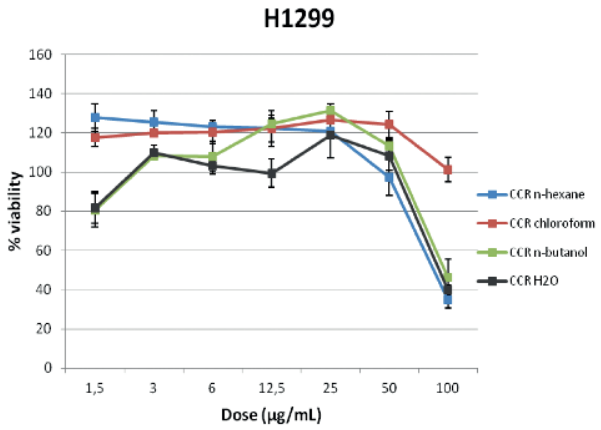

Figure 2a. The cytotoxic effects with different concentrations of the root extracts of *C. canadensis* on H1299 cell lines

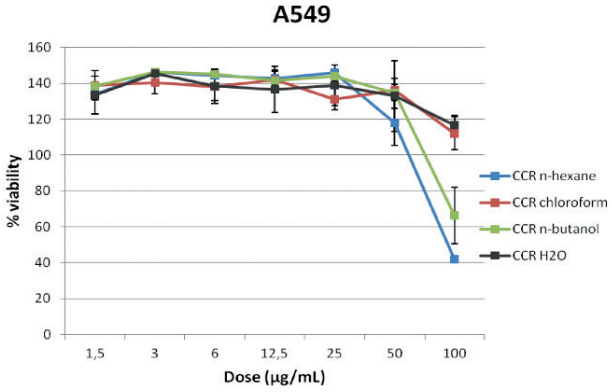

Figure 2b. The cytotoxic effects with different concentrations of the root extracts of *C. canadensis* on A549 cell lines

studies demonstrated earlier cytotoxic effect of the extracts of *C. canadensis* of different origin having varying levels of inhibition on various cancer cell lines (26,34-37). For instance; *n*-hexane, chloroform and aqueous MeOH extracts partitioned from MeOH extract of the aerial parts, flowers and roots of *C. canadensis* and the H_2O extracts prepared from the residual plant materials were investigated for their cytotoxic properties on HeLa, MCF-7 and A431 cell lines using the MTT assay. The *n*-hexane phase of the roots exhibited markedly antigrowth effects on the cell lines (62.4-70.1%) at 10 µg/mL, and the $CHCl_3$ phase of the roots demonstrated moderate antiproliferative activity (39.3-47.9%) at the same concentration (34). According to the bioactivity-guided fractionation of the *n*-hexane and chloroform phases of the methanol extract from the roots of *C. canadensis*, two new unusual C_{10} γ-dihydropyranone derivatives (conyzapyranone A and conyzapyranone B), as well as 2 γ-lactone acetylene derivatives (e.g. 4*E*,8*Z*-matricaria-γ-lactone), triterpenes, sterols (e.g. spinasterol), a hydroxy fatty acid and a flavonoid were isolated. Among them, conyzapyranone B, 4*E*,8*Z*-matricaria-γ-lactone and spinasterol were found to have remarkable antiproliferative activity against HeLa, MCF-7 and A431 cell lines (26). In other study, cytotoxic activities of petroleum ether, ethyl acetate and methanol extracts of the aerial parts of *C. canadensis* were investigated on Hep-2 using methylene blue assay at 24, 48 and 72 h of incubation. At 72 h of incubation, the most active extracts were found to be ethyl acetate and petroleum ether extracts with IC_{50} values 45 and 50 µg/mL, respectively (36). In another study, erigeronol, a new triterpene derivative, was isolated from *C. canadensis* as a potent cytotoxic compound with IC_{50} value of 7.77±0.47 µg/mL on melanoma B16 cell line by the MTT method (37). In these studies, triterpenes, C_{10} acetylene derivatives and dihydropyranones have mainly found as effective cytotoxic constituents in *C. canadensis* (26,37). In our study, terpenes and flavonoids were principally detected in the root extracts according to the preliminary phytochemical analysis.

The present investigation represents a preliminary screen for the cytotoxic effect of *C. canadensis* in human lung cancer cell lines. In accordance with the National Cancer Institute Guidelines, extracts with IC_{50} values ‹20 µg/mL were accepted as active (40). This study resulted in moderate cytotoxic activity compared to the previous studies against the selected cell lines which might be attributed to usage of different cell lines as well as the diverse phytochemical composition in the extracts. The present results are also in accordance with ethnomedicinal uses of the plant reported by Hartwell (Hartwell, 1968).

In conclusion, we provided the first evidence for cytotoxic effects of *C. canadensis* against A549 and H1299 cancer cell lines although it shows the cytotoxic activity at relatively higher doses.

ACKNOWLEDGEMENTS

The authors would like to thank to Prof. Dr. Mecit Vural from the Department of Botany, Faculty of Science, Gazi University, Ankara, Turkey for the identification of the plant.

REFERENCES

1. World Health Organization, WHO Library Cataloguing-in-Publication Data World Health Statistics 2010, Who Press, Geneva 27, Switzerland, World Health Organization 2010.
2. Demain AL, Vaishnav P, Natural products for cancer chemotherapy, Microbial Biotechnol, 5(6), 687-699, 2011.
3. Mondal S, Bandyopadhyay S, Ghosh MK, Mukhopadhyay S, Roy S, Mandal C, Natural products: Promising resources for cancer drug discovery, Anticancer Agents Med Chem 12(1), 49-75, 2012.
4. Jeffrey C, Compositae - Introduction with key to tribes. In: Kadereit JW, Jeffrey C, eds. The Families and Genera of Vascular Plants: VIII, Flowering Plants Eudicots Asterales, Springer-Verlag: Berlin, Germany, 61-86, 2007.
5. Graham JG, Quinn ML, Fabricant DS, Farnsworth NR, Plants used against cancer - An extension of the work of Jonathan Hartwell, J Ethnopharmacol 73, 347-377, 2000.
6. Zheng GQ, Cytotoxic terpenoids and flavonoids from *Artemisia annua*, Planta Med 60, 54-57, 1994.
7. Woerdenbag HJ, Merfort I, Passreiter CM, Schmidt TJ, Willuhn G, Vanuden W, Pras N, Kampinga HH, Konings AWT, Cytotoxicity of flavonoids and sesquiterpene lactones from *Arnica* species against the Glc-4 and the Colo-320 cell lines, Planta Med 60, 434-437, 1994.
8. Koukoulitsa E, Skaltsa H, Karioti A, Demetzos C. Dimas K, Bioactive sesquiterpene lactones from *Centaurea* species and their cytotoxic/cytostatic activity against human cell lines in vitro, Planta Med 68, 649-652, 2002.
9. Modzelewska A, Sur S, Kumar SK, Khan SR, Sesquiterpenes: Natural products that decrease cancer growth, Curr Med Chem Anticancer Agents 5, 477-499, 2005.
10. Pan L, Lantvit DD, Riswan S, Kardono LBS, Chai HB, de Blanco EJC, Farnsworth NR, Soejarto DD, Swanson SM, Kinghorn AD, Bioactivity-guided isolation of cytotoxic sesquiterpenes of *Rolandra fruticosa*, Phytochemistry 71, 635-640, 2010.
11. Zhang S, Won YK, Ong CN, Shen HM, Anti-cancer potential of sesquiterpene lactones: bioactivity and molecular mechanisms, Curr Med Chem Anticancer Agents 5, 239-249, 2005.
12. Patel D, Shukla S, Gupta S, Apigenin and cancer chemoprevention: Progress, potential and promise, Int J Oncol 30, 233-245, 2007.
13. Grierson AJC, *Conyza* Less. In: Davis PH, ed. Flora of Turkey and the East Aegean Islands, Vol 5, pp 132-133, Edinburgh at the University Press: Edinburgh, 1975.
14. Davis PH, Mill RR, Kit T, *Conyza* Less. In: Davis PH, Mill RR, Kit T, eds. Flora of Turkey and the East Aegean Islands, Vol 10, pp 161-162, Edinburgh at the University Press: Edinburgh, 1988.
15. Weaver SE, The biology of Canadian weeds *Conyza canadensis*, Can J Plant Sci 8, 867-875, 2001.
16. Metwally AM, Saleh MRI, Aggag M, Khafagy SM, Phytochemical investigation of *Erigeron crispus*, Planta Med 23, 281-285, 1973.
17. Li TSC, Chinese and Related North American Herbs: Phytopharmacology and Therapeutic Values, CRC Press: Boca Raton, Florida, 2002.

18. Gruenwald J, Brendler T, Jaenicke C, Physician's Desk Reference for Herbal Medicines, 3rd ed, Thomson Medical Economics Montvale: NJ, USA, 2004.
19. Hartwell J, Plants used against cancer: A survey, Lloyd 31, 71-170, 1968.
20. Bohlmann F, Jakupovic J, 8-Oxo-*alpha*-selinene and new scopoletin derivatives from *Conyza* species, Phytochemistry 18, 1367-1370, 1979.
21. Mukhtar N, Iqbal K, Anis I, Malik A, Sphingolipids from *Conyza canadensis*. Phytochemistry 61, 1005-1008, 2002.
22. Mukhtar N, Iqbal K, Malik A, Novel sphingolipids from *Conyza canadensis*, Chem Pharm Bull 50, 1558-1560, 2002.
23. Li X, Pan J, Gao K, γ-Pyranone derivatives and other constituents from *Erigeron annuus*, Pharmazie 61, 474-477, 2006.
24. Xie WD, Gao X, Jia ZJ, A new acetylene and a new triterpenoid from *Conyza canadensis*, Arch Pharm Res 30, 547-551, 2007.
25. Ding X, Su Y, Guo H, Yang F, Mao H, Gao X, Zhu Z, Tu G, Phenypropanoid esters from horseweed (*Conyza canadensis*) and their inhibitory effects on catecholamine secretion, J Nat Prod 73, 270-274, 2010.
26. Csupor-Löffler B, Hajdú Z, Zupkó I, Molnár J, Forgo P, Vasas A, Kele Z, Hohmann J, Antiproliferative constituents of the roots of *Conyza canadensis*, Planta Med 77, 1183-1188, 2011.
27. Lenfeld J, Motl O, Trka A, Anti-inflammatory activity of extracts from *Conyza canadensis,* Pharmazie 41, 268-269, 1986.
28. Olas B, Saluk-Juszczak J, Pawlaczyk I, Nowak P, Kolodziejczyk J, Gancarz R, Wachowicz B, Antioxidant and antiaggregatory effects of an extract from *Conyza canadensis* on blood platelets in vitro, Platelets 17, 354-360, 2006.
29. Shah NZ, Mir AK, Muhammad N, Azeem S, Antimicrobial and phytotoxic study of *Conyza canadensis*, Middle-East J Med Pl Res 1, 63-67, 2012.
30. Shah NZ, Mir AK, Muhammad N, Azeem S, Rauf A, Studies on the chemical constituents and antioxidant profile of *Conyza canadensis*, Middle-East J Med Pl Res 1, 32-35, 2012.
31. Edziri HL, Laurent G, Mahjoub A, Mastour M, Antiviral activity of *Conyza canadensis* (L.) Cronquist extracts grown in Tunisia, Afr J Biotechnol 10, 9097-9100, 2011.
32. Ni LX, Hao XY, Li SY, Chen SJ, Ren GX, Zhu L, Inhibitory effects of the extracts with different solvents from three compositae plants on cyanobacterium *Microcystis aeruginosas*, Sci China Chem 54, 1123-1129, 2011.
33. Shakirullah M, Ahmad H, Shah MR, Ahmad I, Ishaq M, Khan N, Badshah A, Khan I, Antimicrobial activities of conyzolide and conyzoflavone from *Conyza canadensis*, J Enzym Inhib Med Chem 26, 468-471, 2011.
34. Réthy B, Csupor-Löffler B, Zupkó I, Hajdú Z, Máthé I, Hohmann J, Rédei T, Falkay G, Antiproliferative activity of Hungarian Asteraceae species against human cancer cell lines Part I, Phytother Res 21, 1200-1208, 2007.
35. Choi HJ, Wang HY, Kim YN, Heo SJ, Kim NK, Jeong MS, Park YH, Kim S, Composition and cytotoxicity of essential oil extracted by steam distillation from horseweed (*Erigeron canadensis* L.) in Korea, Han'guk Eungyong Sangmyong Hwahakhoeji 51, 55-59, 2008.
36. Hayet E, Maha M, Samia A, Ali MM, Souhir B, Abderaouf K, Mighri Z, Mahjoub A, Antibacterial, antioxidant and cytotoxic activities of extracts of *Conyza canadensis* (L.) Cronquist growing in Tunisia, Med Chem Res 18, 447-454, 2009.
37. Yan MM, Li TY, Zhao DQ, Shao S, Bi SN, A new derivative of triterpene with anti-melanoma B16 activity from *Conyza canadensis*, Chinese Chem Lett 21, 834-837, 2010.
38. Wagner H, Bladt S, Plant Drug Analysis: A Thin Layer Chromatography Atlas, 2nd ed, Springer-Verlag: Berlin, Germany, 2001.
39. Yu J, Yue W, Wu B, Zhang, L, PUMA Sensitizes Lung Cancer Cells to Chemotherapeutic Agents and Irradiation, Clin Cancer Res 12, 2928-2936, 2006.
40. Suffness MS, Pezzuto MJ, Assays related to cancer drug discovery, In: Dey PM, Harborne JB, eds. Methods in Plant Biochemistry, pp 71-133, Academic Press: London, UK, 1991.

Received : 20.05.2016
Accepted : 02.06.2016

Turk J Pharm Sci 13(3), 347-350, 2016
DOI: 10.4274/tjps.2016.11

SHORT COMMUNICATION

Antioxidant and Anticholinesterase Activities of Essential Oil of *Alseodaphne peduncularis* Meisn

Alseodaphne peduncularis Meisn. Uçucu Yağının Antioksidan ve Antikolinesteraz Aktivitesi

Wan Mohd Nuzul Hakimi Wan SALLEH, Farediah AHMAD*

Department of Chemistry, Faculty of Science, Universiti Teknologi Malaysia, 81310 Johor Bahru, Johor, MALAYSIA

ABSTRACT

This study was designed to investigate the antioxidant and anticholinesterase activities of the essential oils from *Alseodaphne peduncularis* Meisn. GC and GC/MS analysis of the leaves oil showed thirty one components representing 72.6% of the oil. The most abundant components were β-caryophyllene (24.0%), δ-cadinene (15.9%) and germacrene B (12.2%). The antioxidant activity was determined by DPPH (1,1-diphenyl-2-picrylhydrazyl) radical scavenging and total phenolic content assays, while anticholinesterase activity assessed by measuring inhibition of acetylcholinesterase (AChE) and butyrylcholinesterase (BChE) enzymes. The essential oil showed weak activity in the DPPH radical scavenging (IC_{50} of 253.2 µg/mL) and phenolic content (32.5 mg GA/g), while moderate inhibition activity against AChE (I: 45.2%) and BChE (I: 48.6%).
Key words: Essential oil, *Alseodaphne peduncularis*, Antioxidant activity, Anticholinesterase activity, Lauraceae

ÖZ

Bu çalışma *Alseodaphne peduncularis* Meisn. uçucu yağının antioksidan ve antikolinesteraz aktivitelerini araştırmak için tasarlanmıştır. GC ve GC/MS analizleri yaprak yağında %72,6 oranında otuz bir bileşen bulunduğunu göstermiştir. En çok bulunan bileşenler β-karyofilen (%24,0), δ-kadinen (15,9) ve germakren B (%12,2) dir. Antioksidan aktivite DPPH (1,1- difenil-2-pikrilhidrazil) radikal süpürme ve toplam fenolik içerik yöntemleriyle değerlendirilirken, antikolinesteraz aktivite asetilkolinesteraz (AChE) ve bütirilkolinesteraz (BChE) enzim inhibisyonu ölçülerek değerlendirilmiştir. Uçucu yağ, zayıf DPPH radikal süpürme aktivitesi (IC_{50} değeri 253,2 mg/mL) ve fenolik içerik (32,5 mg GA/g) gösterirken, AChE (I: %45,2) ve BChE (I: %48,6) inhibisyon aktivitesi orta düzeydedir.
Anahtar kelimeler: Uçucu yağ, *Alseodaphne peduncularis*, Antioksidan aktivite, Antikolinesteraz aktivite, Lauraceae

INTRODUCTION

Alseodaphne is a genus of small to medium sized trees of the wet evergreen tropical forests. The genus is having more than fifty species and distributed in tropical belt of Cambodia, China, Indonesia, Laos, Malaysia, Myanmar, Philippines, Sri Lanka, Thailand, Vietnam and India. There is no information in the literature regarding medicinal uses of genus Alseodpahne. Most of the species of genus are unexplored, both, pharmacologically and phytochemically (1). Previous phytochemical investigations of Alseodaphne have resulted in the isolation of alkaloids (aporphines, bisbenzylisoquinoline, morphinandienones) (2), lactones (3), neolignans (4) and phenanthrenes (5). The isolated constituents of genus *Alseodaphne* might become useful as a source of pharmacologically interesting molecules.

A. peduncularis is a shrub or sometimes a small tree of up to 6-12 m height. The twigs colour is whitish. The leaves/stalk is slender and around 0.51 cm long in size. The blade is membranous and lanceolate with drying greenish brown colour. The midrib rise above and secondary nerves is about 610 pairs, curving and joining near margin and rise on both surfaces. The tertiary nerves are reticulate and visible on both the surfaces. The colour of the flowers is greenish. The shape of fruits is ellipsoid or globose with a dark purple colour and on enlarged red perianth tube (1).

To the best of our knowledge there is no report on the chemical compositions of the essential oil of *A. peduncularis*, therefore we would like to report their chemical composition and their antioxidant and anticholinesterase activities.

*Correspondence: E-mail: farediah@kimia.fs.utm.my Phone: +607-5534137

MATERIALS AND METHODS

Plant materials

A sample of *A. peduncularis* was collected from Hutan Simpan Bangi, Selangor in September 2015, and identified by Dr. Shamsul Khamis from Institute of Biosience (IBS), Universiti Putra Malaysia (UPM). The voucher specimen (SK2955/16) were deposited at the Herbarium of IBS, UPM.

Solvents and chemicals

Antioxidant: 1,1-Diphenyl-2-picrylhydrazyl (DPPH), gallic acid and butylatedhydroxytoluene (BHT) were obtained from Sigma-Aldrich (Germany). Analytical grade methanol, ethanol and dimethylsulfoxide (DMSO), HPLC grade chloroform, Folin-Ciocalteu's reagent, anhydrous sodium sulphate, and sodium carbonate were purchased from Merck (Germany). Anticholinesterase: AChE enzyme (Type-VI-S, EC3.1.1.7), butyrylcholinesterase enzyme (BChE; EC3.1.1.8), acetylthiocholine iodide, butyrylthiocholine chloride, 5,5′-dithio-bis(2-nitrobenzoic)acid (DTNB), and galantamine were purchased from Sigma-Aldrich (Germany).

Extraction of essential oils

The fresh leaf (300 g) was subjected to hydrodistillation in an all glass Dean-stark apparatus for 6 hours. The oils obtained were dried over anhydrous magnesium sulfate and stored at 4-6˚C. The oil yield (w/w) was 1.55 g (0.52%) based on the fresh weight.

Gas chromatography (GC)

GC analysis were performed on a Hewlett Packard 6890 series II A gas chromatograph equipped with an Ultra-1 column (100% polymethylsiloxanes) (25 m long, 0.33 µm thickness and 0.20 mm inner diameter). Helium was used as a carrier gas at flow rate of 0.7 mL/min. Injector and detector temperature were set at 250 and 280˚C, respectively. Oven temperature was kept at 50˚C, then gradually raised to 280˚C at 5˚C/min and finally held isothermally for 15 min. Diluted samples (1/100 in diethyl ether, v/v) of 1.0 µL were injected manually (split ratio 50:1). The injection was repeated three times and the peak area percents were reported as means ± SD of triplicates. Calculation of peak area percentage was carried out by using the GC HP Chemstation software (Agilent Technologies).

Gas chromatography-mass spectrometry (GC-MS)

GC-MS chromatograms were recorded using a Hewlett Packard Model 5890A gas chromatography and a Hewlett Packard Model 5989A mass spectrometer. The GC was equipped with Ultra-1 column (25 m long, 0.33 µm thickness and 0.20 mm inner diameter). Helium was used as a carrier gas at a flow rate of 1 mL/min. Injector temperature was 250˚C. Oven temperature was programmed from 50˚C (5 min hold) at 10˚C/min to 250˚C and finally held isothermally for 15 min. For GC-MS detection, an electron ionization system, with ionization energy of 70 eV was used. A scan rate of 0.5 s (cycle time: 0.2 s) was applied, covering a mass range from 50-400 amu.

Identification of components

The constituents of the oil were identified by comparison of their mass spectra with reference spectra in the computer library (Wiley) and also by comparing their retention indices, with data in the literature (6). The quantitative data were obtained electronically from FID area percentage without the use of correction factor.

Antioxidant activity

DPPH radical scavenging

The free radical scavenging activity was measured by the DPPH method with minor modifications (7). Each sample of stock solution (1.0 mg/mL) was diluted to final concentration of 1000-7.8 µg/mL. Then, a total of 3.8 mL of 50 µM DPPH methanolic solution (1 mg/50 mL) was added to 0.2 mL of each sample solution and allowed to react at room temperature for 30 min. The absorbance of the mixtures was measured at 517 nm. A control was prepared without sample or standard and measured immediately at 0 min. Lower absorbance of the reaction mixture indicates higher free radical scavenging activity, and vice versa. The percent inhibitions (I%) of DPPH radical were calculated as follow:

I% = [Ablank – Asample/ Ablank] ×100

where Ablank is the absorbance value of the control reaction and Asample is the absorbance values of the test samples. The sample concentration providing 50% inhibition (IC_{50}) was calculated by plotting inhibition percentages against concentrations of the sample. All tests were carried out in triplicate and IC_{50} values were reported as means ± SD of triplicates.

Total phenolic content (TPC)

Total phenolic contents of the essential oils were determined as described previously (8). A sample of stock solution (1.0 mg/mL) was diluted in methanol to final concentrations of 1000 µg/mL. A 0.1 mL aliquot of samplewas pipetted into a test tube containing 0.9 mL of methanol, then 0.05 mL Folin-Ciocalteu's reagent was added, and the flask was thoroughly shaken. After 3 min, 0.5 mL of 5% Na_2CO_3 solution was added and the mixture was allowed to stand for 2 h with intermittent shaking. Then, 2.5 mL of methanol was added and left to stand in the dark for 1 h. The absorbance measurements were recorded at 765 nm. The same procedure was repeated for the standard gallic acid solutions. The concentration of total phenolic compounds in the oils was expressed as mg of gallic acid equivalent per gram of sample. Tests were carried out in triplicate and the gallic acid equivalent value was reported as mean ± SD of triplicate.

Anticholinesterase activity

AChE/BChE inhibitory activity of the essential oils was measured by slightly modifying the spectrophotometric

Table 1. Constituents identified from the essential oil of *A. peduncularis*

No	Components	KI[a]	Percentage (%)
1	δ-Elemene	1335	1.5
2	α-Cubebene	1345	0.5
3	α-Ylangene	1373	0.1
4	α-Copaene	1374	2.5
5	β-Copaene	1374	0.8
6	Isoledene	1375	0.3
7	β-Cubebene	1387	0.4
8	α-cis-Bergamotene	1411	0.4
9	**β-Caryophyllene**	1417	**24.0**
10	α-trans-Bergamotene	1432	0.1
11	γ-Elemene	1434	5.2
12	α-Guaiene	1437	0.0
13	6,9-Guaiadiene	1442	0.6
14	cis-Cadina-1(6)4-diene	1461	0.2
15	trans-Cadina-1(6)4-diene	1475	0.4
16	γ-Muurolene	1478	0.9
17	β-Selinene	1489	0.6
18	β-Guaiene	1492	0.1
19	γ-Amorphene	1495	0.3
20	Valencene	1496	0.3
21	Cubebol	1514	0.3
22	**δ-Cadinene**	1522	**15.9**
23	α-Cadinene	1537	0.1
24	γ-Cadinene	1543	0.2
25	Germacrene B	1559	**12.2**
26	(E)-Nerolidol	1561	0.1
27	Spathulenol	1577	0.2
28	Caryophyllene oxide	1582	0.8
29	Globulol	1590	0.2
30	Epicubenol	1627	1.0
31	trans-Longipinocarveol	1634	0.2
32	t-Muurolol	1644	1.9
33	β-Eudesmol	1649	0.1
34	α-Bisabolol	1685	0.1
35	Phytol	1942	0.1
Group components			
	Sesquiterpene hydrocarbons		67.6
	Oxygenated sesquiterpenes		5.0
Identified components (%)			**72.6**

[a]Kovat's indices (KI) experimental: n-alkanes (C_9-C_{30}) were used as reference points in the calculation of KI

method developed by Ellman et al. (9) and Orhan et al. (10). Electric eel (Electrophorus electricus) AChE and horse serum BChE were used, while acetylthiocholine iodide (AChI) and butyrylthiocholine chloride (BChI) were employed as substrates of the reaction. DTNB acid was used for the measurement of the anticholinesterase activity. Briefly, in this method, 140 µL of sodium phosphate buffer (pH 8.0), 20 µL of DTNB, 20 µL of essential oils and 20 µL of AChE/BChE solution were added by multichannel automatic pipette in a 96-well microplate and incubated for 15 min at 25˚C. The reaction was then initiated with the addition of 10 µL of AChI/BChI. Hydrolysis of AChI/BChI was monitored by the formation of the yellow 5-thio-2-nitrobenzoate anion as a result of the reaction of DTNB with thiocholines, catalyzed by enzymes at 412 nm utilizing a 96-well microplate reader (Epoch Micro-Volume Spectrophotometer). Percentage inhibition (I%) of AChE/BChE was determined by comparison of rates of reaction of samples relative to blank sample (EtOH in phosphate buffer pH 8) using the formula:

I%=[E-S/E]×100

where E is the activity of enzyme without test sample and Sis the activity of enzyme with test sample. The experiments were done in triplicate. Galantamine was used as reference.

Statistical analysis

Data obtained from essential oil analysis and their bioactivities were expressed as mean values. The statistical analyses were carried out by employing one way ANOVA ($p<0.05$). A statistical package (SPSS version 11.0) was used for the data analysis.

RESULTS AND DISCUSSION

Hydrodistillation of the fresh leaves of *A. peduncularis* gave pale yellow oil in 0.52% (w/w). The chemical compositions of the leaves oil of *A. peduncularis* are listed in Table 1. GC and GC-MS analysis of the essential oil had successfully found thirty five components, which accounted for 72.6% of the chromatographical components. Sesquiterpene hydrocarbons were the major components in the essential oil (67.6%) with β-caryophyllene (24.0%) being the most substantial component, followed by δ-cadinene (15.9%) and germacrene B (12.2%). Furthermore, oxygenated sesquiterpenes made

Table 2. Antioxidant and anticholinesterase activities of the essential oil of *A. peduncularis*

Samples	DPPH IC_{50} (µg/mL)[a]	TPC (mg GA/g)[b]	AChE (I%)c	BChE (I%)[c]
Essential oil	253.2	32.5 ± 0.1	45.2 ± 0.2	48.6 ± 0.2
BHT	18.5	-	-	-
Galantamine	-	-	95.9 ± 0.2	88.7 ± 0.2

[a]IC_{50} value at concentrations of 1000-7.8µg/mL; [b]TPC at a concentration of 1 mg/mL;[c]Percentage inhibition at a concentration of 1 mg/mL; ± represents SD of three independent experiments ($p < 0.05$)

up a minor fraction which gave 5.0%, while monoterpenoids were not found in this essential oil.

The antioxidant activities were investigated by DPPH free radical scavenging assay together with the Folin-Ciocalteu assay which evaluated the total phenolic content of the essential oil. The results are displayed in Table 2. The antioxidant activity on DPPH radical scavenging is due to their hydrogen donating ability. The capability of substances to donate hydrogen is able to convert DPPH into their non-radical form DPPH and the reaction can be followed spectrophotometrically (11). The essential oil exhibited weak DPPH radical scavenging activity (IC_{50} of 253.2 µg/mL) compared to standard antioxidant, BHT (IC_{50} of 18.5 µg/mL). The low activity was attributed to the low phenolic content of the essential oil which is responsible for antioxidant activity. This was supported by the results of the Folin-Ciocalteu assay on the essential oils, which showed low amount of phenolic (32.5%). AChE plays an important role in the central nervous system. It is one of the fastest known enzymes and catalyses the cleavage of acetylcholine in the synaptic cleft after depolarisation. Inhibitors of AChE, such as galanthamine, are used frequently in the pharmacotherapy of Alzheimer disease (12). The essential oil indicated moderate AChE and BChE activity at 1000 µg/mL concentration, which gave 45.2% and 48.6% for AChE and BChE activity, respectively. In previous reports, AChE inhibition can be explained by the high content of monoterpenes. It has been mentioned that 1,8-cineole, camphor, α-pinene, β-pinene, borneol, linalool, menthone, carvone, anetole, anisole, have anticholinesterase eactivity (13-15). This current oil lacked the presence of monoterpenes, hence contributed to the low AChE/BChE inhibition.

CONCLUSION

In conclusion, essential oil and their components generally displayed significant bioactivity properties, which are useful as preventive agents from various diseases. In the case of *A. peduncularis* oil, although there is no striking on their bioactivity in the oil, it is still worthwhile to investigate the other parts of the plant as a natural source for essential oil composition or their phytochemical studies.

ACKNOWLEDGMENTS

The authors thank the Ministry of Science, Technology and Innovation Malaysia for financial support under vote QJ130000.2526.03H93 and the Faculty of Science, Universiti Teknologi Malaysia for research facilities.

REFERENCES

1. Bandana KT, Amit A, Devendra SR, Bipin R, Rashmi, Rawat MSM. A review on genus Alseodaphne: Phytochemistry and pharmacology. Mini-Rev Org Chem 9, 433-445, 2012
2. Nafiah MA, Mukhtar MR, Morita H, Ahmad K, Awang K, Hadi AHA. Alkaloids from roots of Alseodaphne corneri Kosterm. Malays J Sci 29, 281-284, 2010.
3. Lee SS, Chang SM, Chen CH. Chemical constituents from Alseodaphne andersonii. J Nat Prod 64, 1548-1551, 2001.
4. Chang H, Liu L, Tu P. Chemical constituents of Alseodaphne hainanensis. Zhongcaoyao 31, 725-727, 2000.
5. Mahmud Z, Khan MN, Lajis NH, Toia RF. Perakensol: Aphenanthrenoid isolated from Alseodaphne perakensis. J Nat Prod 55, 533-535, 1992.
6. Adams RP. Identification of essential oil by gas chromatography-quadrupole/mass spectroscopy. Allured Publishing Corporation, Carol, Stream IL, USA, 2001.
7. Salleh WMNHW, Ahmad F, Khong HY, Zulkifli RM. Chemical compositions and biological activities of essential oils of Beilschmiedia glabra. Nat Prod Commun 10, 1297-1300, 2015.
8. Salleh WMNHW, Ahmad F, Khong HY. Antioxidant and anticholinesterase activities of essential oils of Cinnamomum griffithii and C. macrocarpum. Nat Prod Commun 10, 1465-1468, 2015.
9. Ellman GL, Courtney KD, Andres V, Feather-Stone RM. A new and rapid colorimetric determination of acetylcholinesterase activity. Biochem Pharmacol 7, 88-95, 1961.
10. Orhan I, Aslan S, Kartal M, Sener B, Baser KHC. Inhibitory effect of Turkish Rosmarinus officinalis L. on acetylcholinesterase and butyrylcholinesterase enzymes. Food Chem 108, 663-668, 2008.
11. Soares JR, Dinis TCP, Cunha AP, Almeida LM. Antioxidant activity of some extracts of Thymus zygis. Free Radic Res 26, 469-478, 1997.
12. Loizzo MR, Menichini F, Conforti F, Tundis R, Bonesi M, Saab AM, Statti GA, de Cindio B, Houghton PJ, Menichini F, Frega NG. Chemical analysis, antioxidant, antiinflammatory and anticholinesterase activities of Origanum ehrenbergii Boiss and Origanum syriacum L. essential oils. Food Chem 117, 174-180, 2009.
13. Savelev S, Okello E, Perry NS, Wilkins RM, Perry EK. Synergistic and antagonistic interactions of anticholinesterase terpenoids in Salvia lavandulaefolia essential oil. Pharmacol Biochem Behav 75, 661-668, 2003.
14. Sajjadi SE, Shahpiri Z. Chemical composition of the essential oil of Salvia limbata C.A. Mey. Daru J Pharm Sci 12, 94-97, 2004.
15. Picollo MI, Toloza AC, Mougabure CG, Zygadlo J, Zerba E. Anticholinesterase and pediculicidal activities of monoterpenoids. Fitoterapia 79, 271-278, 2008.

Received : 28.03.2016
Accepted : 12.05.2016

Turk J Pharm Sci 13(3), 351-357, 2016
DOI: 10.4274/tjps.2016.12

REVIEW ARTICLE

Nano Chemotherapeutics in Bone Metastasis and Targeting

Kemik Metastazlarında Nano Kemoterapötikler ve Hedeflendirilmeleri

Müge KILIÇARSLAN*, Miray GÖRGÖZ

Ankara University, Faculty of Pharmacy, Department of Pharmaceutical Technology, 06100 Tandoğan, Ankara, TURKEY

ABSTRACT

Due to the increase of cancer incidence in recent years, contemporary studies have focused on the identification, diagnosis and treatment of this disease. It is rather difficult to treat cancer without harming normal cells. Thus, studies exploring nano systems that are targeted to the cancerous cells are drawing attention. The frequent formation of metastasis in the bone tissue of certain cancers, such as the breast and prostate, has increased the mortality risk from these cancers. For this reason, preventing metastasis by targeting metastatic bone tissue with anti-neoplastic agents without damaging healthy soft tissue has become a subject of interest for many researchers. In addition to the therapeutic properties of bisphosphonates for bone metastases that form osteoclastic and osteoblastic, its affinity to hydroxyapatite, the main mineral of bone tissue, has been extensively studied as a targeting agent for bone diseases. With the conjugation of bisphosphonates to the nanoparticulate systems, nanoparticles loaded with the active ingredient are transmitted solely to the diseased bone tissue. Then, with the help of a nanostructured system, the bisphosphonates are localized only in the tumor containing diseased bone tissue, and the chemotherapeutic agent is released in a controlled manner. In this review, current approaches targeting bone metastases, and especially studies conducted with nanostructured drug carrier systems, are assessed.

Key words: Nano chemotherapeutics, Bone metastasis, Bisphosphanates, Nanoparticles, Drug targeting

ÖZ

Kanser hastalığının son yıllarda artan insidansı nedeniyle güncel çalışmalar bu hastalığın tanı, teşhis ve tedavisi üzerine yoğunlaşmıştır. Normal hücrelere zarar vermeden hastalığın tedavisi oldukça güçtür. Bu nedenle sadece kanserli hücreye hedeflendirilmiş nano sistemler ile yapılan çalışmalar dikkat çekmektedir. Yaygın olan meme ve prostat kanserleri gibi hastalıkların metastazının sıklıkla kemik dokusunda meydana gelmesi hastanın yaşam kalitesini azaltmasından öte bu kanser türlerinin ölüm riskini artırmaktadır. Bu amaçla sağlıklı yumuşak dokuya zarar vermeden anti-neoplastik ajanların doğrudan metastaz meydana gelmiş kemik dokusuna hedeflendirilmesi ile metastazın önlenmesi veya tedavisi çoğu araştırıcının üzerinde çalıştığı konular arasına girmiştir. Osteoklastik veya osteoblastik şekilde oluşan kemik metastazları için bifosfonatların tedavi edici özelliklerine ek olarak kemik dokusunun ana minerali olan hidroksiapatite olan afinitesi nedeni ile kemik hastalıkları için hedefleme ajanı olarak da oldukça yaygın şekilde çalışma konusu olmuştur. Bifosfanatların nanopartiküler sistemlere konjugasyonu ile de etkin madde yüklü nanopartiküller sadece hasta kemik dokusuna iletilmekte, nano yapı sayesinde de sistemin tümörlü dokuda lokalize olup kemoterapötik ajanı kontrollü olarak salması sağlanmaktadır. Bu derleme ile kemik metastazlarına hedeflemedeki güncel olan yaklaşımlar, özellikle nano yapılı ilaç taşıyıcı sistemler ile yapılan çalışmalar tartışılarak değerlendirilmiştir.

Anahtar kelimeler: Nano kemoterapotikler, Kemik metastazı, Bifosfonatlar, Nanopartiküller, İlaç hedefleme

INTRODUCTION

Recent developments in nanotechnology have advanced the direction of biomedical applications and the optimization of therapies. Nano chemotherapeutics have continued to be the center of interest due to several distinguishing attributes, including: the surface area of their delivery systems, which is greater than a micrometer; several unique structural properties; high residency time in the circulatory system; configurability for the diagnosis and treatment of many diseases; ability to target various bioactive agents and organs; ability to travel in the tissue through capillaries; and their relatively easy uptake by the cells. Especially the production of nanoparticles that can deliver chemotherapeutic agents to cancerous tissues and thus, blocking the inadequate selectivity of conventional cancer drugs are very promising (1-3). Aside from their targeting ability, another property that attracts attention of nanoparticles is their ability to facilitate the delivery of different chemotherapeutic agents together, thereby increasing the efficiency of the treatment (4).

*Correspondence: E-mail: muge.kilicarslan@pharmacy.ankara.edu.tr Phone: +90 505 501 73 50

Bone diseases are disorders related to the skeletal system and include disorders that restrict basic movements. These disorders disrupt the balance between bone resorption and formation (5). Since there is no effective treatment for multiple bone disorders, such as arthritis, osteoarthritis, osteosarcoma, and metastatic bone cancer, new drugs and new drug delivery systems that performed efficiently and safely in clinical treatments must be developed immediately. However, for most of bone diseases that cause bone disturbances, such as bone cancer, the main concern is maintaining a balance between the efficiency and the adverse effects of the treatment (6). To address this, conducted studies have revealed that a potential strategy in order to increase treatment efficiency is the preparation and application of targeted nano technological systems. Although nano systems have not yet been clinically used for the treatment of bone cancer, studies about the design of multifunctional nanoparticles in the treatment of multiple bone diseases are encouraging.

RESULTS AND DISCUSSION

Bone metastasis and treatment approaches

The spread of cancer from its initiation site to other parts of the body is called as metastasis. Metastasis occurs when cells separate from the tumor and spread to other parts of the body, either through blood circulation or the lymph ducts, as shown in Figure 1. With this movement, cancer cells can spread to distant tissues and organs. While many cancer cells that separate from the main tumor disappear without causing any harmful effects, some of them settle in new areas and start to proliferate and form new tumors (7). Most of the cancer patients dies from tumor cells that have caused metastasis in other parts of the body (8-10). However, different types of cancer have different dispositions toward different body areas, with the most extensive metastasis observed in the liver, lung, brain and bone (7,11).

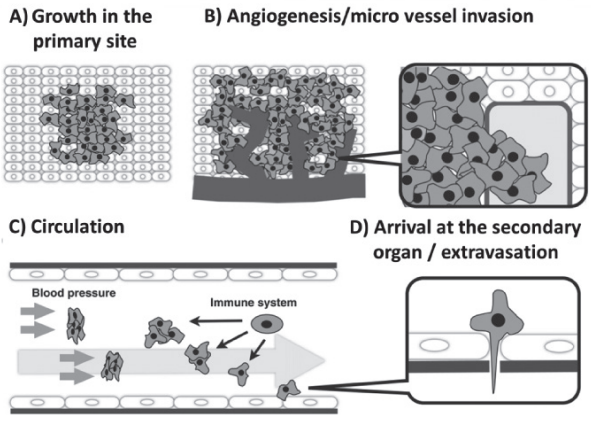

Figure 1. Metastasis stages of cancerous cells A) Proliferation of the tumor in primary area B) Increase of vascularization and transfer of tumor cells into capillaries C) Participation of tumor cells into blood circulation D) Arrival of tumor cells in secondary area where vascularization and extravasation will occur (figure was used with permission of researchers) (22)

When the cancer spreads to the bone, this is referred to as "bone metastasis". Some cancers begin in the bone and are called primary bone cancers, such as osteosarcoma, chondrosarcoma, and Ewing's sarcoma. Especially in adults, bone metastasis is observed more often than bone cancer. Furthermore, tumors that cause breast, lung, and prostate cancer usually metastasize in the bones (6,7,12-15).

The skeletal system is the basic framework of the body and is composed of bone tissue, which consists of a fibrous collagen structure, and calcium phosphate minerals. Hydroxyapatite is the main mineral component of bones. These minerals confer to the bone rigidity and strength for carrying the body by attaching the cells (16-18). Bone tissue harbors two basic cells in its structure-osteoblasts that allow the formation of new bone and osteoclasts that degrade aged bone. The degradation of old cells and the formation of new bone tissue are synchronous processes. Through these two mechanisms, bone tissue preserves its strength (19-21).

It is generally agreed that due to its rich nourishment and stable environment, tumors migrate to bone (23). Additionally, adhesive molecules produced by tumor cells facilitate their binding to the bone. As a result of this adhesion, the production of angiogenic and bone resorbing factors increase, thereby accelerating the proliferation of the tumor in bone tissue. Furthermore, the bones fulfill the storage function for several growth factors. These growth factors are actively released during bone resorption, forming an environment where tumor cells can develop and proliferate. This phenomenon is explained by the "seed and soil" theory (21,24).

The aim of treatment is to prevent tumor growth and eliminate symptoms. Treatment is applied either systemically or locally, with the former preferred in cases where the cancer has spread to more than one bone. However, local treatment is

Table 1. Advantages and disadvantages of nanosystems used in targeting (28,30,32)

Advantages	Disadvantages
- Longer residence time in blood circulation - Ability to localize in the cancerous area because of higher permeation and retention properties of the neoplastic tissue - Reconstructability - Allowance of polymeric nanoparticles to multifaceted modification (such as surface modification with polyethylene glycol [PEG]) - Ability to directly adhere to the tumor by employing the ligands, which have different affinities to biological targets in active targeting	- Although nanoparticles have an affinity to accumulate in the tumor area, their efficiency is dependent upon their complete release of the active substance - Weak tumor penetration of nanopharmaceuticals - Complexity of nanoparticle design and active targeting that can be beneficial in a potential application for a specific therapy - Lack of combined nanoformulation applications that comply with the diet combinations that are applied in clinical usage (difficulty preparing a patient-specific combination) - Passage requirement of some biological membranes, muscle tissue and fibroblast-based cell layers between cancer cells and endothelial cells

preferred when the cancer has spread to only one bone or a small area. Systemic treatments can be provided through hormone therapy, chemotherapy and the administration of drugs orally or via injection. While radiotherapy and surgical procedures are mostly utilized for local therapy (25), in cancer types that have specifically spread to the bone, radiopharmaceuticals and bisphosphonates are used, and at times, systemic and local therapies are used in conjunction. Targeted drugs follow the cancer cells directly; therefore, healthy normal cells are not damaged during treatment. These types of drugs can also be combined with chemotherapy and hormone therapy (25-28).

Nanosystems and tumor targeting

Nanotechnological targeting can be performed actively or passively. Some advantages and disadvantages of using nanosystems to target tumor tissue are shown in Table 1. Some of the passively targeted nanopharmaceuticals that have been approved for clinical usage include Myocet®, Doxil®, Daunoxome®, Abraxane® and Genexol-PM® (1,29). Because of being largely impossible to facilitate the accumulation of active substances in the impact area with passive targeting, researches tend to be directed toward actively targeted nano-formulations. With active targeting in cancer therapy, transmitting toxic drugs to healthy tissue is minimized or eliminated, and the therapeutic efficacy of actively targeted nanoparticles is higher than non-targeted nanoparticles (30). Some external stimulants, such as light, heat, ultrasound waves, and magnetic areas are applied in order to release of drug to the areas desired to be affected to eliminate disadvantages of targeted nanosystems. These systems are called triggered release systems (1,31).

Targeting of nano chemotherapeutics to the bone

Bisphosphonates are the predominant group used in the treatment of bone metastasis and bone targeting (33-35). Bisphosphonates have high bone affinity and are released into bone tissue by instilling or grafting them over the nanoparticles that are loaded with other active substances (6,36). Table 2 lists some examples of active substances, ligands, and production methods which are used in different nanosystems (nanoparticle, dendrimer, liposome, and nanocomplex) for bone targeting.

Biological activity of bisphosphonates was first discovered in 1968, and they were soon prescribed to treat osteoporosis (21). These drugs effect by slowing down the activity of the osteoclast cells and, therefore, are especially effective in treating osteoclastic metastasis (7,33,37). They are also effective in terms of reducing apoptosis related to cell permeability, and they reduce the capillary vascularization of endothelial tissue (21). Bisphosphonates can reduce cancer related bone pain, bone damage, and high blood calcium concentrations; they are also capable of averting bone fractures (10). Because they show high affinity towards bone, bisphosphonates are generally utilized as imaging agents conjugated with radiopharmaceuticals. Furthermore, they can be conjugated with active substances such as estradiol, prostaglandin, diclofenac, fluoroquinolone, cisplatin, methotrexate, technetium hydroxyethylene diphosphonate, technetium methylene diphosphonate, samarium, lexidronam. Peptides and proteins have also been conjugated with bisphosphonates for bone targeting (10,14,21,43-45).

Utilizing bisphosphonates for the targeting of nanoparticulate systems has many advantages. Nitrogenous bisphosphonates contain primer amines and carboxylic acid. If they are conjugated with the nanoparticle via degradable bonds, they become pharmaceutically active and will even show synergy with a suitable active substance (21).

Table 2. Bone targeted nano systems

Formulations	Ligands	Active ingredients	Polymer/Lipid	Production method	Particle size	Ref.
Nano structured ceramic implants	Calcium phosphate and hydroxyapatite	-	-	Precipitation	8.84 µm and 5.21 µm	(38)
Nano complex	Hydroxyapatite	BMP-2 Titanium	-	Ionic interaction	150-250 nm	(39)
Nanoparticle	Hydroxyapatite	-	-	Precipitation	20-40 nm	(18)
Nanoparticle	Alendronate	Estrogen	Polyethylene glycol- Poly(lactic-co-glycolic acid) block copolymer	Dialysis method	43.5-57.3 nm	(40)
Dendrimer	Alendronate	Paclitaxel	Hydroxypropyl methacrylamide (HPMA)	Conjugation	95 nm	(41)
Dendrimer	Alendronate	Paclitaxel	Polyethylene glycol	Conjugation	190 nm	(23)
Radiopharmaceutics and bisphosphonate complex	Hydroxyethylidene-1,1-diphosphonate	Rhenium-186 (^{186}Re)	-	Conjugation	-	(42)
Liposome	RGD peptide	Cisplatin	Phosphatidylcholine, cholesterol, 1,2-distearoyl-sn-glycero-3-phosphoethanolamine-N-[maleimide (polyethylene glycol)-2000]	Extrusion of suspensions	214.7 nm	(9)

Zoledronic acid (ZOL) is a nitrogen-containing bisphosphonate with anticancer activity. ZOL increases apoptosis, prevents the formation of new veins that will ensure the blood supply to the tumor, decreases the level of vascular endothelial growth factor (VEGF), and decreases substance adhesion activity towards the tumor and osteoclast cells. Chaudhari et al. developed targeted drug release systems for bone metastasis containing docetaxel loaded nanoparticles formed from PLGA (poly(lactic-co-glycolic acid)), which have been approved by the FDA for use with ZOL on humans. In this study, nanoparticles were prepared by forming a PLGA-PEG-ZOL conjugate. According to the results obtained from the *in vitro* drug release experiments, the release model is biphasic. The initial burst release was due to the release of drug located on and near the surface of the nanoparticles. In the second phase, the release was slower and controlled by diffusion rate of drug across the polymer matrix. In addition, as a result of the bone affinity tests, no significant differences were observed in bone adhesion between the conjugate nanoparticles and the solutions containing only ZOL. The distribution of radiolabeled particles among the body and bone affinity of these particles were compared with the blood concentrations of the PLGA-PEG-ZOL nanoparticles. At the end of 24 hours, it was observed that 50 times more PLGA-PEG-ZOL conjugate was present in the bone compared to PLGA-PEG nanoparticles. Furthermore, the bone adhesion ratio of the PLGA-PEG-ZOL nanoparticles was found 3.5 times increased compared to normal bone. The authors postulated that the reason for this phenomenon was the loss of lining wherein surrounds the healthy bone in diseased bone tissue. This lining prevents zoledronate from binding, thus its affinity to diseased tissue (osteoporosis, bone metastasis, etc.) is much higher (10).

Li et al. stated that prostate cancer, believed to be osteoblastic, shows osteolytic character at the initial stage of bone metastasis. Therefore, they argued that by targeting to the bone metastasis area that contains both osteolytic and osteoblastic drug molecules, the bone tumor related alterations will be prevented (14). In another study, researchers produced nanoparticles conjugated with alendronate (ALE) for calcification, which is a pathological bone metastasis *in vivo.* Calcification forms as a result of the deposition of calcium in normal tissues, such as veins, nerves and breast tissues, which is similar to embryonic osteogenesis. Generally, lesions formed as a result of calcification are benign; however, in prostate and breast cancer, this situation is reversed. It has been observed that surface of the nanoparticles formed for this purpose is primarily covered with polydopamine, which provides adhesive properties, and conjugation of the particle surface is facilitated. Then, ALE can easily be conjugated with the particle surface, ensuring that it will act as both an active substance and a targeting agent (46).

In a study conducted by Clementi et al. (2011), ALE and paclitaxel (PTX) were prepared in dendrimer form together and separately, and conjugates were obtained. The purpose of this study was to investigate the effect of PEG when used as a carrier on cytotoxic PTX and ALE. Active targeting to the bone by virtue of ALE and passive targeting with an endothelial permeation retention effect were successful. In addition, by increasing the dimensions of the PEG conjugation relative to the free drug, the deposition in the tumor tissue increased (23). In another study by the same research group, bone metastasis caused by breast cancer was targeted using micelles with a dendrimer structure. Cell culture experiments were performed using preparation of the same conjugates over MDA-MB-231 human breast cancer cells and 4T1 mouse breast cancer cells. For both cell types, conjugate formation did not cause any loss of effect. In addition, *in vivo* antitumor activity determination study showed that after 15 days, the highest tumor healing could be provided with the PTX-PEG-ALE conjugate. Deposition in the tumor was monitored by using a non invasive monitoring system, and at the end of 8 hours, the PTX-PEG-ALE conjugate showed the highest deposition. When the distribution in the body was investigated, it was found that the PTX-PEG-ALE conjugate bound to the tumor with a higher ratio than the conjugate formed between PTX and ALE or PTX and PEG (12).

In another study, H40-star-PEG/ALE micelles were obtained and targeted delivery of doxorubicin to the bone was successful. In this micelle, H40 polyester formed the hydrophobic nucleus part and served as storage for the hydrophobic active substance. ALE was the bone targeted fragment. PEG formed the hydrophobic arms of the star shaped micelle. Release profiles of the micelles loaded with doxorubicin were investigated at pH 4 and pH 7.4. For both pH, the burst effect was quiet fast. The release rate observed in pH 5 was faster than the physiological pH. The reason for these differences was protonation of the amino group of doxorubicin in an acidic environment and low speed degradation of the micelle nucleus at low pH. The authors stated that this drug release rate was promising for pH dependent release systems to bone tumors (43).

Miller et al. aimed to facilitate the targeting of PTX to bone by utilizing ALE. Owing to conjugation with the N-(2-Hydroxypropyl) methacrylamide (HPMA) copolymer, PTX was targeted to metastatic bone regions. It was determined that the passage of the conjugate from the leaking tumor area and its exit from the exterior of the vein were passive. Furthermore, a normal blood vein would not allow the conjugate to pass due to its size; thus, it was ensured that the conjugate would only target the tumor area. HPMA can be dissolved in water and is among the carriers that are biocompatible and non-toxic, and it does not stimulate the immune system. These macromolecules do not diffuse in normal blood veins, but they selectively accumulate in tumor areas because of the increased permeability and retention (IPR) effect. In addition, since the blood brain barrier cannot be overcome with this conjugation, the neurotoxic side

effects formed by PTX are prevented, and residence time in the circulation is extended (41).

Currently, the most popular nano systems for local substance release are magnetic nanoparticles. The disadvantage of these methods is low target cell selectivity, and the requirement to place the patient in a magnetic area for long periods of time (23). One study observed the effect of magnetic nanoparticles on *in vitro* osteoblasts, and according to the cell culture results collected on the fifth and eighth days, it was found that γ-Fe_2O_3 magnetic nanoparticles significantly increased osteoblast density compared to the control group. Then, these nanoparticles were coated with calcium phosphate for the treatment of bone disorders, and in order to prevent agglomeration, were distributed in bovine serum albumin or citric acid. With the presence of this coating inside the bovine serum albumin, by day one, osteoblast density had significantly increased compared to the control group (47).

The performed studies show that modifying the polymeric structure does not significantly increase the targeting binding ratio of processes to the bone tissue, but the presence of the higher binding affinity ligands increased the adsorption. Moreover, it was stated that multiple types of ligand conjugations give better bindings. However, increasing number of the ligands in the nanostructure and increasing the ligand size are not advantageous, once the size of nanoparticles is increased then nanoparticles cannot be used in every formulation (21,48).

When metastasis is generated in bone, acid base balance of the tissue where metastasis is formed is disturbed, due to the protons and hydrolases that are given to the medium by the osteoclast cells. Here, the organic and mineral structure of the bone matrix disintegrates, and the pH decreases to 4.5 in the medium where bone resorption occurs. Because of this, pH sensitive bone specific drug release systems have drawn considerable attention. Ye et al. obtained ALE-monoethyl adipate-(hydrazone)-doxorubicin conjugate by conjugating monoethyl adipate, ALE, and doxorubicin with an amide bond and a hydrazone bond, respectively. It was determined that with conjugation, binding of doxorubicin to the bone increased significantly. In addition, the authors found that in *in vitro* release tests conducted under different pH conditions, a pH dependent release was observed in conjugates with the hydrazone bond, but not in conjugates with the amide bond (49).

Bone binding and drug release

In bone targeted systems, *in vitro* binding tests are performed by determining the binding of particles to hydroxyapatite. These tests are generally based on the addition of a nanoparticle suspension over bone powder or hydroxyapatite in a test tube. Then, the mixture is incubated, and after a predetermined period of time, centrifuged. The particular system is then analyzed inside the supernatant using a suitable analysis method (48). A binding test was performed using the above mentioned method. Figure 2 shows a graph comparing the bone binding capacities of micelles that were conjugated with ALE and those which were not conjugated with ALE. It shows that the bone binding ratio of the nano sized conjugate formed with ALE was 70% after 5 minutes, while the conjugates not bound with ALE showed no significant binding (43).

In another study bone binding kinetics of nanoparticles conjugated with ZOL and ZOL solution was investigated and it was determined that the utilization of ZOL as nanoparticle surface ligand did not cause any effect loss in terms of bone binding (10).

In vitro drug release studies are generally performed in buffer mediums that mimic 37°C, lysosomal (pH 5), and physiological mediums (pH 7.4) with the incubation of a sufficient amount of conjugate in a proper way (23,43). Chen et al. investigated the

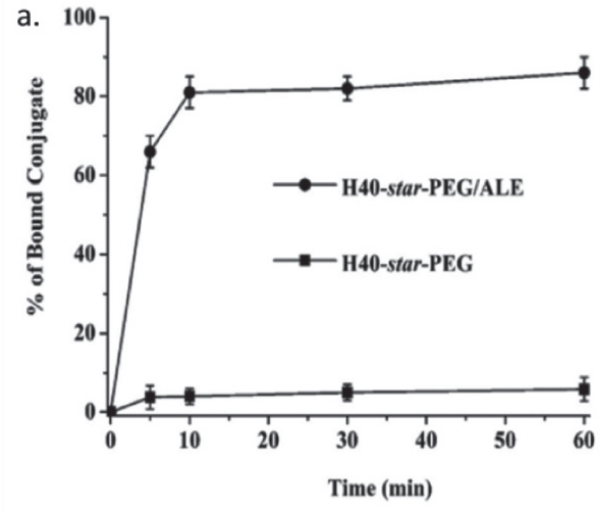

Figure 2. H-40-star-PEG/ALE and H-40-star-PEG micelles *in vitro* bone binding kinetics (figure was used with permission of researchers) (43)

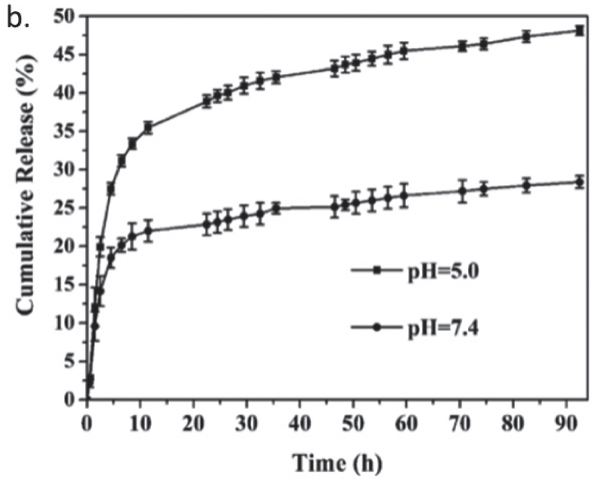

Figure 3. *In vitro* active substance release graphic of doxorubicin loaded Boltorn H40-PEG conjugate, which was conjugated with ALE in pH 5.0 vs. pH 7.4 buffer mediums (figure was used with permission of researchers) (43)

in vitro drug release rate of doxorubicin loaded Boltorn-H40-PEG conjugate, which was conjugated with ALE by incubating it in pH 5 and pH 7.4 buffer mediums. According to the obtained results (Figure 3), pH-dependent drug release was observed in the established particulate. These results showed that the obtained micelles could provide more efficient treatment at the tumor containing area of the bone (43).

Although the *in vitro* drug release studies will give information about release rate, the antineoplastic effect in the metastatic tissue cannot be analyzed in these tests. In addition, even though a reduction in the tissue containing tumor can be observed in the *in vivo* experiments, whether the anticancer agent harms the healthy cells cannot be determined or not. Therefore, conducting cell culture experiments is important to show that targeting can be performed. It is important to prove that the nanoparticles do not show a non-proliferative effect on healthy cells, with regard to showing that the prepared system does not harm healthy tissue. For non healthy cells that develop bone metastasis, generally sarcoma, breast or prostate cancer cells are used (9,23,46,50).

CONCLUSION

As a result of the review we performed, it is determined that the most frequently used approach for targeted delivery of anticancer agents to areas containing tumors in the bone is conjugation of bisphosphonates to nano particulate systems. Bisphosphonates' affinity to hydroxyapatite shows that these molecules are ideal molecules for bone targeting. This conjugation was generally formed by conjugating bisphosphonates to the particle surface. The usability of bisphosphonates as active substances, especially in osteoclastic metastasis, make these molecules advantageous. Concurrently, it was shown in many studies that both the targeting and the anticancer effect of the active substance of bisphosphonates, such as zoledronate, ZOL and ALE, which were bound to nanoparticles loaded with active substances used for the treatment of cancer, can be increased with a synergic effect. Nano particulate systems that are conjugated with bisphosphonates and/or other ligands with bone affinity are promising therapies in the treatment of bone cancer or bone metastasis, as well as other bone diseases.

REFERENCES

1. Sanna V, Pala N, Sechi M. Targeted therapy using nanotechnology: focus on cancer. Int J Nanomedicine 9, 467-83, 2014.
2. Cegnar M, Kristl J, Kos J. Nanoscale polymer carriers to deliver chemotherapeutic agents to tumours. Expert Opin Biol Ther 5(12), 1557-69, 2005.
3. Wang M , Thanou M. Targeting nanoparticles to cancer. Pharmacol Res 62(2), 90-9, 2010.
4. Kemp JA, Shim MS, Heo CY, Kwon YJ. "Combo" nanomedicine: Co-delivery of multi-modal therapeutics for efficient, targeted, and safe cancer therapy. Adv Drug Deliv Rev 98, 3-18, 2016.
5. Rodan GA , Martin TJ. Therapeutic approaches to bone diseases. Science 289(5484), 1508-14, 2000.
6. Gu W, Wu C, Chen J, Xiao Y. Nanotechnology in the targeted drug delivery for bone diseases and bone regeneration. Int J Nanomedicine 8, 2305-17, 2013.
7. American Cancer Society, Bone Metastasis. 2014.
8. Mundy GR. Metastasis to bone: causes, consequences and therapeutic opportunities. Nat Rev Cancer 2(8), 584-93, 2002.
9. Wang F, Chen L, Zhang R, Chen Z, Zhu L. RGD peptide conjugated liposomal drug delivery system for enhance therapeutic efficacy in treating bone metastasis from prostate cancer. J Control Release 196, 222-33, 2014.
10. Ramanlal-Chaudhari K, Kumar A, Megraj-Khandelwal VK, Ukawala M, Manjappa AS, Mishra AK, Monkkonen J, Ramachandra-Murthy RS. Bone metastasis targeting: a novel approach to reach bone using Zoledronate anchored PLGA nanoparticle as carrier system loaded with Docetaxel. J Control Release 158(3), 470-8, 2012.
11. Krzeszinski JY , Wan Y. New therapeutic targets for cancer bone metastasis. Trends Pharmacol Sci 36(6), 360-73, 2015.
12. Miller K, Clementi C, Polyak D, Eldar-Boock A, Benayoun L, Barshack I, Shaked Y, Pasut G, Satchi-Fainaro R. Poly(ethylene glycol)-paclitaxel-alendronate self-assembled micelles for the targeted treatment of breast cancer bone metastases. Biomaterials 34(15), 3795-806, 2013.
13. Yuasa T, Yamamoto S, Urakami S, Fukui I, Yonese J. Denosumab: a new option in the treatment of bone metastases from urological cancers. Onco Targets Ther 5, 221-9, 2012.
14. Li Y, Kong D, Ahmad A, Bao B, Sarkar FH. Targeting bone remodeling by isoflavone and 3,3'-diindolylmethane in the context of prostate cancer bone metastasis. PLoS One 7(3), e33011, 2012.
15. Mai J, Huang Y, Mu C, Zhang G, Xu R, Guo X, Xia X, Volk DE, Lokesh GL, Thiviyanathan V, Gorenstein DG, Liu X, Ferrari M, Shen H. Bone marrow endothelium-targeted therapeutics for metastatic breast cancer. J Control Release 187, 22-9, 2014.
16. Poologasundarampillai G, Wang D, Li S, Nakamura J, Bradley R, Lee PD, Stevens MM, McPhail DS, Kasuga T, Jones JR. Cotton-wool-like bioactive glasses for bone regeneration. Acta Biomater 10(8), 3733-46, 2014.
17. Hench LL, Roki N, Fenn MB. Bioactive glasses: Importance of structure and properties in bone regeneration. J Mol Struct 1073, 24-30, 2014.
18. Pathi SP, Lin DD, Dorvee JR, Estroff LA, Fischbach C. Hydroxyapatite nanoparticle-containing scaffolds for the study of breast cancer bone metastasis. Biomaterials 32(22), 5112-22, 2011.
19. Wang Y , Grainger DW. RNA therapeutics targeting osteoclast-mediated excessive bone resorption. Adv Drug Deliv Rev 64(12), 1341-57, 2012.
20. Konermann A, Staubwasser M, Dirk C, Keilig L, Bourauel C, Gotz W, Jager A, Reichert C. Bone substitute material composition and morphology differentially modulate calcium and phosphate release through osteoclast-like cells. Int J Oral Maxillofac Surg 43(4), 514-21, 2014.
21. Schroeder A, Heller DA, Winslow MM, Dahlman JE, Pratt GW, Langer R, Jacks T, Anderson DG. Treating metastatic cancer with nanotechnology. Nat Rev Cancer 12(1), 39-50, 2012.
22. Futakuchi M, Fukamachi K, Suzui M. Heterogeneity of tumor cells in the bone microenvironment: Mechanisms and therapeutic targets for bone metastasis of prostate or breast cancer. Adv Drug Deliv Rev 99(Pt B), 206-11, 2016.

23. Clementi C, Miller K, Mero A, Satchi-Fainaro R, Pasut G. Dendritic poly(ethylene glycol) bearing paclitaxel and alendronate for targeting bone neoplasms. Mol Pharm 8(4), 1063-72, 2011.
24. Roodman GD. Mechanisms of bone metastasis. N Engl J Med 350(16), 1655-64, 2004.
25. Blackburn G, Scott TG, Bayer IS, Ghosh A, Biris AS, Biswas A. Bionanomaterials for bone tumor engineering and tumor destruction. J Mater Chem B 1(11), 1519-1534, 2013.
26. Mohamed M, Borchard G, Jordan O. *In situ* forming implants for local chemotherapy and hyperthermia of bone tumors. J Drug Del Sci Tech 22(5), 393-408, 2012.
27. Brannon-Peppas L , Blanchette JO. Nanoparticle and targeted systems for cancer therapy. Adv Drug Deliv Rev 64, 206-212, 2012.
28. Singh R , Lillard JW, Jr. Nanoparticle-based targeted drug delivery. Exp Mol Pathol 86(3), 215-23, 2009.
29. Lammers T, Kiessling F, Hennink WE, Storm G. Drug targeting to tumors: principles, pitfalls and (pre-) clinical progress. J Control Release 161(2), 175-87, 2012.
30. Steichen SD, Caldorera-Moore M, Peppas NA. A review of current nanoparticle and targeting moieties for the delivery of cancer therapeutics. Eur J Pharm Sci 48(3), 416-27, 2013.
31. Ji W, Wang H, van den Beucken JJ, Yang F, Walboomers XF, Leeuwenburgh S, Jansen JA. Local delivery of small and large biomolecules in craniomaxillofacial bone. Adv Drug Deliv Rev 64(12), 1152-64, 2012.
32. Farokhzad OC, Cheng J, Teply BA, Sherifi I, Jon S, Kantoff PW, Richie JP, Langer R. Targeted nanoparticle-aptamer bioconjugates for cancer chemotherapy in vivo. Proc Natl Acad Sci U S A 103(16), 6315-20, 2006.
33. Clezardin P, Benzaid I, Croucher PI. Bisphosphonates in preclinical bone oncology. Bone 49(1), 66-70, 2011.
34. Yang L, Webster TJ. Nanotechnology controlled drug delivery for treating bone diseases. Expert Opin Drug Deliv 6(8), 851-64, 2009.
35. Gittens SA, Bansal G, Zernicke RF, Uludag H. Designing proteins for bone targeting. Adv Drug Deliv Rev 57(7), 1011-36, 2005.
36. Verron E, Khairoun I, Guicheux J, Bouler JM. Calcium phosphate biomaterials as bone drug delivery systems: a review. Drug Discov Today 15(13-14), 547-52, 2010.
37. Kurban S, Mehmetoğlu İ. Osteoprotegerin, Rank ve Rank Ligandı. Turk J Biochem 32(4), 178-184., 2007.
38. Balasundaram G, Webster TJ. Nano-structured Biodegradable Ceramics for the Prevention and Treatment of Bone. NSTI-Nanotech, 2006.
39. Bae SE, Choi J, Joung YK, Park K, Han DK. Controlled release of bone morphogenetic protein (BMP)-2 from nanocomplex incorporated on hydroxyapatite-formed titanium surface. J Control Release 160(3), 676-84, 2012.
40. Choi SW, Kim JH. Design of surface-modified poly(D,L-lactide-co-glycolide) nanoparticles for targeted drug delivery to bone. J Control Release 122(1), 24-30, 2007.
41. Miller K, Erez R, Segal E, Shabat D, Satchi-Fainaro R. Targeting bone metastases with a bispecific anticancer and antiangiogenic polymer-alendronate-taxane conjugate. Angew Chem Int Ed Engl 48(16), 2949-54, 2009.
42. Ogawa K , Mukai T. Targeted imaging and therapy for bone metastases: control of pharmacokinetics of bone-targeted radiopharmaceuticals. J Drug Deliv Sci Tech 19(3), 171-176, 2009.
43. Chen H, Li G, Chi H, Wang D, Tu C, Pan L, Zhu L, Qiu F, Guo F, Zhu X. Alendronate-conjugated amphiphilic hyperbranched polymer based on Boltorn H40 and poly(ethylene glycol) for bone-targeted drug delivery. Bioconjug Chem 23(9), 1915-24, 2012.
44. Tautzenberger A, Kovtun A, Ignatius A. Nanoparticles and their potential for application in bone. Int J Nanomedicine 7, 4545-57, 2012.
45. Coleman R. Bone targeted treatments in cancer – The story so far. J Bone Oncology, 2016.
46. Li N, Song J, Zhu G, Shi X, Wang Y. Alendronate conjugated nanoparticles for calcification targeting. Colloids Surf B Biointerfaces 142, 344-50, 2016.
47. Pareta RA, Taylor E, Webster TJ. Increased osteoblast density in the presence of novel calcium phosphate coated magnetic nanoparticles. Nanotechnology 19(26), 265101, 2008.
48. Hruby M, Etrych T, Kucka J, Forsterova M, Ulbrich K. Hydroxybisphosphonate-containing polymeric drug-delivery systems designed for targeting into bone tissue. J Appl Polym Sci 101(5), 3192-3201, 2006.
49. Ye WL, Zhao YP, Na R, Li F, Mei QB, Zhao MG, Zhou SY. Actively targeted delivery of doxorubicin to bone metastases by a pH-sensitive conjugation. J Pharm Sci 104(7), 2293-303, 2015.
50. Daubine F, Cortial D, Ladam G, Atmani H, Haikel Y, Voegel JC, Clezardin P, Benkirane-Jessel N. Nanostructured polyelectrolyte multilayer drug delivery systems for bone metastasis prevention. Biomaterials 30(31), 6367-73, 2009.

Received: 27.07.2016
Accepted: 04.08.2016

2016 Author Index - 2016 Yazar Dizini

2016 Author Index - 2016 Yazar Dizini

2016 Subject Index

2016 Subject Index

2016 Konu Dizini

2016 Konu Dizini